WALTER J. ARABASZ

CHARACTERISTICS OF COAL-MINING-INDUCED AND TECTONIC SEISMICITY, WASATCH PLATEAU, UTAH

by

Walter J. Arabasz
Department of Geology and Geophysics
University of Utah
Salt Lake City, Utah 84112-1183

Final Report

to

National Science Foundation
Division of Earth Sciences
Seismology Program
Washington, D.C.

Grant No. EAR-8319661

Principal Investigator: Walter J. Arabasz

Award Period: April 1, 1984 to November 30, 1985

Part III-le. Technical Description of Project and Results

March 1986

Any opinions, findings, and conclusions and recommendations expressed in this publication are those of the authors and do not necessarily reflect the views of the National Science Foundation.

CHARACTERISTICS OF COAL-MINING-INDUCED AND TECTONIC SEISMICITY, WASATCH PLATEAU, UTAH

by

Walter J. Arabasz
Department of Geology and Geophysics
University of Utah
Salt Lake City, Utah 84112-1183

Final Report

to

National Science Foundation
Division of Earth Sciences
Seismology Program
Washington, D.C.

Grant No. EAR-8319661

Principal Investigator: Walter J. Arabasz

March 1986

TABLE OF CONTENTS

SUMMARY OF COMPLETED PROJECT

The primary purpose of this project was the simultaneous field investigation of mining-related and tectonic earthquakes (neighboring both laterally and vertically) in the eastern Wasatch Plateau of central Utah. During June to August 1984, a collaborative field experiment was carried out in the East Mt.-Gentry Mt.-Joes Valley area of the Wasatch Plateau by the University of Utah (with the support of this NSF award), the U.S. Bureau of Reclamation, and Woodward-Clyde Consultants of San Francisco. Up to 40 analog and digital seismographs were operated simultaneously within a 40x25 km area in the eastern part of the Basin & Range (BR)-Colorado Plateau (CP) transition. Multiple objectives included: (1) precise resolution of intense mining-related seismicity—both at and below levels of active underground coal mining; (2) source characterization of the mining-related and neighboring tectonic earthquakes, especially in relationship to an inferred subjacent detachment and young normal faulting in the Joes Valley area; (3) digital recording of steeply incident waves, both at underground mine level and at surface, to investigate path/site effects on high-frequency spectral content; and (4) spatial mapping of stress orientation within the BR-CP transition.

Thousands of seismic events (M<2), predominantly mining-related, were recorded. In the vicinity of East Mountain—the primary focus of the University of Utah efforts—475 hypocentral solutions (and 13 focal mechanisms) were determined using a 20-station local array. Important results include: (1) clustering of accurately-located foci near sites of active mining, with focal depths predominating within 1 km below mine level; (2) sparse seismicity (<4.4 km deep) in the vicinity of multiple late Pleistocene-Holocene(?) normal fault scarps in the Joes Valley area; (3) bracketing of a lateral change in stress orientation within the BR-CP transition involving a reorientation of maximum principal stress from the vertical (normal faulting) to the horizontal (reverse faulting); and (5) documentation of near-surface effects on high-frequency seismic waves based on simultaneous surface/subsurface (600 m depth) recordings.

DESCRIPTION OF PROJECT

This project represents the latest part of a multi-stage investigation of the seismotectonics of the Basin and Range (BR)-Colorado Plateau (CP) transition in Utah by the principal investigator. Earlier NSF awards for this work included Grant EAR-7723706 ("High-Resolution Seismicity, the Mechanics of Active Faulting, and Crustal Deformation Across the Basin and Range-Colorado Plateau/Rocky Mountain Transition") and Grant EAR-8008799 ("Seismological Studies Across the Basin and Range-Colorado Plateau Transition in Utah"). A key overview of this work is given by Arabasz and Julander (1986).

As described briefly in the preceding Summary, a multi-institutional seismic-monitoring experiment was carried out during June to August 1984 in the eastern Wasatch Plateau of central Utah. For convenience, the field experiment will be referred to as the EWP-84 experiment (for eastern Wasatch Plateau, 1984). The experiment involved collaborative efforts by the University of Utah (U of U), the U.S. Bureau of Reclamation (USBR), and Woodward-Clyde Consultants (WCC) of San Francisco, California.

The field experiment was conceived as basic research to investigate the seismotectonics of the seismically active eastern Wasatch Plateau. Planning of the experiment dates from submission in August 1983 of the research proposal to the National Science Foundation by W.J. Arabasz upon which this award and report are based. The proposal included letters of intention from both the U.S. Bureau of Reclamation and Woodward-Clyde Consultants to participate with independent funding in the proposed seismic-monitoring experiment in order to pursue objectives of respective engineering interest.

Funding to the University of Utah was awarded by the National Science Foundation in April 1984, and the collaborative field experiment was successfully carried out during the summer of 1984. Up to 40 analog and digital seismographs were operated simultaneously within a 40 by 25 km area encompassing the central and northern parts of Joes Valley as well as the adjacent areas of East Mountain and Gentry Mountain to the east (Figure 1).

In addition to the multiple objectives outlined in the preceding Summary, the cooperative experiment also as also carried out for: (1) an assessment of the level of microseismicity in the Joes Valley area and implications of observational seismology for an earthquake hazard evaluation of Joes Valley dam (USBR), and (2) an investigation of near-field ground motion at mine level (WCC).

Given the collaborative involvement of the three research groups, the basic strategy in the field experiment was to establish three discrete subarrays (focused on three respective targets within the study area) while forming a broad-aperture network to cover the study area with a station spacing of about 10 km or less. Dense station coverage in the East Mountain and Gentry Mountain areas was essential for investigating very shallow, mining-related seismicity, especially for focal-depth control. The broad-aperture network, on the other hand, was designed to ensure an adequate geographic distribution of stations for uniform detection throughout the study area, good azimuthal control for earthquake epicenters, and adequate focal-depth and focal-sphere control for earthquakes that might occur in the 5-15 km depth range.

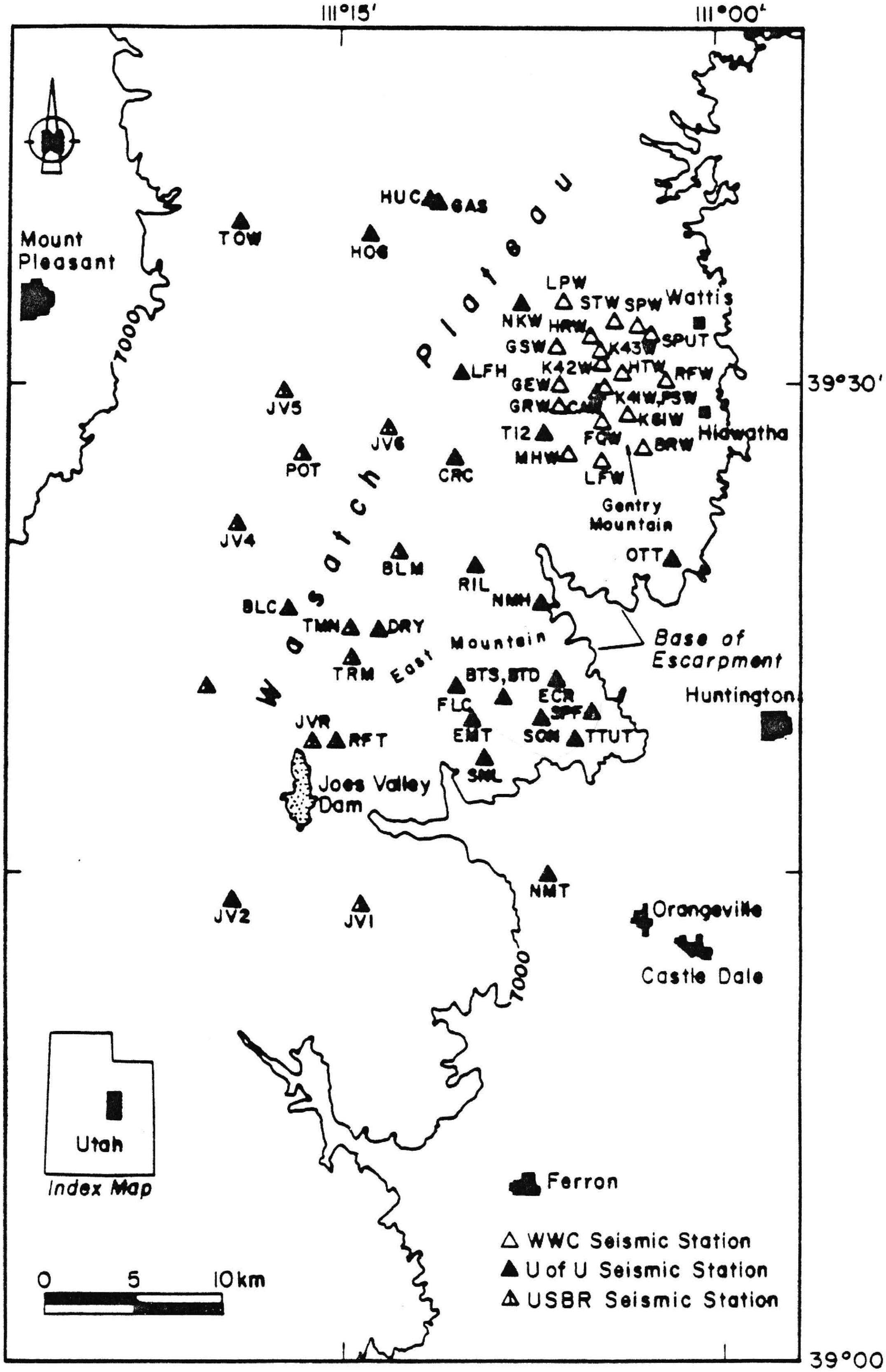

Figure 1. Station map showing all seismograph stations operated during the EWP-84 field experiment.

A primary target area selected by the U of U was the East Mountain area, which includes the Deer Creek Mine and the Wilberg Mine, two major underground coal mines of the eastern Wasatch Plateau. In addition, the U of U assumed the responsibility of deploying seismographs to supplement array coverage by the USBR and to ensure skeletal station coverage throughout the study area. The USBR equipment involved telemetry capabilities such that six stations (JV1-JV6, Figure 1) were installed by helicopter along the high-elevation flanks of the Joes Valley graben, and signals were telemetered by radio to two recording sites. Topographic relief in the study area exceeds 1400 m. The principal target of the WCC subarray was the Gentry Mountain area—the location of the King Mine, another major underground coal mine.

The study area is covered by the University of Utah's regional seismic telemetry network such that seismic events larger than about magnitude 1.5 in the study area are routinely located. As part of the EWP-84 experiment, two seismic telemetry stations were installed at stations TTUT and SPUT (Figure 1), and signals were telemetered to the University of Utah campus in Salt Lake City for temporary recording as part of the U of U regional seismic network. Data from stations TTUT and SPUT were recorded continuously on helicorder drum recorders (at a recording speed of 60 mm/min) from mid-June to the end of August 1984.

An effective broad-aperture network operated in the study area from about July 6 to August 12, 1984—effectively the same period of operation as the USBR sub-array in the Joes Valley area. Supplemental coverage of the study area during this period was provided chiefly by U of U stations. Dense-array coverage of the East Mountain area by U of U stations was in place from the last week of June to about July 27. For the Gentry Mountain area, dense-array coverage by WCC stations was in place from about July 13 to August 25.

After completion of the EWP-84 experiment, separate funding was provided to the University of Utah for analysis of the analog data collected by the USBR. Basically, the intention was to achieve processing of the USBR-collected data for hypocenter location, source mechanism (where possible), and magnitude of seismic events—in conjunction with the analysis of data recorded by the University of Utah and Woodward-Clyde Consultants. Reports to the U.S. Bureau of Reclamation by Arabasz and Williams (1986) and Arabasz (1986) summarize results of those corollary efforts.

A summary of reports and publications resulting from this grant is presented in a following section entitled "Publication Citations." Scientific results from the research efforts are then presented in the section entitled "Results" in the form of a manuscript, a brief technical report, and three selected abstracts.

References

(See Publication Citations on following page.)

PUBLICATION CITATIONS

Arabasz, W.J., 1986. Seismotectonics of the Basin and Range–Colorado Plateau transition in Utah (abstract): Geol. Soc. Am. Abstracts with Programs 18 (in press).

Arabasz, W.J. and D.R. Julander, 1986. Geometry of seismically active faults and crustal deformation within the Basin and Range–Colorado Plateau transition in Utah, in Extensional Tectonics of the Basin and Range Province: A Perspective, L. Mayer, Editor, Geol. Soc. Am. Special Paper 208 (in press).

Arabasz, W.J., J.C. Pechmann, D. Williams, R.A. Martin, Jr., C.K. Wood, I.G. Wong, J.R. Humphrey, and J.A. Adams, 1985. Collaborative study of coal-mining induced and tectonic seismicity, eastern Wasatch Plateau, central Utah—A preliminary report (abstract): Earthquake Notes 55 (1), 24.

Williams, D.J., and W.J. Arabasz, 1985. Mining-related seismicity in the East Mountain area, Wasatch Plateau, central Utah (abstract): EOS, Trans. Am. Geophys. Union 66, 954-955

Williams, D.J., 1986. Mining-related and tectonic seismicity in the East Mountain area, Wasatch Plateau, central Utah: M.S. Thesis, University of Utah, Salt Lake City, Utah.

Publications in Preparation:

Pechmann, J.C.: Observation of near-surface apparent attenuation from surface and subsurface recordings of a nuclear explosion (in prep. for Geophys. Res. Letters).

Williams, D.J. and W.J. Arabasz: Mining-related and tectonic seismicity in the East Mountain area, Wasatch Plateau, Central Utah (in prep. for Bull. Seism. Soc. Am.).

Technical Reports (Based, in part, on results from this project):

Arabasz, W.J., 1985. Interpretation of instrumental seismicity and contemporary tectonics of the eastern Wasatch Plateau relevant to seismic exposure of the Joes Valley and Scofield dams: Technical Report, Contract No. 4 PG 40 13210, U.S. Bureau of Reclamation, Denver, Colorado.

Arabasz, W.J. and D.J. Williams, 1985. Analysis and summary of seismographic data recorded in vicinity of Joes Valley Dam, Emery County Project, eastern Wasatch Plateau, Utah: Technical Report, Contract No. 4 PG 40 13210, U.S. Bureau of Reclamation, Denver, Colorado.

RESULTS

As outlined in the Publication Citations, scientific results from research supported by this grant have been summarized in an M.S. thesis, three abstracts, two reports, and one publication in press; two additional manuscripts are in preparation for publication. Salient results of the research are presented here in three parts: (1) a full technical report by W.J. Arabasz and D.J. Williams of the details and results of the 1984 Eastern Wasatch Plateau seismic monitoring experiment—specifically for the effort supported by this grant to the University of Utah; (2) a brief summary by J.C. Pechmann of an f_{max} experiment in which digital recordings were made of a nuclear explosion both at underground mine level and at the surface to investigate near-surface effects on high-frequency spectral content; and (3) the text of three abstracts published by the principal investigator and scientific collaborators.

Part I

MINING-RELATED AND TECTONIC SEISMICITY IN THE EAST MOUNTAIN AREA, WASATCH PLATEAU, CENTRAL UTAH

by

D. J. Williams and W. J. Arabasz

Department of Geology and Geophysics

University of Utah

March 1986

ABSTRACT

As part of a larger multi-institutional field experiment during the summer of 1984 investigating the seismicity of the eastern Wasatch Plateau a 20-station array of portable seismographs was operated for 1 month in the East Mountain area, an area of active underground coal mining. Eight stations of the array were concentrated on top of East Mountain at an average spacing of 3 km, including 2 key digital stations, with one 600 m below surface at mine level. Principal objectives relate to (1) precise resolution of seismicity in the East Mountain area, especially for seismic events below mine level, given experiment design and station spacing; and (2) determination of focal mechanisms for seismic events at mine level, below mine level, and extending laterally outside of the mining area. Secondary objectives include: (3) evaluation of evidence for temporal variation in mining-related seismicity in so far as the eight-week monitoring period of the 1984 study bracketed a two-week vacation shutdown of mining activity; and (4) improved resolution of seismicity at mine level to address, to whatever degree possible, the spatial correlation with active coal extraction. Available high-resolution seismic profiles and drill-hole sonic logs were used for a refined velocity model. Accurately-located epicenters cluster within an area < 2.5 km in diameter that encompasses four zones of significant coal extraction during the study period, Accurate focal depths indicate clustering down to 500 m below mine level, with the deepest reliably located event to 4.4 km. Continuous monitoring for a 60-d period (June 15-Aug. 15) bracketed a 16-d mining shutdown (July 7-

22) during which significant seismicity, comparable to that observed before the shutdown, was observed. P-wave first motions indicate two populations of events: (1) enigmatic events located at or above to mine level with ubiquitous dilatational first motions, and (2) double-couple mechanisms, predominantly of compressional type (thrust and ss), with NW- to NE-trending P-axes. Normal-faulting mechanisms for two earthquakes 3.0 km and 4.4 km deep suggest a change to an extensional stress state 10 km to 15 km west of the mining area where late Pleistocene-Holocene (?) normal fault scarps are observed at the surface.

TABLE OF CONTENTS

ACKNOWLEDGMENTS

Numerous individuals made contributions relating to various aspects of the acquisition, analysis, and interpretation of data presented in this report. R.A. Martin, Jr., of the U.S. Bureau of Reclamation (USBR), I.G. Wong of Woodward-Clyde Consultants (WCC), and J.C. Pechmann of the University of Utah (U of U) were primary co-investigators (together with W.J. Arabasz) in the 1984 Eastern Wasatch Plateau field experiment.

The following individuals were part of the respective field groups: D.C. Martin, E. McPherson, T.L. Olson, J.F. Peinado, K.A. Poulson, and J.K. Whipp (U of U); R. LaForge, R.A. Hansen, and C.K. Wood (USBR); and J.A. Adams and I.G. Humphrey (WCC). D.T. Loeb, T.L. Olson, J.F. Peinado, and R.M. Smith helped at the University of Utah in the analysis of data for this report; W.D. Richins and D. Cameron kindly provided computer assistance.

The cooperation of officials of Utah Power & Light Company was crucial to the 1984 field experiment--notably in connection with investigations of mining-related seismic activity in the East Mountain area; R.C. Fry provided key assistance, and T.W. LLoyd helped with subsurface operation of seismographs. J.F. Niebergall, W.E. Nowak, C. Reed, and S. Robison of the U.S. Forest Service provided useful help relating to site selection for the temporary network and especially to compilation of information on seismic exploration activity and active mining in the study area.

Primary support for this research was provided by the National Science Foundation, Grant No. EAR-8319661. Additional support for data analysis was provided by U.S. Bureau of Reclamation Contract No. 4PG 40 13210.

INTRODUCTION

During June to August 1984, a multi-institutional seismic-monitoring experiment was carried out in the East Mountain-Joes Valley-Gentry Mountain area of the eastern Wasatch Plateau in central Utah (Figure 1). For convenience, the field experiment will be referred to as the EWP-84 experiment (for eastern Wasatch Plateau, 1984). The field experiment involved collaborative efforts by the University of Utah (U of U), the U.S. Bureau of Reclamation (USBR), and Woodward-Clyde Consultants (WCC) of San Francisco, California.

The EWP-84 experiment was part of a multi-year study of the seismotectonics of the transition between the Basin and Range (BR) and Colorado Plateau (CP) provinces begun by the University of Utah in 1979 (McKee,1982; McKee and Arabasz, 1982; Julander, 1983). A summary paper of results achieved prior to the EWP-84 experiment has been prepared by Arabasz and Julander (1986). The reader is referred to the latter paper for extensive background information on the BR-CP transition. Background information presented here focuses on aspects of the seismicity and tectonics directly relevant to the study area of this report.

Purpose and scope. The EWP-84 experiment had multiple objectives relating to earthquake occurrence (both tectonic and mining-related), source characterization, and stress state throughout a broad region of the eastern Wasatch Plateau (Arabasz et al., 1985). Up to 40 analog and digital seismographs were operated simultaneously within a 40 by 25 km area encompassing the central and northern parts of Joes Valley as well as the adjacent areas of East Mountain and Gentry Mountain to the east (Figure 2). This report represents only one facet of the EWP-84 experiment, as explained next, and focuses on the East Mountain area.

The spatial coincidence of intense microseismicity with active underground coal mining in the East Mountain area had been established by earlier study (Mckee, 1982; McKee and Arabasz, 1982). The previous results raised the expectation of finding (1) abundant seismic events at and below mine level (approximately 0.6 km below surface) with focal depths less than 4 km, and (2) sporadic seismic events even deeper (down to 16 km). Those earlier results had also defined the need for areal mapping of changes in stress orientation in the area between the eastern Wasatch Plateau and the eastern Basin and Range province. Figure 3 shows that in the vicinity of the study area there are reverse-faulting focal mechanisms in the eastern Wasatch Plateau, reflecting horizontal compression , and normal-faulting mechanisms, reflecting horizontal extension, more than 50 km to the west.

Two aspects of the EWP-84 experiment design for East Mountain should be emphasized. First, broad-aperture coverage had to be maintained (discussed later), which limited the number of instruments that could be concentrated on East Mountain, allowing a station spacing of 2-3 km. Second, only one seismograph package could be deployed underground at mine level, and only by mining personnel. (Safety problems precluded access to mine level, a decision by the mine operators that was later vindicated by the Wilberg Mine disaster in December 1984 in which there were 27 fatalities.) Accordingly, the intention was not to resolve the precise location of seismic events at mine level (which would have required a station spacing of hundreds of meters), but rather to achieve hypocentral resolution of the sub-mine seismicity.

The primary objectives of this thesis are: (1) precise hypocentral resolution of intense microseismicity in the East Mountain area, especially for seismic events below mine level, given the experiment design and station spacing; and (2) determination of focal mechanisms for seismic events at mine level, below mine level, and extending laterally outside of the mining area. Secondary objectives include: (3) evaluation of evidence for temporal variation in mining-related seismicity in so far as the eight-week monitoring period of the 1984 study bracketed a two-week vacation shutdown of mining activity; and (4) improved resolution of seismicity at mine level to address, to whatever degree possible, the spatial correlation with active coal extraction.

Geologic and tectonic setting. the study area lies along the eastern part of the Wasatch Plateau, one of the dominant topographic features in central Utah. The plateau rises to an elevation of more than 3,000 m. An erosional escarpment with as much as 800 m of relief forms its eastern margin; its western boundary is formed by the Wasatch Monocline, which has almost 2000 m of relief between the top of the plateau and the floor of the Sanpete Valley. The plateau exposes nearly flat-lying sandstones and shales of Cretaceous to Tertiary age; post-Eocene strata are absent (Hinze, 1973). In the East Mountain area, the Blackhawk Formation of the Cretaceous Mesa Verde Group contains major coal seams. Two prominent coal seams located approximately 600 m below the top of the plateau crop out along the eastern escarpment and are the focus of active mining of central importance to this report.

Complex sets of northerly-trending faults extend along the entire length of the Wasatch Plateau (Figure 1). One of the most prominent fault zones forms the Joes Valley graben, which extends 120 km from north to south and has displacements up to 750 - 900 m on its bounding faults (Doelling, 1972; Spieker, 1949). Multiple displacements of late Pleistocene-Holocene (?) age have been exposed by trenching on three faults of the Joes Valley zone north of Joes Valley Dam (Figure 1). The trenching was carried out by the USBR on the two graben bounding faults and an intra-graben fault. Single-event vertical displacements range from less than 1 m to 5 m, and the recurrence interval of surface rupture on a single fault is estimated to be 10,000 to 30,000 years (L. Foley, U.S. Bureau of Reclamation, personal communication, 1986).

East of the Joes Valley graben, vertical displacements diminish to a range of a few hundreds to a few tens of meters or less (Doelling, 1972). Studies of slickenslides exposed in coal-mine workings along the eastern Wasatch Plateau show evidence of mixed strike-slip and normal faulting, the latter being generally younger (G.L. Hunt, Cyprus Mining Company, personal communication, 1985).

According to structural interpretations of Standlee (1982), which are based upon extensive industry subsurface data in central Utah, major eastward-directed thrusting in Late Cretaceous to Paleocene time extended eastward beneath the Wasatch Plateau and occurred on a detachment surface within incompetent strata above the Triassic- Jurassic Navajo Sandstone (see Figure 4). Backsliding along such a detachment over a west-facing subsurface ramp, as shown in Figure 4, is inferred to have created the Wasatch Monocline during an episode of "thin-skinned" horizontal extension during Late Tertiary-Recent time (Royse, 1983). Details of Figure 4 will be described further in the DISCUSSION section.

General seismicity. Figure 5 shows all earthquakes of magnitude 2 or greater located within the study area by the University of Utah regional seismic network from 1962 through 1984. Also included in this figure are 22 earthquakes of magnitude 3 or greater from the historical record dating back to 1850. The two largest shocks in the sample are (1) a magnitude 5 earthquake, located approximately 10 km west of Mt. Pleasant, that occurred in 1876, and (2) another magnitude 5 earthquake located 5 km southwest of Ephriam that occurred in 1961. Since 1962, no instrumentally recorded earthquake larger than magnitude 3.7 has occurred within the study area. In the general vicinity of East Mountain the largest earthquake since 1962 was one of magnitude 3.2 in 1977. The epicenters shown in Figure 5 could have a horizontal error of as much as 10 km and focal depth control is poor. In Figure 5 the majority of the diffuse seismicity appears randomly scattered. The relation of this diffuse seismicity to geologic structure is unclear. There is an apparent clustering of epicenters with the southern part of the Frontal

Fault zone of the Wasatch Plateau in the southwest portion of the figure and near the northern end of the Joes Valley fault zone. (See Arabasz and Julander, 1986, McKee and Arabasz, 1982, and Arabasz et al.,1980, for other details of the regional seismicity.)

The relatively intense clustering of epicenters along the margin of the Wasatch Plateau and along the Book Cliffs north of Price coincides with areas of underground coal mining. McKee (1982) noted a general correlation of mining-related seismicity with areas having coal extraction rates greater than 500,000 tons per year. In the Sunnyside mining district about 40 km east of Price, Smith et al. (1974) found that mining-related seismicity occurred just below the level of mine workings. Seismic events recorded in the vicinity of coal mines in and near the study area have multiple origins (see McKee, 1982; Wong, 1985), including: (1) shear failures, gas "outbursts", and roof collapses in the immediate vicinity of mine workings, and (2) earthquakes presumed to reflect tectonic stress release on faults either within the area of mine workings or at some depth below.

EARTHQUAKE FIELD EXPERIMENT

Network design. The EWP-84 experiment involved operation of a temporary network of up to 40 portable analog and digital seismographs in the study area (Figure 2). Field recording was carried out during a nine-week period between June 21 and August 25, 1984. Figure 2 and Appendix A summarize basic information on the geographic distribution and operational dates of stations included in the temporary network. Given the joint involvement of the three research groups, the basic strategy in the field experiment was to establish three discrete subarrays (focused on three respective targets within the study area) while forming a broad-aperture network to cover the study area with a station spacing of about 10 km or less. Dense station coverage in the East Mountain and Gentry Mountain areas was essential for investigating shallow, mining-related seismicity, especially for focal-depth control. The broad-aperture network, on the other hand, was designed to ensure an adequate geographic distribution of stations for uniform detection throughout the study area, good azimuthal control for earthquake epicenters, and adequate focal-depth and focal-sphere control for earthquakes that might occur in the 5-15 km depth range.

From June 26 to July 27, 1984, eight University of Utah seismographs were concentrated on top of East Mountain with an average station spacing of 2.5 km. This included two key digital event recorders, one located within the Wilberg Mine, the other 600 m above, on top of the plateau. The data from this recording period form the core of this thesis. Supplementary information from longer recording of the broad-aperture network is also included.

The study area is covered by the University of Utah's regional seismic telemetry network (see Figure 5) such that seismic events larger than about magnitude 1.5 in the study area are routinely located. As part of the EWP-84 experiment, two seismic telemetry stations were installed at stations TTUT and SPUT (Figure 2), and signals were telemetered to the University of Utah campus in Salt Lake City for temporary recording as part of the U of U regional seismic network (see, for example, Richins and others, 1984). Data from stations TTUT and SPUT were recorded continuously on helicorder drum recorders (at a recording speed of 60 mm/min) from mid-June to the end of August 1984 (see Appendix A).

Instrumentation. The majority of portable seismographs deployed as part of the EWP-84 experiment were analog instruments of the smoked-paper type (Sprengnether Model MEQ-800). Vertical-component, 1-second-period seismometers were used throughout. For six of the USBR stations (JV1-JV6, Figure 2 and Appendix A), signals from remote sites were telemetered by radio to two recording sites where data were recorded on groups of smoked-paper-type recorders. Analog recordings for the portable seismographs were made at speeds either of 60 mm/min or 120 mm/min. Crystal clocks were synchronized with WWV radio signals for accurate time reference.

In addition to operating smoked-paper type seismographs, each of the research groups deployed a small number of digital-event-recorders (DER's) with 1-second seismometers for supplemental recording of waveform data. The University of Utah deployed three DER's fabricated at the U of U, each in a three-component mode. Two temporary telemetry stations installed by the U of U (stations TTUT and SPUT, Figure 2 and Appendix A) were of the standard short-period type, also with 1-second, vertical-component seismometers.

METHODS OF ANALYSIS

Velocity structure. Upper-crustal velocity structure was specially investigated for the EWP-84 study area to provide a refined velocity model for the accurate location of seismic events. The model is based on available results from high-resolution seismic-reflection profiles and borehole sonic logs. Fortunately, the geological make-up of the study area involves a nearly horizontally-layered stratified section of sedimentary rocks (see Figure 6). With the exception of the 750-900 m vertical displacement on the Joes Valley fault zone, fault displacements in the EWP-84 study area are in the range of a few hundred to a few tens of meters or less as noted eariler.

McKee (1982) developed a simplified one-dimensional velocity model for the upper-crust in the eastern Wasatch Plateau by extrapolaton from the Book Cliffs area, 60 km to the east, where reversed refraction profiling had been carried out by Tibbetts and others (1966). Assuming local datums of 2,750 m and 2,850 m above sea level for parts of the eastern Wasatch Plateau, McKee's (1982) upper-crustal velocity model has a layer 3.75 km thick with P-wave velocity, V_p, of 4.3 km/sec, overlying a layer more than 20 km thick with V_p=6.0 km/sec.

Figure 7 shows the location of high-resolution seismic-reflection profiles in the East Mountain area contracted by Utah Power and Light

Co. and completed during 1980-82. The profiling involved frequencies up to 256 Hz, 6-12 fold coverage, 50-ft trace spacing, and penetration to 2.0 sec or roughly about 1,800 m below a datum 2,900 m above sea level. From stacking velocities reported for the profiles, vertical interval velocities were approximated for this study by the commonly-used Dix solution (e.g., Lindseth, 1982, p. 8.14).

Figure 8 summarizes the interval-velocity data derived from the high-resolution reflection profiling. A relatively steep velocity gradient within the uppermost kilometer is apparent. At depths below about 1 km, the vertical interval velocities are judged to be unreliable because the reflection profiling involved relatively small offsets. Under these circumstances, travel paths for reflections from deeper horizons approach the vertical leading to large uncertainties in resolving vertical interval velocities for the deeper layers (e.g., Lindseth, 1982). Accordingly, velocities for 1.1 km to 5 km below datum were determined from sonic logs of the Texas International Petroleum #41-33 well, which is located in the southern portion of the study area (Figure 7). These logs were examined to determine vertical velocity changes. A mean value of velocity was estimated visually from the sonic curve for discrete intervals ranging in thickness from 5 to 250 m for which the curve could be approximated by straight-line segments. From these velocities an average velocity, over a specific depth, was calculated by summing the interval travel times, corresponding to each mean value velocity, and dividing by total depth.

The mean-value velocities for the discrete intervals varied less than 35% over the total depth for each average velocity. From a depth of 3.78 km below datum to 4.04 km below datum the interval velocity was constant so an average velocity was not calculated.

Figure 6 summarizes the combination of interval-velocity and sonic-log velocity data from which a generalized velocity model was developed for the study area. In the upper part of the figure, the stair-step profile represents an approximation of mean values of the velocity gradient documented in Figure 8 to a depth of 1.0 km below datum. Below that depth, interval velocities are generalized from the sonic-log data, as described above.

McKee (1982) empirically determined ratios of P-wave to S-wave velocities from local earthquake travel-times in the Gentry Mountain and East Mountain areas. For the common assumption that Poisson's ratio equals 0.25, V_p/V_s is equal to 1.73, which is the average of values of 1.69 and 1.76 determined by McKee (1982) for the Gentry Mountain and East Mountain areas, respectively. Accordingly, Poisson's ratio is simply assumed equal to 0.25 to derive corresponding S-wave velocities from the P-wave velocity structure. The following velocity model (with datum=2,900 m above sea level) is thus assumed as a good approximation for the study area:

Depth below datum (km)	P-wave velocity(km/sec)	S-wave velocity (km/sec)
0.0-0.1	2.40	1.39
0.1-0.2	2.70	1.56
0.2-0.3	3.00	1.73
0.3-0.4	3.30	1.91
0.4-0.6	3.60	2.08
0.6-0.8	3.80	2.20
0.8-1.94	4.04	2.33
1.94-2.38	4.40	2.54
2.38-3.78	4.84	2.79
3.78-4.04	5.81	3.35
4.04-	6.18	3.57

From well logs, stratigraphic columns, and formation thickness in the eastern Wasatch Plateau (Hinze, 1973), the following velocity discontinuities are attributed to formation boundaries: the discontinuity at 1.94 km below datum is interpreted to be the contact between the top of the Dakota Sandstone and the base of the overlying Mancos Shale; that at 2.38 km below datum, the boundary between sandstones and shales of the Morrison Formation and the Entrada Sandstone; and that at

3.78 km below datum, the boundary between sandstones and siltstones of the Moenkopi Formation and the Kaibab Limestone.

Hypocentral resolution. Hypocentral locations were calculated with version 1 of the computer program HYPOINVERSE (Klein,1978), an earthquake location program which uses a generalized inverse method. Inputs to the program include: P and S arrival times accurate to +-0.1 seconds, station locations, and a crustal velocity model. Version 1 of HYPOINVERSE accepts a crustal velocity model with homogeneous layers. The outputs of this program which will be of interest here are:

1) the year (YR), day (DATE) and origin time (ORIG TIME), in Universal Coordinated time;

2) location coordinates in degrees and minutes of north latitude (N-LAT) and west longitude (W-LONG);

3) depth (DEPTH) in kilometers below datum;

4) a local magnitude (MAG; see Magnitude estimation);

5) total number of P- and S-wave arrival times (N);

6) GAP, the largest azimuthal separation between stations, measured from the epicenter;

7) DMIN, the epicentral distance in kilometers to the closest recording station;

8) ERZ and ERH, which are simplified errors derived from the lengths and directions of the principle axes of the error ellipsoid; and

9) RMS, the root-mean-square error of the travel time residuals determined by the equation

$$RMS= ((W_i R_i)^2/N)^{0.5}$$

where, R_i is the observed minus the computed arrival times of the P, S, or

S-P data at the i-th station; W_i is the relative weight given

to the i-th station (0.0 for no weight through 1.0 for full weight)

for the type of data (P, S, or S-P); and N is the total number

of P- and S-wave arrival times.

(The RMS error reflects both systematic and random errors. Because

random errors are usually smaller than systematic errors the RMS

is a measure of incompatibility of the velocity model and poor

picking and timing errors.

The issue of focal-depth resolution is critical to investigating the association of earthquakes with mining activity in the East Mountain area and for reliable focal mechanisms. The depth solution obtained from HYPOINVERSE depends on many factors, a critical one being the distance to the closest station. As a rule, the depth solution is assumed accurate when there is a station located within one focal depth of the epicenter. The standard program output for the error estimate for depth is a statistical measure and is an imperfect measure of accuracy. Other output parameters such as GAP, and ERH give an incomplete indication of the reliability of the true depth solution. For these reasons special efforts were made to analyze selected earthquake locations for the uniqueness and stability of hypocentral-depth determination. The procedure used follows Johnston et al. (1984). Each event was located with HYPOINVERSE using a range of fixed depths incremented from 0.01 to 20.0 km below datum. Incremental steps varied from 0.2 to 0.5 km and were selected to sample and bracket velocity intervals and steps in the adopted velocity model. RMS travel-time residuals taken from the range of hypocentral solutions were plotted as a function of the fixed focal depth (see Figure 9a). Next, the same seismic events were processed again with HYPOINVERSE using the same range of incremental depths as trial focal depths, but with the focal depth unconstrained allowing an iterative focal-depth solution to be determined. Figure 9b illustrates the result of such a procedure in which the final focal depth is plotted as a function of the trial or starting depth. Apart from special testing, the trial depth was routinely set at 4.0 km for general processing.

Detailed information provided by results such as in Figure 9 allow the evaluation of the uniqueness of a minimum in the RMS function and also the stability of a focal-depth solution as a function of trial focal depth. Where there is a distinctive minimum in the former and stability in the latter (as in Figure 9) one can be confident that the solved focal depth is reliable and not an artifact of either an arbitrary trial focal depth or discontinuities within the assumed velocity model.

Magnitude estimation. Total signal duration, from P-wave onset to the point where the coda amplitude decreases to the pre-earthquake level, was used as an estimator of earthquake size. Signal durations measured on helicorder seismograms for station TTUT, one of the temporary telemetry stations operated by the U of U, are the most reliable link to the calibrated scale for coda-magnitude estimates of local magnitude (M_L) developed for the University of Utah's regional seismic telemetry network. The relevant equation determined by Griscom and Arabasz (1979) for multiple measurements of coda duration from the U of U seismic network is:

$$M_L = -3.13 + 2.74 \log \tau + 0.0012 \Delta \qquad (1)$$

where $\log \tau$ is the average logarithm of total signal duration measured in seconds from P-wave onset, and Δ is the average epicentral distance in kilometers. The standard error of estimation is 0.27. Because coda-magnitude scales cannot be extrapolated below about $M_L = 1.5$ without special calibration (e.g., Bakun and Lindh, 1977), magnitudes less than 1.5 indicated in this report cannot be considered reliable.

The smaller values do, however, provide some measure of relative size.

Throughout the analysis of the EWP-84 data, a measure of signal duration was consistently documented together with every P-wave arrival. In general, there appears to be a consistent relation between signal durations measured on the smoked-paper seismograms and those measured on seismograms for station TTUT. The TTUT measurements are greater, on average, by a factor of 1.5 to 2.0 than those for the smoked-paper seismograms, which would cause magnitude estimates based on the latter and equation (1) to be systematically lower by 0.2 to 0.3 of a unit of magnitude compared to station TTUT. Therefore all magnitudes listed for the 1984 data set were calculated from the duration of the event at station TTUT.

Fault-plane solutions. Unless specified otherwise, fault-plane solutions were attempted only for events with well constrained focal depths. Two methods were employed. The first was the standard stereographic projection of P-wave first motions. For selected events with appropriate data, attempts were made to apply the method of Kisslinger (1980), which involves the inversion of SV-to-P amplitude ratios as measured on vertical-component seismograms. Procedures for application of the latter technique are described in detail by Arabasz and Julander (1986).

Fault-plane solutions based on P-wave first motions are susceptible to systematic error because of sensitivity to focal-depth error and velocity structure. This often results because of interpretive bias when nodal planes are determined by "eye-ball" fitting. Special efforts that were used to address uncertainty in focal depth and velocity structure have already been described. To minimize bias in nodal-plane determination, the computer algorithm FOCPLT, developed by Whitcomb and Garmany (Whitcomb, 1973), was acquired and implemented at the University of Utah by J.C. Pechmann. As described by Pechmann (1983, p. 27), FOCPLT "...tests a grid of trial mechanisms spaced at approximately 5 degree intervals on the focal sphere and then chooses a mechanism which minimizes the number of first motion readings in error. Less reliable readings are given half the weight of other readings, and a linear function is used to downweight stations within 3 degrees of a nodal plane."

OBSERVATIONS

General remarks. A total of 475 seismic events were located and used for the analysis in this study. The entire data set was scrutinized to obtain a subset of 201 well-located events meeting the following criteria (see Methods of Analysis): (1) N > 5 (2) GAP < 250 degrees (3) RMS < 0.40 sec (4) ERH < 2.0 km (5) ERZ < 2.0 km. This subset of events will be referred to as subset A. Subset A encompasses a 37-day period from July 6 to August 11, 1984.

Epicentral pattern and focal-depth distribution. Figure 10 shows the epicenters of all 475 seismic events located in this study from the EWP-84 data set; the largest magnitude is 2.0. A first-order feature of the epicentral pattern is the intense clustering of seismicity in the vicinity of East Mountain. There is a discrete secondary cluster in the Gentry Mountain area, which was the target of separate study by the WWC group. Outside the East Mountain and Gentry Mountain mining areas, seismicity is scattered along and to the east of the plateau escarpment. West of the mining areas the epicentral density decreases rapidly, but scattered epicenters locate along the Joes Valley fault zone. The 201 epicenters of subset A are shown in Figure 11 with respect to the same base map as Figure 10. The requirement for good azimuthal control has effectively screened out the majority of events east of the escarpment and outside the local seismic network. Those epicenters should not be considered reliable. The remaining seismic events now to be discussed in more detail are those with epicenters clustered on East Mountain and the two located within Joes Valley.

The seismicity concentrated beneath East Mountain was first analyzed to check the temporal correlation of seismic occurrence with active mining. A two-week vacation shutdown of the Deer Creek and Wilberg mines from July 7 at 00:00 to July 23 at 24:00 (GMT) was bracketed by two weeks of seismographic recording before the shutdown and by two weeks of subsequent recording after mining activity resumed. Station TTUT, located on East Mountain, provided continuous recording from June 1, 1984, through August 30, 1984. Figure 12 is a histogram of the number of events of magnitude greater than or equal to 1 recorded by station TTUT during a total period encompassing two weeks prior to the mining shutdown, two weeks of no mining activity, and two weeks of subsequent mining activity. Note that the seismic activity does not completely cease during the mining shutdown period and at least in part compares to the level of activity before the shutdown.

To investigate the spatial correlation of seismic activity with active mining, epicenters of subset A were superposed on detailed maps of the Deer Creek and Wilberg mine workings, respectively shown in Figures 13 and 14. The areas of active coal extraction from June 15 to August 31, 1984, are specially indicated in each figure. Note that the Wilberg Mine is located approximately 50 m below the Deer Creek Mine. Circles of radius 900 m, corresponding to the mean epicentral precision plus two standard deviations, were drawn about each site of active mining. The majority of the seismicity in map view correlates with the active mine faces. In one exception near the bottom of Figure 13, there is a group of events which do not correlate with active mining. Of these events, 67 percent occurred during the mining shutdown, but during the shutdown scattered events also occurred in the circumscribed areas. Depth distribution will next be considered.

A process of rigorous focal-depth testing was performed on subset A to verify focal-depth reliability for as many events as possible. One of the most important criteria for these data was the epicentral distance in kilometers (DMIN) to a station closest to the event. Criteria to be met were: N>= 5, GAP <= 200, and RMS <= 0.25 second. Next, for each qualifying event an analysis of RMS versus depth and focal-depth stability was completed (see Methods of Analysis). Events for which an RMS minimum and focal-depth stability could be established were grouped into another subset. This refined subset containing events whose focal-depth reliability has been rigorously tested will be referred to as the "best" subset.

Figure 15 shows cross-section views, keyed to Figure 11, of hypocenters belonging respectively to subset A (Figure 15a) and its corresponding subset having "best" focal depths (Figure 15b). First the "best" foci are considered. Disregarding for the moment the focal-mechanism information, Figure 15b shows concentrated foci within 0.5 km below mine level. There are relatively few accurately located foci above mine level, but the constraints of this subset must be emphasized. Because of the average station spacing of 2.5 km and the criteria for focal depth relability, very shallow focal depths are not well controlled. As discussed previously, a more dense network would have been required to achieve good focal-depth precision above mine level. None of the foci in Figure 15b below the mine workings are deeper than 1.5 km below datum. Deeper foci lie to the west corresponding to the two Joes Valley events, whose reliable depths of 3.0 km and 4.4 km imply that they are tectonic earthquakes.

Given the relatively small number of events in the "best" subset, all data of subset A are next plotted for comparison in Figure 15a. Obvious differences with Figure 15b are the clustering of very shallow events above mine level and location of foci beneath mine workings in the 2 to 3 km depth range below datum. In both plots the majority of sub-mine seismicity lies within 1.0 km of mine level. The deepest reliably located event is at a depth of 4.4 km. The location of the top of the Navajo Sandstone is shown in figure 15 for reference. If a detachment surface lies close to that level (see Figure 4), then only a single event has been located below it.

Fault-plane solutions. One of the primary objectives of this report was stated to be the determination of focal mechanisms for seismic events at mine level, below mine level, and extending laterly outside the mining area. Background information on previous results and the need for mapping areal changes in stress orientation (see Figure 3) was presented in the Introduction.

The following basic strategy was used. First, attention was placed on the subset of seismic events in the "best" focal-depth group. These foci included events clustered in the immediate vicinity of East Mountain together with the two earthquakes in Joes Valley. Thus it was straightforward to consider them in cross-section view (as done in Figure 15b) along the line of section shown in Figure 11. Some seismic events were later selected from the remainder of subset A (Figure 15a) to gain additional information on focal mechanisms for the relatively deepest events directly below the area of mining. Finally, another group of seismic events was selected, chiefly from subset A, to study a class of events having all dilatational first motions.

A total of seventeen single-event and two composite fault-plane solutions were determined. Epicenters for the corresponding events are labeled in Figure 11; all lie within 3 km of the line of section. In addition to data illustrated in the following text, Appendix B contains a summary of hypocentral information for the 19 fault-plane solutions, stereographic plots for solutions 1-13, and data for RMS and depth-stability tests for selected earthquakes.

All fault-plane solutions herein are equal-area, lower-hemisphere sterographic projections of the focal sphere. Filled-in circles correspond to compressional first motions; open circles indicate dilatational first motions. With the exception of solution 2e (Figure 17e), which was determined with the computer program AMPRAT, all solutions were determined with the computer program FOCPLT (see METHODS OF ANALYSIS). For the FOCPLT solutions, triangles indicate the locations of the P-axis, T-axis, and the alternative slip vectors (corresponding to the poles of the auxiliary nodal planes). The P-axis and T-axis respectively bisect the dilatational and compressional quadrants of the focal sphere.

Figure 15b gives an overview of focal mechanism data for the "best" focal depth set. This includes (1) five fault-plane solutions sampled from the 0.6 km to 1.0 km depth range at or slightly below mine level, (2) two solutions for events roughly one km below mine level, and (3) two solutions for deeper earthquakes west of the mining area. The two deepest events shown on the left of Figure 15b locate beneath Joes Valley (Figure 11). Figure 16a shows the first-motion information for solution 1 at its free depth of 3.0 km. This solution shows oblique slip with a predominance of normal faulting. To test the sensitivity of the solution to focal depth, and hence velocity structure, alternative solutions were determined by fixing the depth at 3.1 km (Figure 16b), 2.3 km (Figure 16c), and 3.7 km (Figure 16d). The first two alternatives (b,c) indicate the predominance of normal faulting, but the third (d) involves a significantly different pattern of take-off directions on the focal sphere corresponding to critically-refracted ray paths. The resulting focal mechanism (Figure 16d) has reversed quadrants such that the mechanism is compressional with nearly pure reverse slip on either nodal plane. From the results for the nearby second earthquake in Joes Valley, presented next, one can argue that the normal-fault-type solution for this first earthquake is more likely.

Solution 2 (Figure 17a) is for the 4.4-km-deep event beneath Joes Valley and shows a normal-faulting mechanism with nearly pure dip slip.

Again, to test the sensitivity of the solution to focal depth, alternative solutions were determined assuming focal depths of 5.0 km (Figure 17b), 3.5 km (Figure 17c), and 2.5 km (Figure 17d). The consistency of a normal-fault-type mechanism is apparent, with slightly rotated, but generally northerly-trending nodal planes. An independent fault-plane solution for this same event was determined from SV/P amplitude ratios, using the computer algorithm LAMPRAT. Figure 17e shows the result of this procedure. The solution violates a few of the first-motions but is consistent with the previous results in that the focal mechanism has a dilatational cap. The consistency of a normal-fault-type mechanism between 2.5 km and 5.0 km makes it unlikely that the compressional alternative for solution 1 at 3.7 km depth (Figure 16d) is valid. The free-depth solutions of normal-faulting type (solutions 1a and 2a) are preferred.

In Figure 15b thirteen events in the outlined box range in depth from mine level (0.60 km) down to 1.0 km. Five fault-plane solutions for events sampled from this box are systematically shown as solutions 3 through 7 (see Appendix B). In general, mechanisms 3-6 are consistent in that all are compressional mechanisms with an implied predominance of reverse slip on planes of moderate dip. Solution 7, a composite of seven events at 0.6 (+,- 0.1) depth is of the same type. Inconsistency of these events is seen in the fact that they have divergent orientations of P-axis, presumably approximating the direction of maximum horizontal compression.

Solutions 8 and 9 in Figure 15b show a contradiction in the first-motion quadrants. Solution 8 has a free depth of 1.4 km. The data quality is good and there are no first motions in disagreement with the solution (Appendix B). To test the stability of the mechanism to focal depth, the depth sequentially was held at depths of 0.6 km, 1.0 km, 1.6 km, and 2.0 km. The resulting mechanism was consistently compressional, with only minor change in P-axis orientation for each depth (see Appendix B).

Solution 9 (Figure 15b, Appendix B.) is a composite of two events, each well constrained to be at 1.5 km depth. This solution was also analyzed for its sensitivity to focal depth. The focal mechanism stays dilatational for depths of 2.0 km, 1.6 km, 1.4 km, and 1.0 km. At a fixed depth at 0.6 km, however, the focal mechanism becomes compressional, showing a change in the pattern of take-off directions on the focal sphere. The data of Figure 15b show convincing evidence for compressional-type mechanisms at or slightly below mine level. Whether or not there is a change in stress orientation below mine level cannot be simply resolved by solutions 8 and 9, although solution 8 of the compressional type is more reliable.

Next, focal mechanism information was added from subset-A events in the 2 km to 4 km depth range below the mining area (Figure 15a). The focal depths for these events are not strictly as reliable as for the "best" set, but the solutions are informative. Four events beneath the mining area in Figure 15a between 2.3 km and 3.4 km depth had an adequate number of first-motion observations and were systematically tested for focal-depth relability. Results presented in Appendix B show variable quality in terms of distinct RMS minima and focal depth stability. Event 11 at 2.7 km depth has the highest-quality focal depth; for the other three events the depth stability was good, but RMS-versus-depth profiles would allow events 10 and 12 to have a depth less than 1 km, while event 13 might be as shallow as 1.7 km. The resulting fault-plane solutions (10 to 13) for the free focal depths are schematically shown in Figure 15a. As a group the mechanisms are consistent and of compressional type. Alternative fault-plane solutions for a range of focal depths are included in Appendix B. For each event the mechanism is not sensitive to depth. Solution 11 at 2.7 km depth and solution 13 at 3.4 km depth (perhaps as shallow as 1.7 km) provide a good basis for inferring reverse-type faulting 1 km to 2 km below mine level. Solutions 10 and 12 show the same type mechanism but their precise depth location must be considered uncertain.

Dilatational mechanisms. An unexpected result of the data analysis for this thesis was the observation that a significant number of located events appeared to have ubiquitous, dilatational P-wave first motions. A similar result was observed by the WCC group for data in the Gentry Mountain area. There, only about three events out of more than 200 located in that mining area had mixed first motions, and those were not of high quality (I.G. Wong, Woodward-Clyde Consultants, personal communication, 1985). The observations are puzzling but similar to observations made by Kusznir and others (1980) in a study of longwall coal mining in England where the source mechanisms were interpreted to be implosional. The question to be here is whether observations are clearly inconsistent with a double-couple source mechanism.

The events with ubiquitous dilatations were scrutinized to investigate their occurrence. Of the 475 events in the total data set, each one with more than five P-wave first motions that were all dilatational was classified as a beta event. It was found that the beta events made up 25% of the classifiable events located during the mining shutdown and 33% of the classifiable events located during active mining. The beta events were found to have a median and maximum magnitude of 0.8 and 1.8, respectively. For comparison, the non-beta events had a median and maximum magnitude of 0.5 and 2.0, respectively. The two groups thus do not differ significantly in size.

Beta events which satisfied the following criteria were analyzed for their spatial distribution: N >=5, GAP <=200, RMS <=0.5, ERH<=2.5, ERZ <=9.0. Figure 18a shows a stereo-pair plot (keyed to Figure 10) of foci for such beta events located in the East Mountain area. For comparison, another stereo-pair plot is shown in Figure 18b of non-beta events from the some area that belong to subset A. In Figure 18 the horizontal plane drawn within the box is at mine level. For perspective, the foci shown in Figure 18 are basically the same as shown in map view in Figure 13 and 14 where comparison can be made with the areas of active mining.

As a matter of observation, the majority of the beta events locate just below or above mine level. Three of the beta events are included in the "best" located data set. Event 8407240109 has a well constrained depth of 0.7 km, and events 8407250244 and 8407250908 have well constrained depths of 1.2 km. There appears to be two differences in the distribution of beta events compared to the non-beta events. First, the beta events cluster more distinctly in the eastern part of the sample area, corresponding to the most excavated parts of the Deer Creek and Wilberg Mines (Figures 13 and 14). Second, there appear to be more beta events than non-beta events in the southeastern part of the sample area. These observations will be returned to later.

To investigate the source mechanisms for the beta events, focal-mechanism plots were made for all such events included in Figure 18a that had 13 or more first motions. Of seven such events, focal mechanisms are shown for six in Figures 19 and 20 (solutions 14 through 19). (Corresponding hypocentral information is included in Appendix B.) A seventh event was disregarded because its hypocentral depth error was very large. Each of the remaining six events has a free depth at or above mine level; ERZ for these events range from 0.3 km to 2.2 km. DMIN for these events is of the order of 1 km to 3 km (Appendix B), so there is obvious uncertainty in such very shallow focal depths.

In Figures 19 and 20, pairs of fault-plane solutions are shown for each of the six beta events. The solution on the left in each pair corresponds to the free-depth hypocentral location; that on the right, to a fixed-depth location. The reason for the fixed-depth alternative was this. Five of the free-depth locations are above mine level, so the choice was made to test a solution at mine level where anomalous mechanisms might be conceivable. The sixth event, on the other hand, located coincidentally at mine level, so a shallower fixed depth was tried.

The most striking observation of Figures 19 and 20 is that for every mechanism above mine level, the first-motion pattern can be fit by a double-couple mechanism with not a single inconsistent first-motion reading. In every such case the implied mechanism is one reflecting normal faulting with nearly pure dip slip. The implied T-axis orientations, however, are variable. For the corresponding solutions at mine level, four of them (solutions 14b, 15b, 16b, and 17b) show inconsistency with a double-couple interpretation, but one might still argue that the discrepancies do not preclude a double-couple interpretation. If these mechanisms are double-couple, the cap of the focal sphere would be compressional in each case, consistent with the earlier observations for events with mixed first motions at or slightly below mine level. Solutions 18b and 19a are different from the other four at mine level in that the cap of the focal sphere is dilatational. Both imply oblique slip with a predominance of normal faulting.

DISCUSSION

Mining-related seismicity. Previous studies (McKee, 1982; McKee and Arabasz, 1982; see also Osterwald et al., 1971, Wong, 1984, 1985) have established the association of intense microseismicity with underground coal mining in the eastern Wasatch Plateau. For relevant discussion on the relationship of seismicity and coal mining in the Sunnyside coal mining district, 60 km to the east of the Wasatch Plateau, the reader is referred to Smith et at. (1974), who also summerizes earlier work in that area. The triggering of seismic strain release in the immediate vicinity (within 100's of meters) of mine workings is well documented (e.g., Gay and Wainwright, 1984). In the eastern Wasatch Plateau seismicity occurs at distances of kilometers both laterally and vertically from the mines. This seismicity is thought to be the result of slip on faults that are pre-stressed by the existing tectonic environment (Osterwald et al.,1971; Wong, 1984, 1985).

Two dimensional finite element modeling of in-situ stress changes for a typical Wasatch Plateau - Book Cliffs coal mine was performed by Wong (1985). The model is for a 3-meter-thick coal seam with equally spaced pillars, overburden thickness of 610 meters, cliff topography and rock properties appropriate for the geologic make-up of the eastern Wasatch Plateau, and an ambient tectonic horizontal stress of 256 bars obtained from an in-situ stress measurement in the Sunnyside district. Important results of the modeling include: (1) large compressive stress concentrations of up to 700 bars in and near pillars and mine faces; (2) changes in the vertical stress on the order of a few bars or less at depths of 1 to 3 km below the mine workings, sufficient to trigger slip on tectonically pre-stressed reverse faults: and (3) prediction that sub-mine seismicity should predominate beneath and toward cliff topography due to reduction in lateral support. Wong (1985) concludes that the combination of topography, tectonic stress field, pre-existing faults beneath mine workings, and mine-induced stress changes could explain the occurrence of the intense seismicity observed in the eastern Wasatch Plateau.

The results of this study contribute to understanding the mining-related seismicity in the eastern Wasatch Plateau. Again, however, the 1984 field recording in the East Mountain area was not designed for fine spatial resolution at the level of mine workings. Some comment can be made about the temporal variation of seismicity with active mining. During the period of the EWP-84 experiment, recording bracketed a vacation shutdown of the mines. It was found that the number of seismic events per day did decrease the first few days of the mine shutdown, but returned to a level equal to that prior to the shutdown before mining resumed. In at least one area more than 1 km distant from sites of active coal extraction, more seismic events were located during the mining shutdown than during a longer period of active mining. For the East Mountain area, it seems that there is not a simple one-to-one relationship between the timing of mining and the occurrence of seismic events. In a study of the Gentry mountain ates by Osterwald et al. (1971), it was observed that shallow-focus tremors which originated within or near the mining area were actually more frequent on days when no mining was done.

The issue of spatial correlation of seismicity with mining was addressed at least with respect to map view in Figures 13 and 14. Taking into account the average horizontal error of location, the majority of seismic events have epicenters that correlated with sites of active coal extraction. Seismic events are closest and most densely clustered about the mine site DC-A in Figures 13 and 14. This can be explained if the mean ERH of this circumscribed group of events is compared to the other groups. For the events surrounding mine site DC-A, the mean ERH was equal to 0.35 km; for the set of seismic events in the other circumscribed groups, 0.51 km. Another contributing factor relating to epicentral scatter could be the following. Mine sites W-A, W-B, and DC-B are all within parts of the Wilberg and Deer Creek Mines which are honeycombed with mined-out areas. Mine site DC-A, on the other hand is in a distal part of the mine workings. The relative amounts of coal extraction during the recording experiment might be an additional contributing factor. Between June 15 and August 31, 1984, the approximate totals of coal extraction were: 64,000 yd^3 for mine site DC-A, 110,000 yd^3 for DC-B, 120,000 yd^3 for W-A, and 190,000 yd^3 for W-B (D.W. Jense, Utah Power and Light Co., personal communication, 1985). The volume of coal extraction at DC-A, smaller by a factor of 2-3 compared to other sites, conceivably could have resulted in a smaller area of stress redistribution.

Accurately located foci had depths ranging from mine level down to 1.5 km below datum, with the majority of well located events in the 0.6 km to 1.0 km depth range (Figure 15b). The apparent paucity of events at mine level both in Figures 15a and 15b could have several explanations, the first being the issue of station spacing. In Figure 13, note that the seismograph stations (indicated by triangles) systematically are on the order of a kilometer away from most of the seismic events. Therefore, focal depth resolution for events at mine level would generally not be adequate to meet the qualifying criteria imposed on the "best" data set. A second issue might be the typical spectral content of events at mine level. If they are predominately very-high-frequency seismic events with characteristic frequencies in the kHz range (e.g., Hardy, 1975), then they would not be well recorded at distances of kilometers by the seismographs used in this experiment (see also Smith et al., 1974 regarding similar discussion for a recording experiment in the Sunnyside district).

Source mechanisms for the seismic events located at or below mine level were overwhelmingly of the compressional type with the exception of the beta events with ubiquitous dilatational P-wave first motions. These events are puzzling, but their distribution of first motions suggests a working hypothesis to explain their occurrence. Figures 19 and 20 show that the majority of the beta events can be fit with a double-couple normal-faulting mechanism if they in fact occur above mine level. Such a mechanism could reflect subsidence in the overburden above the mine workings. The concentration of the beta events in the eastern part of the mine workings (Figure 18a) where mined-out areas predominate would be consistent with this hypothesis. If the beta events are in fact at mine level, the majority of their alternative fault-plane solutions are of the compressional type, which would agree with the fault-plane solutions for the non-beta events.

Because of the uncertainty in the focal depths for the beta events, whether they occur above or at mine level cannot be totally resolved here. Future experiments clearly should involve the positioning of seismograph stations directly above mining activity at the time so that the first motions recorded at overlying stations would be for upward-traveling rays. This would preclude ambiguity as to the type of quadrant for the cap of the focal sphere. Hence, there would be no argument for distinguishing normal-faulting above mine level from reverse faulting at mine level due to variations of take-off directions as a function of assumed focal depth. In this regard the presence of a near-surface high-velocity gradient in the East Mountain area has critical control on take off directions plotted on the focal sphere. Figure 19 and 20 show how alternative focal depths differing by only 500 m can lead to radically different first-motion patterns.

Seismotectonics. The results of this thesis are relevant to the general seismotectonics of the eastern Wasatch Plateau insofar as they relate to (1) correlation of seismicity with geologic structure, and (2) spatial mapping of stress orientation. The majority of the seismicity located in this study appears to be mining-related and does not correlate simply with mapped faults (Figure 10). Focal mechanisms of reverse faulting type for the seismicity at and below mine level poses the further problem of incompatibility with normal faults exposed at the surface. Outside the mining area, only a few earthquakes were reliably located during this experiment (Figure 11). Correlation with mapped faulting relies on the compatibility of fault type and trend with observed focal mechanisms, as in the case of two earthquakes with epicenters along the Joes Valley Fault Zone.

Figure 4 illustrates one possible scenario for "thin-skinned" horizontal extension in the Wasatch Plateau from interpretations of Standlee (1982) and Royse (1983). This figure shows nonpenetration of the detachment (located above the Navajo Sandstone) by post-Eocene normal faulting in response to the extension of upper-plate rocks above the detachment. Evidence for the existence of the detachment comes from subsurface geophysical exploration of the Castle Valley area, along the eastern margin of the Wasatch Plateau where a system of eastward thrusting dies out just below the surface. Arabasz and Julander (1986) note that the Navajo Sandstone appears to coincide with the lower bound of clustered shallow seismicity located by McKee (1982) beneath the area of active mining in the East Mountain area. They postulate that a detachment structure above the Navajo Sandstone could conceivably exert an important influence on the depth distribution of sub-mine earthquakes.

If a regional detachment extends beneath the eastern Wasatch Plateau, then faults of the Joes Valley graben likely cut it and penetrate to a greater depth. Evidence for this statement is found in the results of the earlier cited trenching by the USBR on the Joes Valley graben-bounding faults. Earthquakes required to generate surface displacements of the order of 1m to 5m would almost certainly be in the magnitude 7.0 +- 0.5 range (see Arabasz and Julander, 1986). Earthquakes of this magnitude moreover would likely nucleate near the base of the seismogenic layer (Das and Scholz, 1983), which is much deeper than the 3 km depth range where the detachment is hypothesized to lie. There is fragmentary but supporting evidence in this study that the Joes Valley faults are not truncated by a detachment at shallow depths. This is given by the earthquake located directly beneath the Joes Valley graben at a depth of 4.4 km, which is below the hypothesized detachment. Because all but one earthquake for this study located above the Navajo Sandstone, the seismicity provides little information as to whether a detachment exists at depth and influences the seismicity in the study area.

Special efforts were made to test the focal depths of the deeper earthquakes located by McKee (1982) in the depth range of 6 km to 15 km beneath the eastern Wasatch Plateau. After relocating these earthquakes with the velocity model determined for this study, and after applying tests for focal-depth stability, it appears that many of those deeper foci do not have a unique RMS minimum at the asserted depth.

Another seismotectonic issue is the lateral change in stress orientation documented within the limited bounds of the study area. The two Joes Valley earthquakes have well constrained normal-faulting mechanisms. This together with the observation of multiple Pleistocene-Holocene (?) normal movements on faults of the Joes Valley graben, imply an extensional stress state. The WNW-ESE orientation of T-axes for the

Joes Valley fault-plane solutions (Figures 16 and 17) is consistent with a mean orientation in the 102 degrees to 282 degrees direction of T-axes for fault-plane solutions in the BR-CP transition zone (Arabasz and Julander, 1986; see also Figure 3). Thus it is reasonable to infer that Basin-and Range extension extends at least as far eastward as the Joes Valley area.

Seismic events in the vicinity of East Mountain showed consistent compressional focal mechanisms down to depths of 1 km to 2 km (Figure 15b). Supplementary focal mechanisms (Figure 15a) allowed the interpretation of reverse-type faulting as deep as 3.4 km beneath the area of mining. These events are assumed to be occurring on faults that are pre-stressed by the existing tectonic environment (Smith et al., 1974; Wong, 1985). This would imply maximum principle stress in the horizontal direction, consistent with a compressional stress regime inferred for the Colorado Plateau Province (Zoback and Zoback, 1980). The combined results of Figure 15 provide key information for the spatial mapping of stress orientation. At depths of 3 km it requires a reorientation of maximum principle stress from the vertical (normal faulting) beneath Joes Valley to horizontal (reverse faulting) beneath East Mountain. This change must occur within 10 km to 15 km. Careful arguments were made earlier about the validity of reverse faulting mechanisms down to at least 2.7 km (below datum) beneath East Mountain. Thus it cannot be argued that the compressional stress state is due to a very localized field induced by mining.

CONCLUSIONS

Results of operation of a 20-station array of portable seismographs during the summer of 1984 in the East Mountain area provide a basis for examining (1) the association of seismicity with active underground coal mining, and (2) the seismotectonics of the Eastern Wasatch Plateau. Important results include the following:

1. From a set of 475 earthquake locations ($M \le 2.1$), a refined subset of 201 hypocenters was used for spatial correlation. Within their epicentral precision, the majority of seismic events correlate in map view with sites of active coal extraction during the recording period. Seismic events surrounding active sites in the older more mined out areas of the underground mine workings have more epicentral scatter than seismic events clustering about an active face in a distal part of the mine workings.

2. Well-located foci ranged from mine level (0.6 km below datum) to 4.4 km below a datum 2.9 km above sealevel. Abundant foci located above mine level are less reliable because of a station spacing of 2 to 3 km. An apparent paucity of foci at mine level may be due to the very high frequency character of seismic events occurring at mine level and their poor recording by the local seismic network. The majority of submine events locate within one kilometer below mine level. Two of the deepest events reliably located in this study are at depths of 3.0 and 4.4 km; they occurred west of the mining area beneath the Joes Valley graben.

3. During the period of the 1984 experiment, recording bracketed a two-week vacation shutdown of the mines. The number of seismic events per day decreased during the first few days of the mine shutdown, but returned to a level equal to that prior to the shutdown <u>before</u> mining resumed. In at least one area more than 1 km distant from sites of active coal extraction, more seismic events were located during the mining shutdown than during a longer period of active mining.

4. Ten of eleven fault-plane solutions for seismic events located at or below mine level are of compressional type and indicate a predominance of reverse faulting. Fault planes and corresponding P-axes for these events show variable orientation. A sizeable group of events recorded with all dilatational P-wave first motions are not necessarily indicative of a non-double-couple source mechanism. These events can be fit with consistent normal-faulting fault-plane solutions if their foci are located above mine level where subsidence in the overburden might be expected.

5. The two earthquakes reliably located beneath Joes Valley (see 2, above) display normal-faulting focal mechanisms in agreement with surface observations of multiple late Pleistocene-Holocene(?) normal fault displacements on faults of the Joes Valley graben. The WNW-ESE orientation of T-axes for these focal mechanisms agrees with previous results for fault-plane solutions within the Basin and Range- Colorado Plateau transition. Basin-range extension is inferred to extend eastward into the Wasatch Plateau as far as the Joes Valley area.

6. Within the bounds of the study area focal mechanisms provide constraints on spatial changes in stress orientation. Seismic events beneath the East Mountain mining area show consistent compressional focal mechanisms down to at least 2.7 km, arguing against a very localized stress field induced by mining. A lateral change in stress orientation is inferred from the Joes Valley area. At a depth of approximately 3 km there appears to be a reorientation of the maximum principle stress from the vertical (normal faulting) beneath Joes Valley to horizontal (reverse faulting) beneath East Mountain.

7. If a regional low-angle detachment structure exists beneath the Eastern Wasatch Plateau, then the faults of the Joes Valley graben are inferred to cut it and penetrate to greater depths. Supporting evidence for this comes from trenching by the U.S. Bureau of Reclamation along the Joes Valley graben, where single event displacements of up to 5 m were found. Such displacements are judged to be incompatible with truncation of the Joes Valley Faults at the 3 km depth of the detachment. The normal-faulting earthquake from this study located below the Joes Valley at a depth of 4.4 km is below the inferred detachment.

ILLUSTRATIONS

Figure

Figure

11. Seismicity map of subset A events. Epicenters for solutions 1-19 are shown. W-E cross-section line keyed to Figure 15.

12. Histogram of the number of events per day of magnitude greater than or equal to 1 recorded on station TTUT, from June 15 to Aug. 15, 1984.

13. Epicentral Plot of events from subset A superimposed on outline of the Deer Creek Mine workings. Squares represent active mine sites within the Deer Creek Mine, ovals, active mine sites within the Wilberg Mine. Circles drawn about each site correspond to the mean epicentral precision plus 2 standard deviations.

14. Epicentral plot of events from subset A superimposed on outline of the Wilberg mine workings. Squares represent active mine sites within the Deer Creek Mine, ovals are active mine sites within the Wilberg Mine. Circles drawn about each site correspond to the mean epicentral precision plus 2 standard deviations.

15. West-East cross-section (keyed to Figure 11) showing distribution of focal depths for subset A (a) and for "best" subset (b). Schematic focal mechanisms shown for solutions 1-13. Dilatational quadrants are white, compressional quadrants black (for single events), hachered (for composite events). Dashed line at top of (a) is the approximate topography.

16. Focal mechanisms for solution 1. Projections are lower-hemisphere, equal-area. Filled in circles represent compressions, open dilatiations. Triangles represent P-axis, T-axis and alternative slip vectors. Symbols h, represents focal depth, R, restricted fixed depth solution. Numbers are the strike and dip of the nodal planes.

17. Focal mechanisms for solution 2 at its free depth (a) and restricted depths (b,c,d), e is the AMPRAT solution at the free depth. Symbols as in Figure 16.

18. Plot of stereographic pairs for beta events (a) and non-beta events (b). Area covered is keyed to rectangle in Figure 10. Direction of view is north.

19. Focal mechanisms for solutions 14-17, beta events. Symbols as in Figure 16.

20. Focal mechanisms for solutions 18 and 19, beta events. Symbols as in Figure 16.

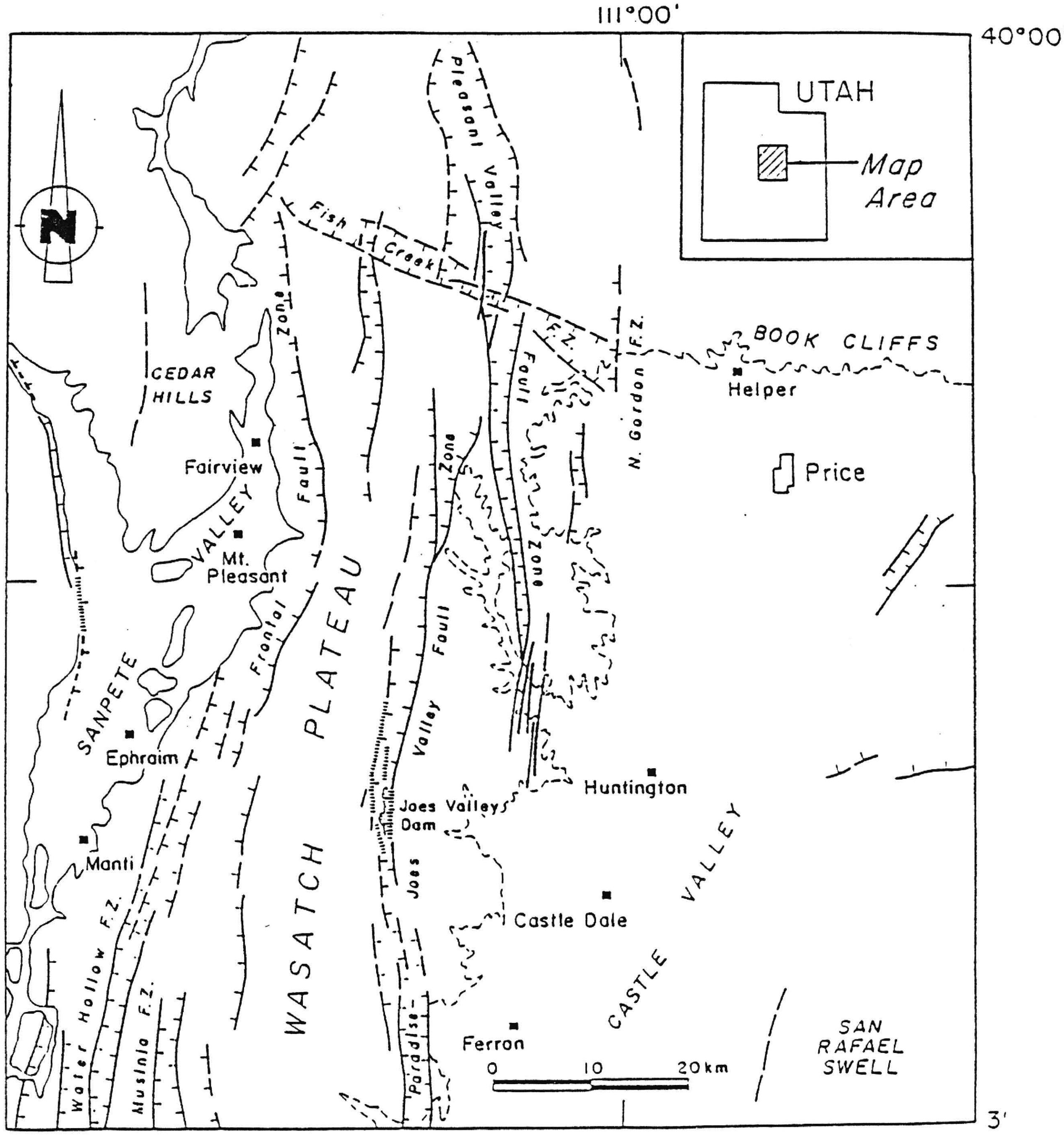
111°00'
40°00'
3'
UTAH
Map Area
CEDAR HILLS
Fairview
Mt. Pleasant
SANPETE VALLEY
Ephraim
Manti
Water Hollow F.Z.
Musinia F.Z.
Frontal Fault Zone
WASATCH PLATEAU
Fish Creek
Pleasant Valley Fault Zone
Joes Valley Fault Zone
Joes Valley Dam
Paradise
F.Z.
N. Gordon F.Z.
BOOK CLIFFS
Helper
Price
Huntington
Castle Dale
CASTLE VALLEY
Ferron
0 10 20km
SAN RAFAEL SWELL

Figure 1

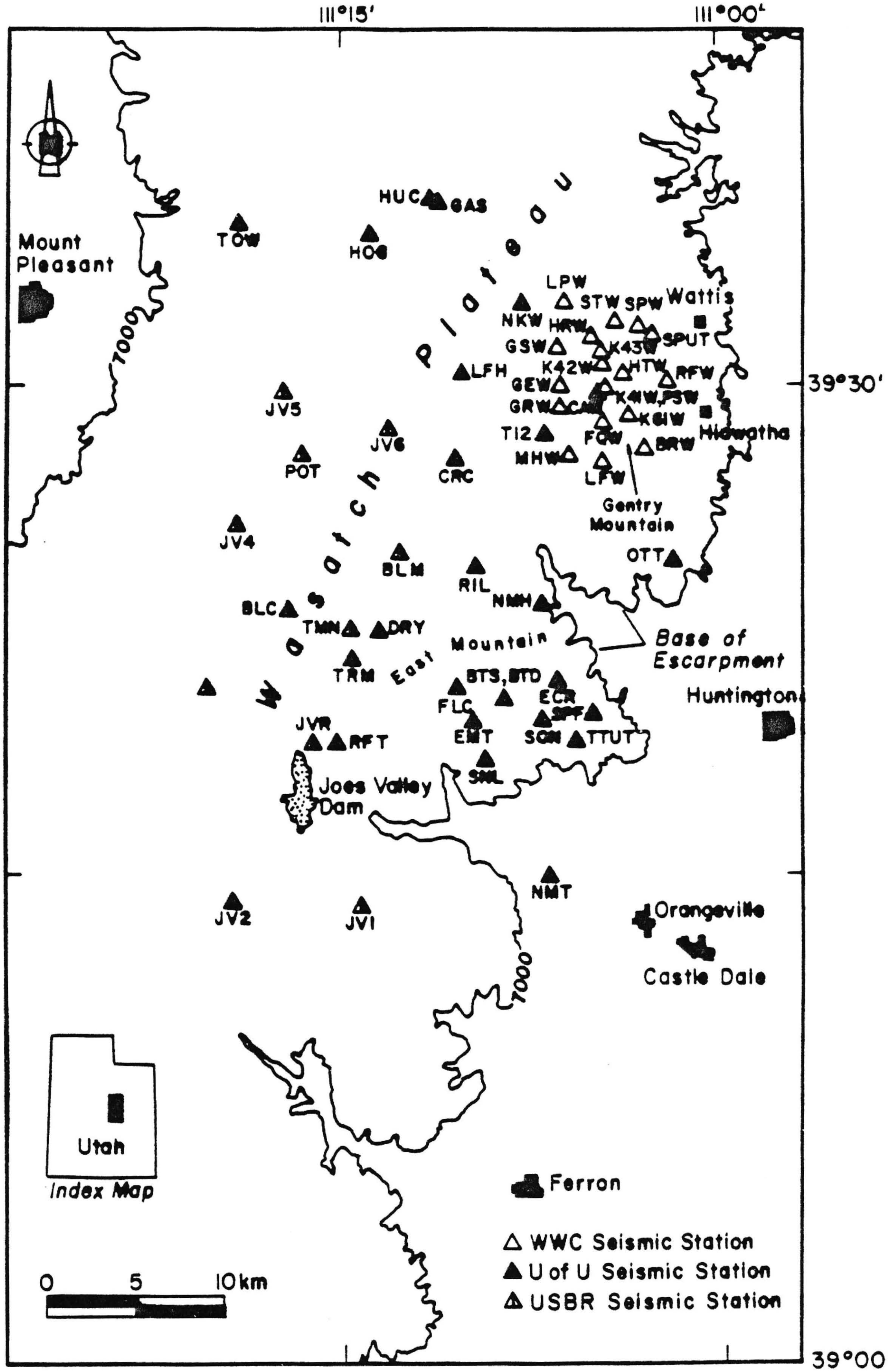

111°15'
111°00'
39°30'
39°00'
Mount Pleasant
7000
TOW
HOG
HUC
GAS
Wasatch Plateau
LPW
STW
SPW
Wattis
NKW
HRW
SPUT
GSW
K43W
LFH
K42W
HTW
RFW
GEW
K41W,FSW
GRW
K61W
T12
FCW
Hiawatha
MHW
BRW
LFW
JV5
JV6
POT
CRC
Gentry Mountain
JV4
BLM
RIL
OTT
NMH
BLC
TMN
DRY
East Mountain
Base of Escarpment
TRM
BTS,BTD
ECR
Huntington
FLC
SPF
EMT
SCN
TTUT
JVR
RFT
SNL
Joes Valley Dam
NMT
JV2
JV1
Orangeville
Castle Dale
7000
Utah
Index Map
Ferron
WWC Seismic Station
U of U Seismic Station
USBR Seismic Station
0
5
10km

Figure 2

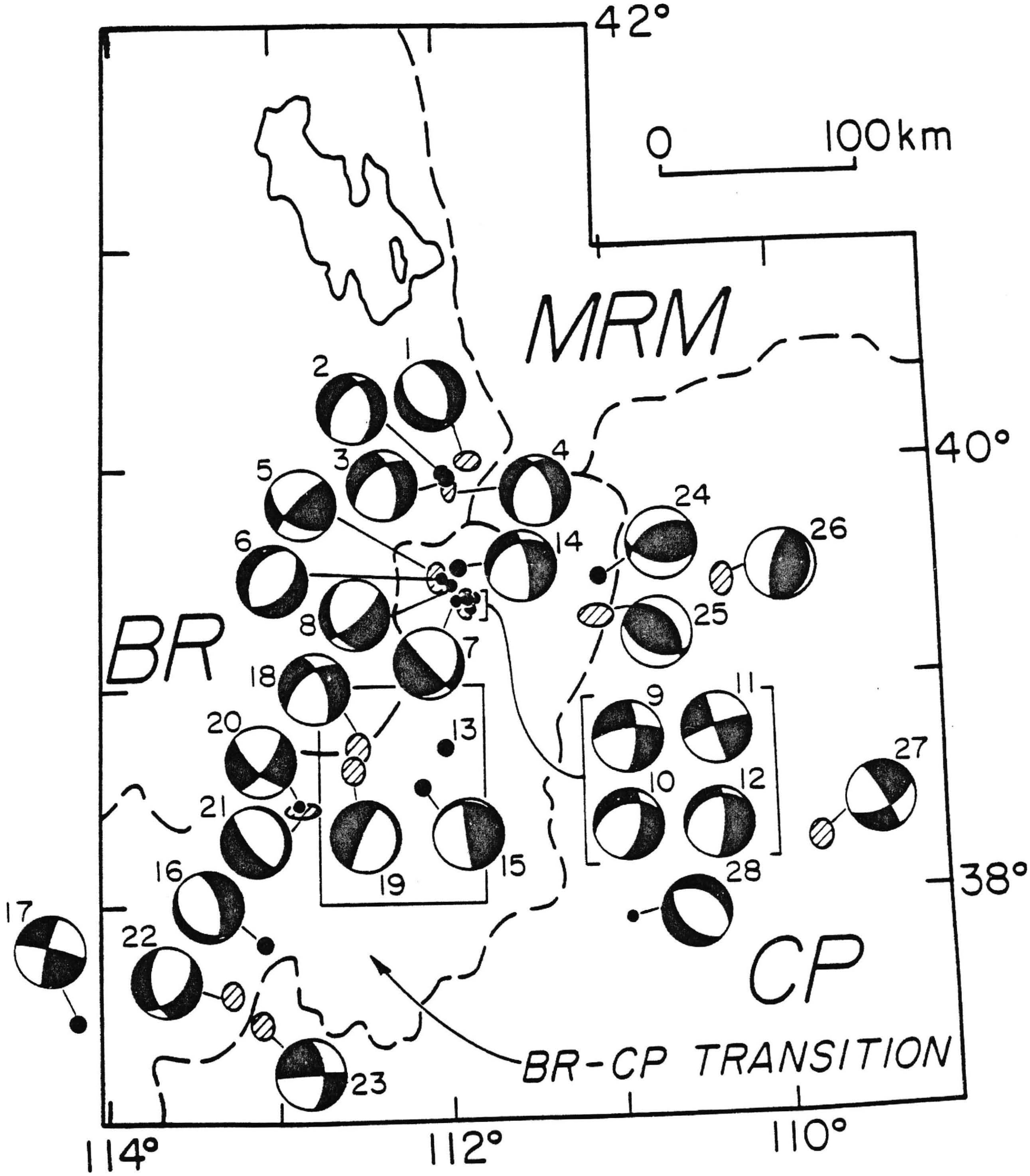
42°
0
100km
MRM
40°
BR
38°
CP
BR-CP TRANSITION
114°
112°
110°
1
2
3
4
5
6
7
8
9
10
11
12
13
14
15
16
17
18
19
20
21
22
23
24
25
26
27
28

Figure 3

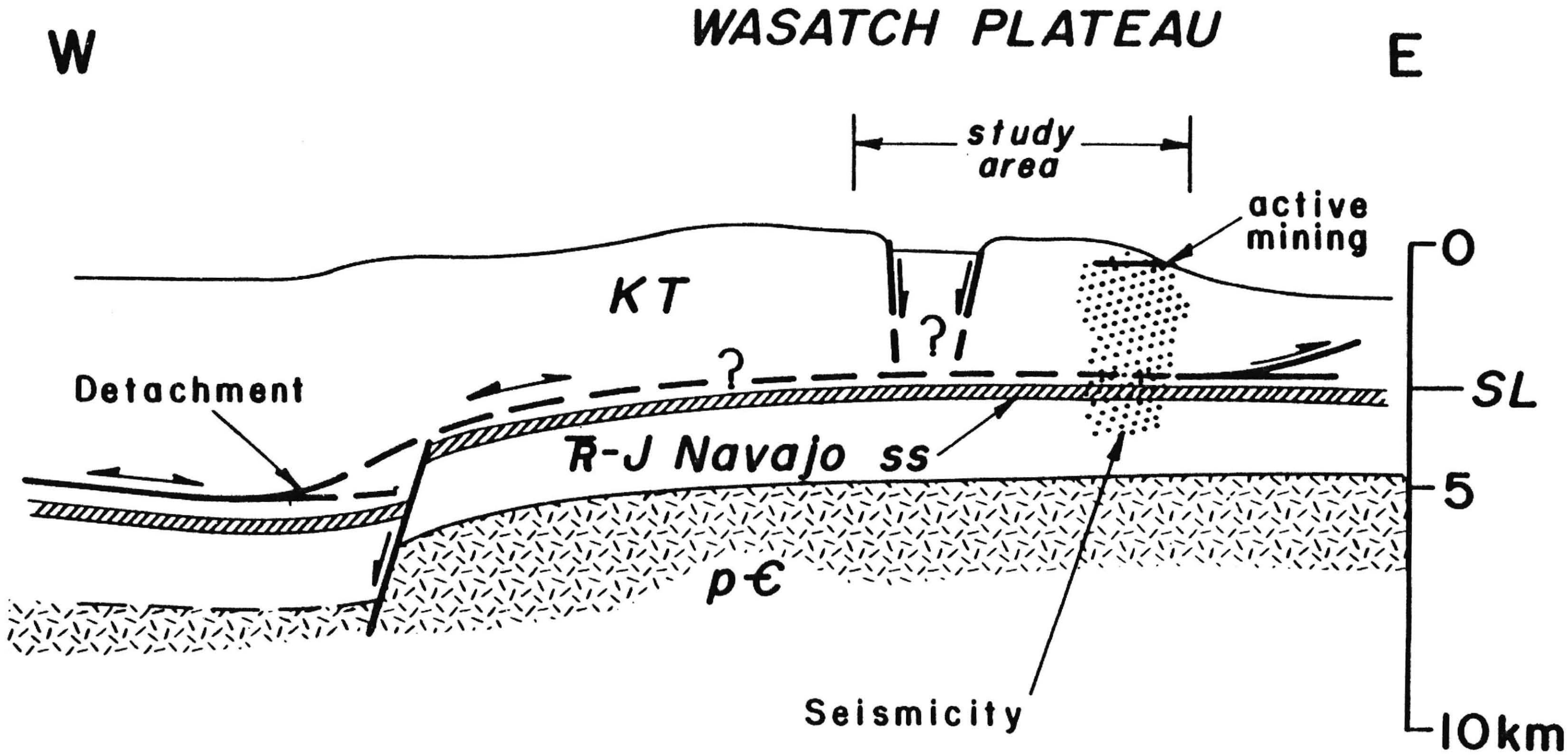
WASATCH PLATEAU
W
E
study
area
active
mining
KT
?
?
Detachment
SL
0
₸-J Navajo ss
5
p-€
Seismicity
10km

Figure 4

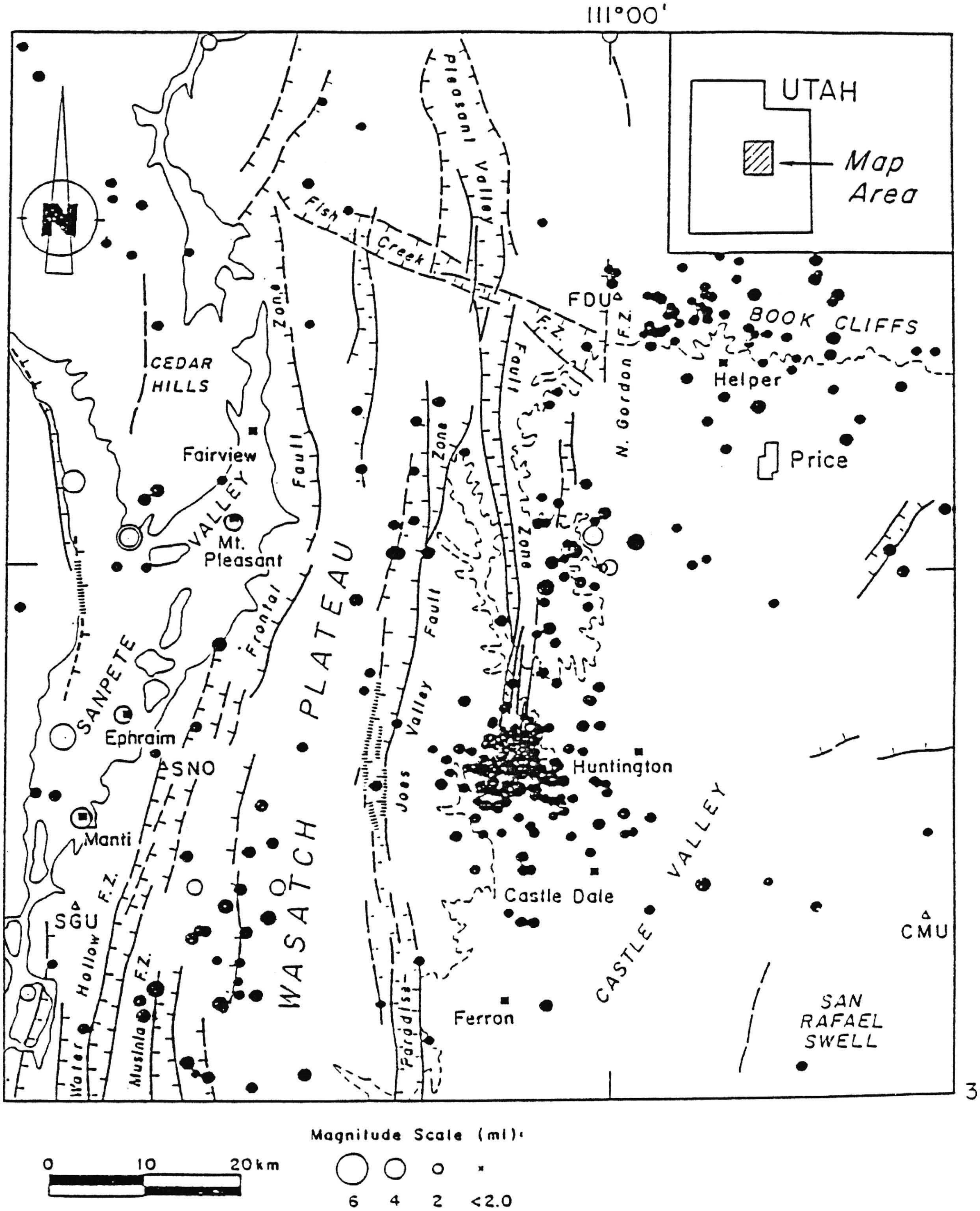

111°00'
UTAH
Map Area
N
Fish Creek
Pleasant Valley
FDU
BOOK CLIFFS
N. Gordon F.Z.
Helper
Price
CEDAR HILLS
Fairview
VALLEY
Mt. Pleasant
Frontal Fault Zone
WASATCH PLATEAU
Joes Valley Fault Zone
SANPETE
Ephraim
SNO
Manti
Huntington
CASTLE VALLEY
Castle Dale
SGU
Water Hollow F.Z.
Musinia F.Z.
Paradise
Ferron
CMU
SAN RAFAEL SWELL
3
Magnitude Scale (ml):
6 4 2 <2.0
0 10 20km

Figure 5

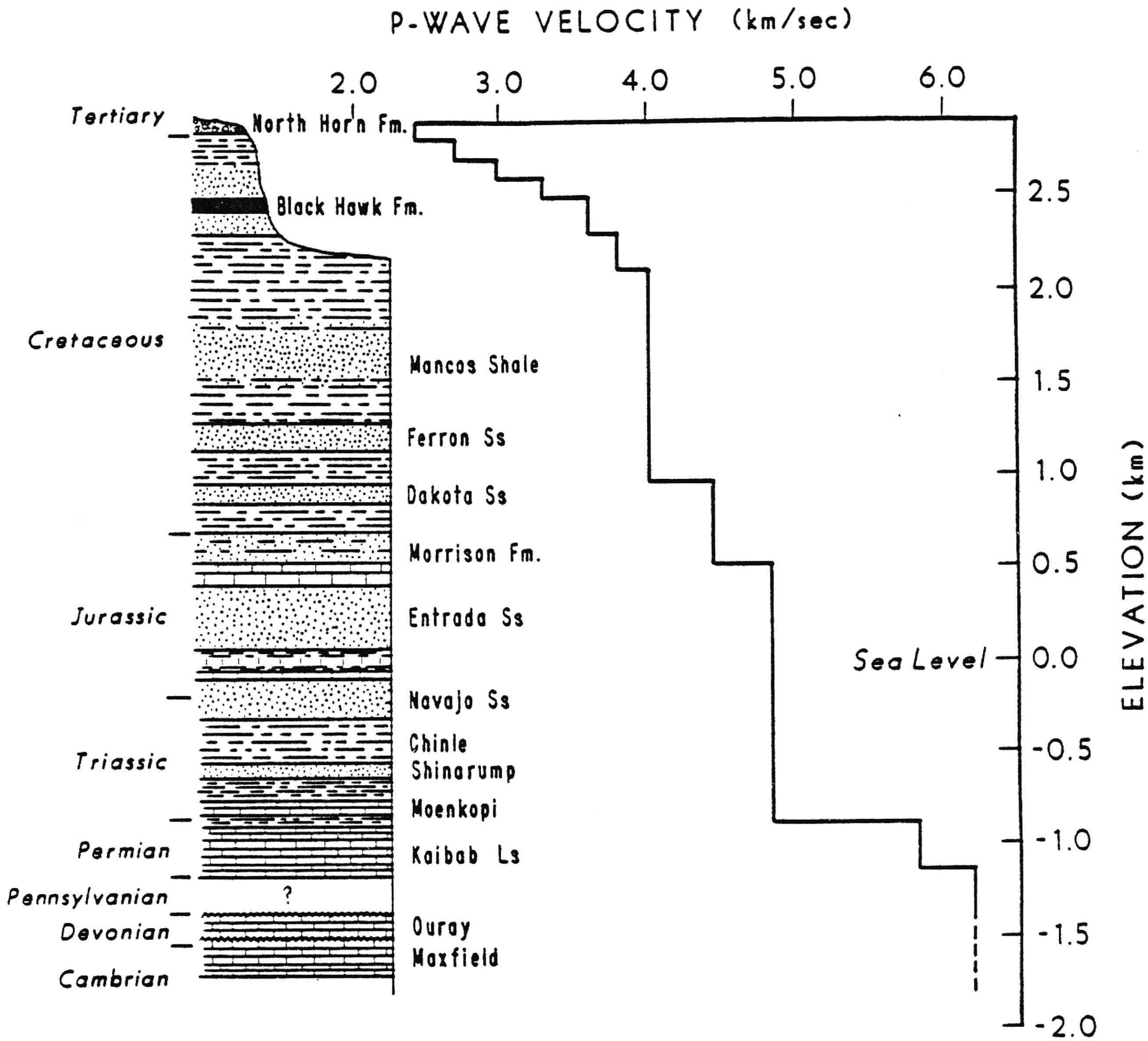
P-WAVE VELOCITY (km/sec)
2.0
3.0
4.0
5.0
6.0
Tertiary
North Horn Fm.
Black Hawk Fm.
Cretaceous
Mancos Shale
Ferron Ss
Dakota Ss
Morrison Fm.
Jurassic
Entrada Ss
Navajo Ss
Triassic
Chinle
Shinarump
Moenkopi
Permian
Kaibab Ls
Pennsylvanian
?
Devonian
Ouray
Maxfield
Cambrian
2.5
2.0
1.5
1.0
0.5
Sea Level
0.0
-0.5
-1.0
-1.5
-2.0
ELEVATION (km)

Figure 6

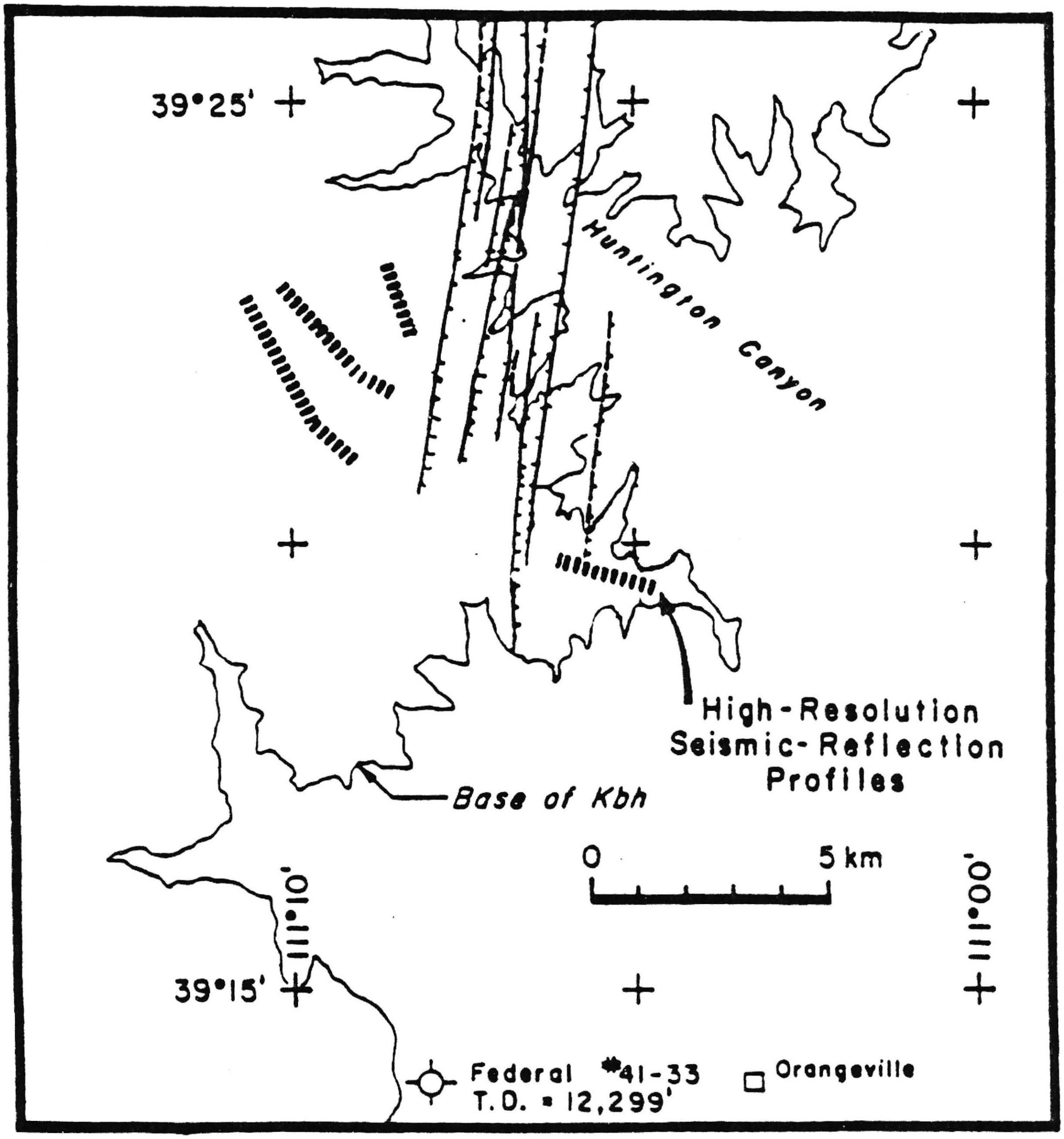
39°25'
Huntington Canyon
High-Resolution
Seismic-Reflection
Profiles
Base of Kbh
0
5 km
111°10'
111°00'
39°15'
Federal #41-33
T.D. = 12,299'
Orangeville

Figure 7

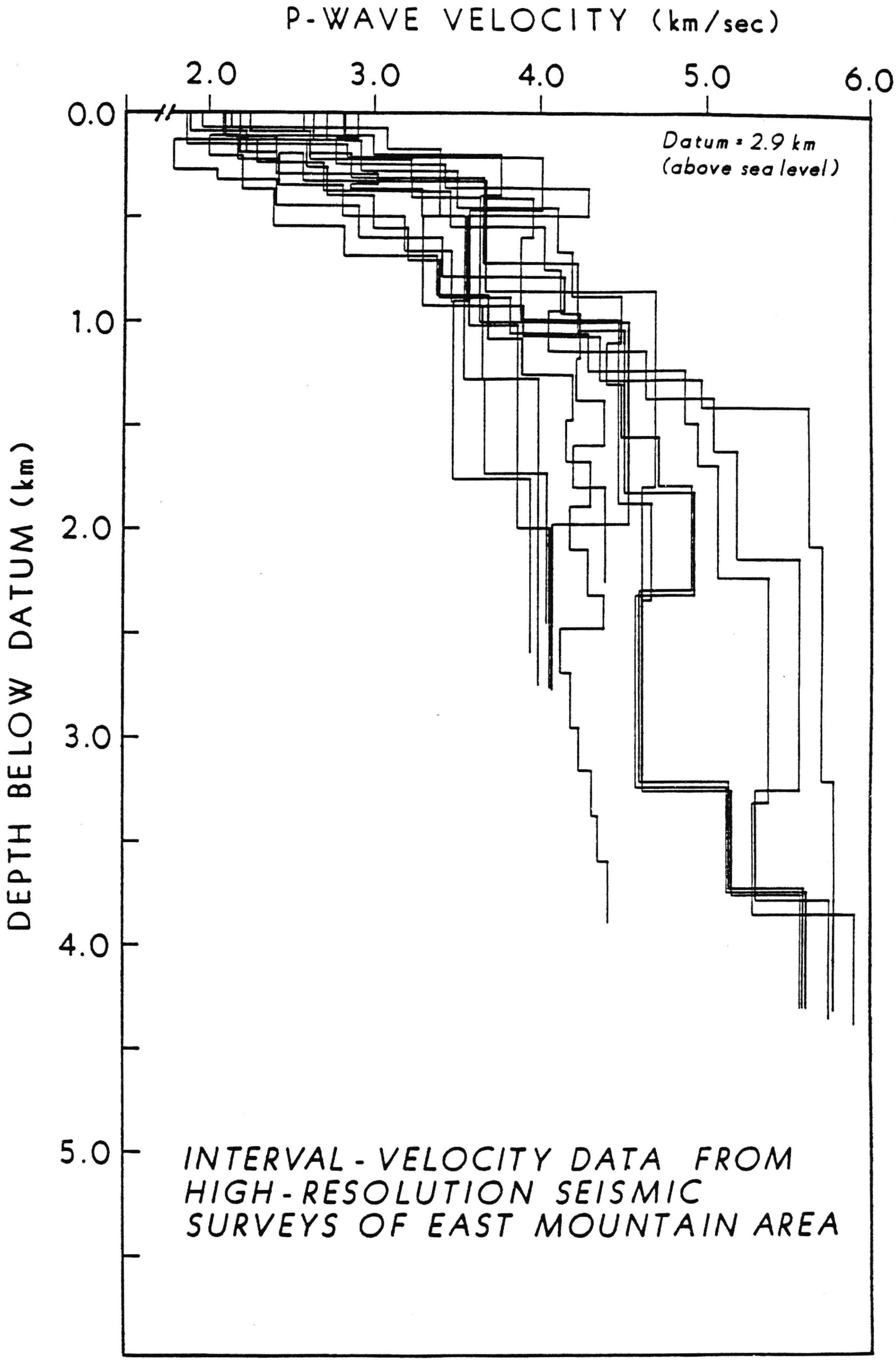
P-WAVE VELOCITY (km/sec)
2.0
3.0
4.0
5.0
6.0
0.0
1.0
2.0
3.0
4.0
5.0
DEPTH BELOW DATUM (km)
Datum = 2.9 km
(above sea level)
INTERVAL-VELOCITY DATA FROM
HIGH-RESOLUTION SEISMIC
SURVEYS OF EAST MOUNTAIN AREA

Figure 8

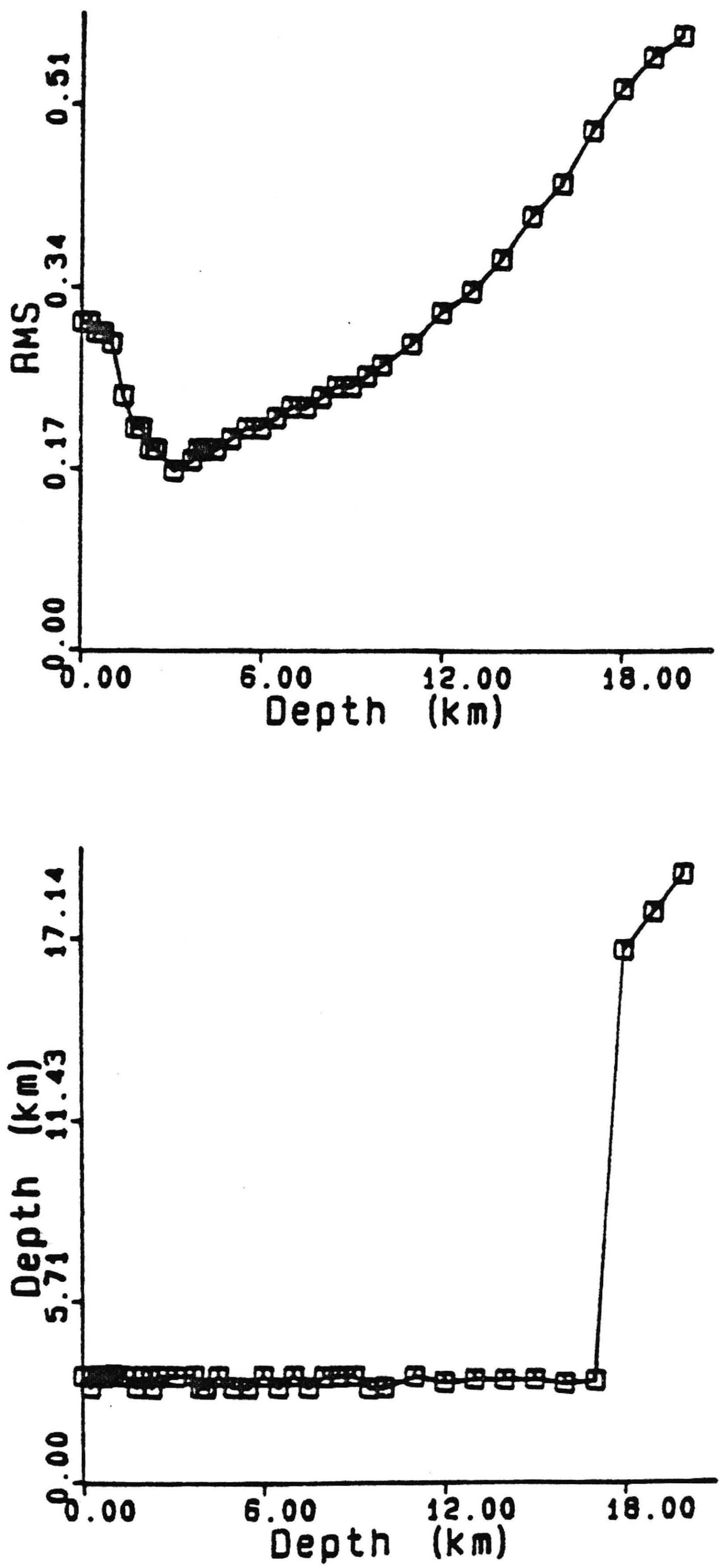

RMS
0.00
0.17
0.34
0.51
0.00
6.00
12.00
18.00
Depth (km)
Depth (km)
0.00
5.71
11.43
17.14
0.00
6.00
12.00
18.00
Depth (km)

Figure 9

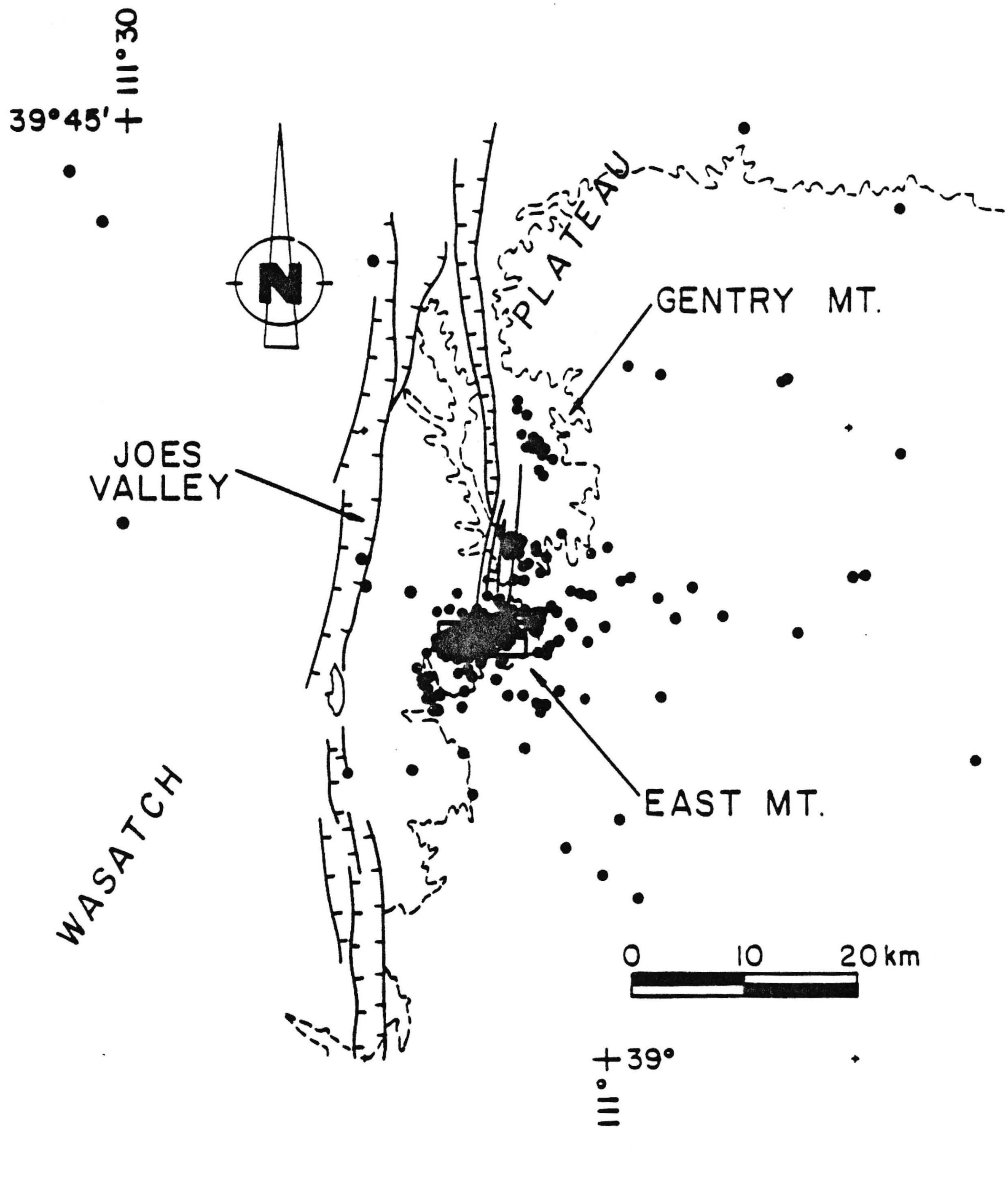
111°30
39°45'
N
PLATEAU
GENTRY MT.
JOES VALLEY
WASATCH
EAST MT.
0 10 20 km
39°
111°

Figure 10

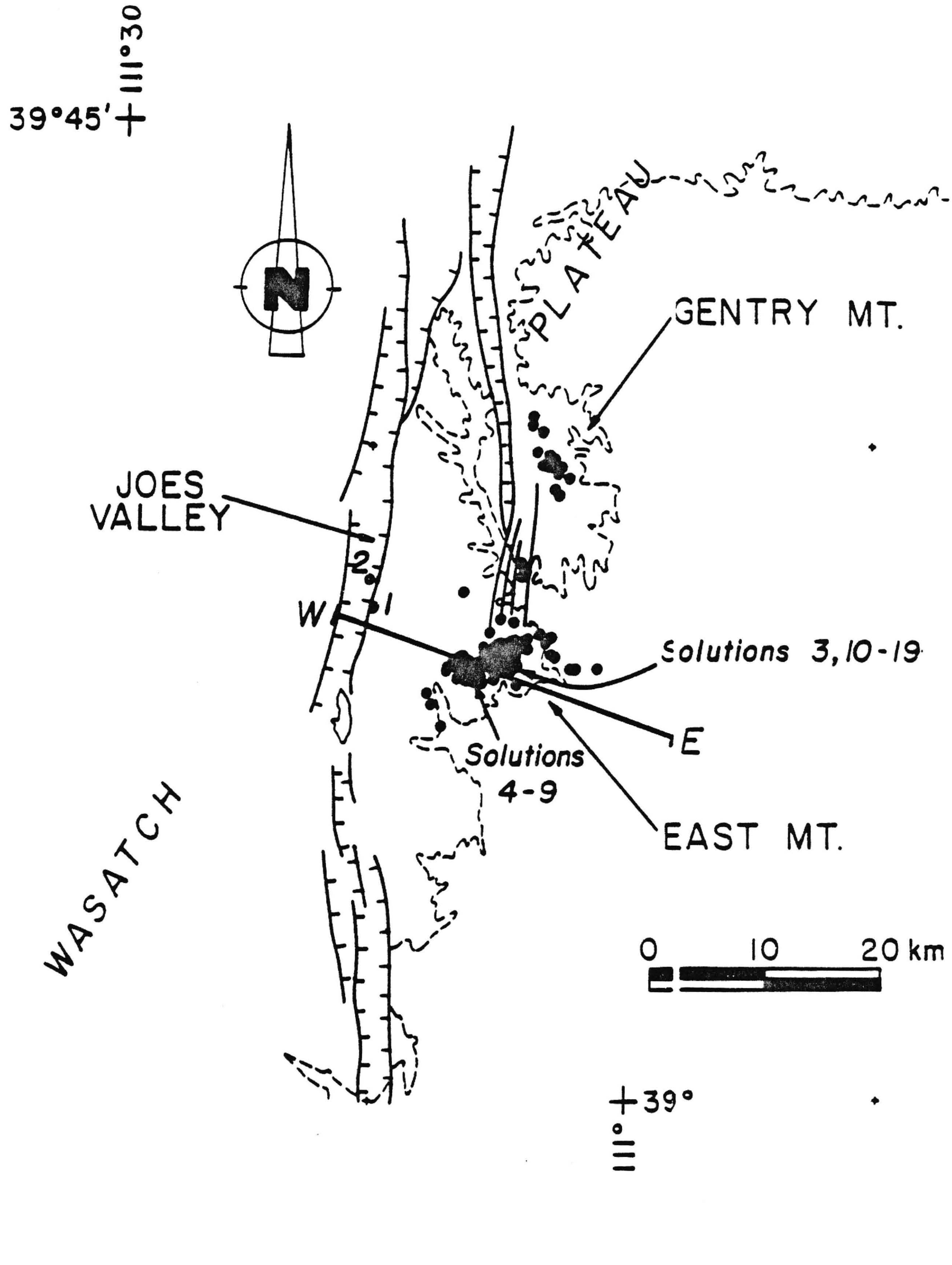
39°45'
111°30
N
PLATEAU
GENTRY MT.
JOES
VALLEY
2
1
W
Solutions 3,10-19
E
Solutions
4-9
EAST MT.
WASATCH
0
10
20 km
39°
111°

Figure 11

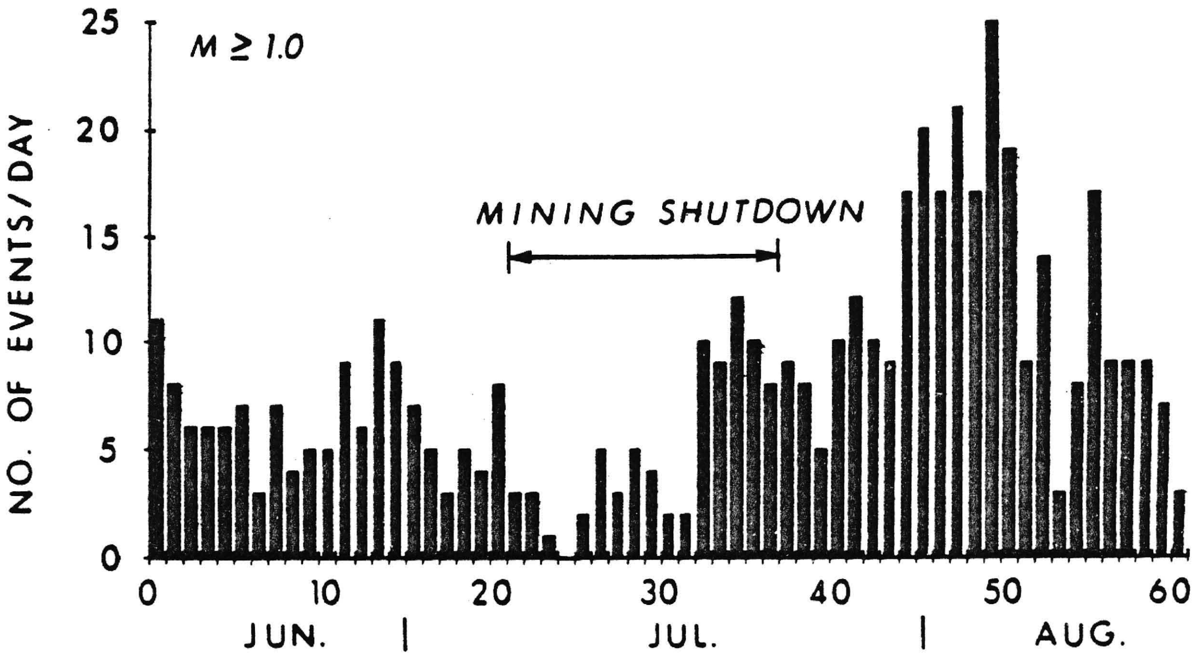

M ≥ 1.0
NO. OF EVENTS/DAY
0
5
10
15
20
25
MINING SHUTDOWN
0
10
20
30
40
50
60
JUN.
JUL.
AUG.

Figure 12

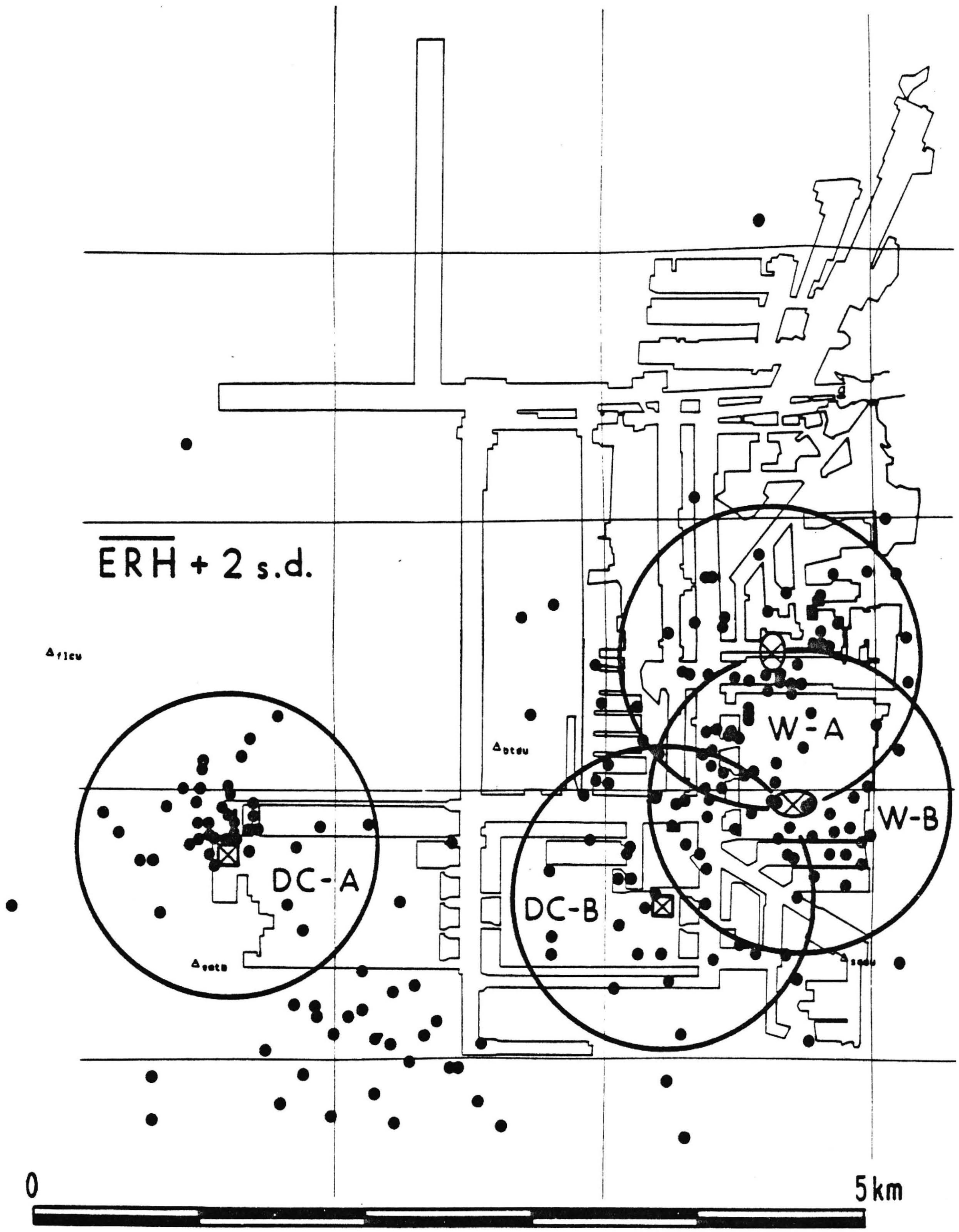

Figure 13

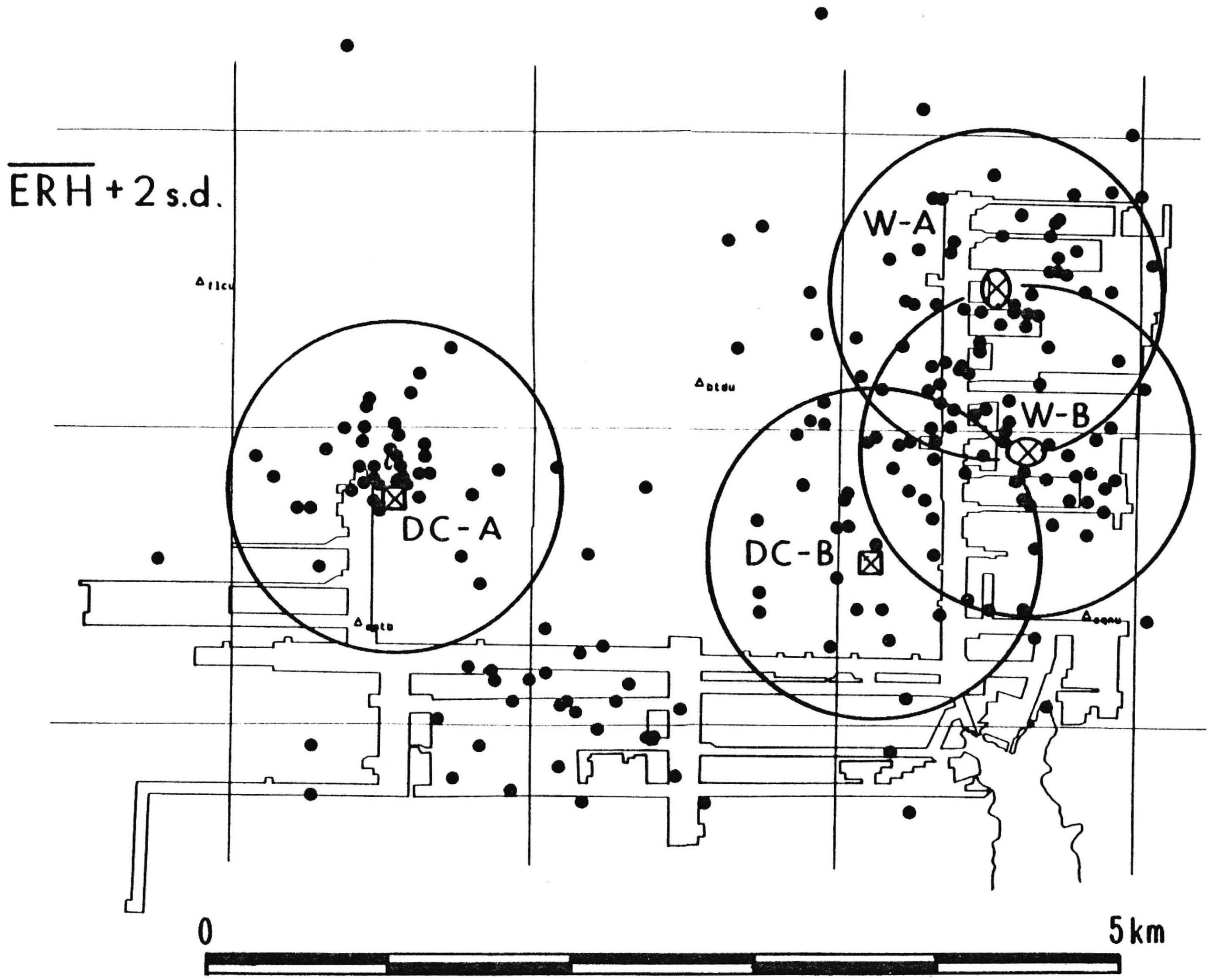

Figure 14

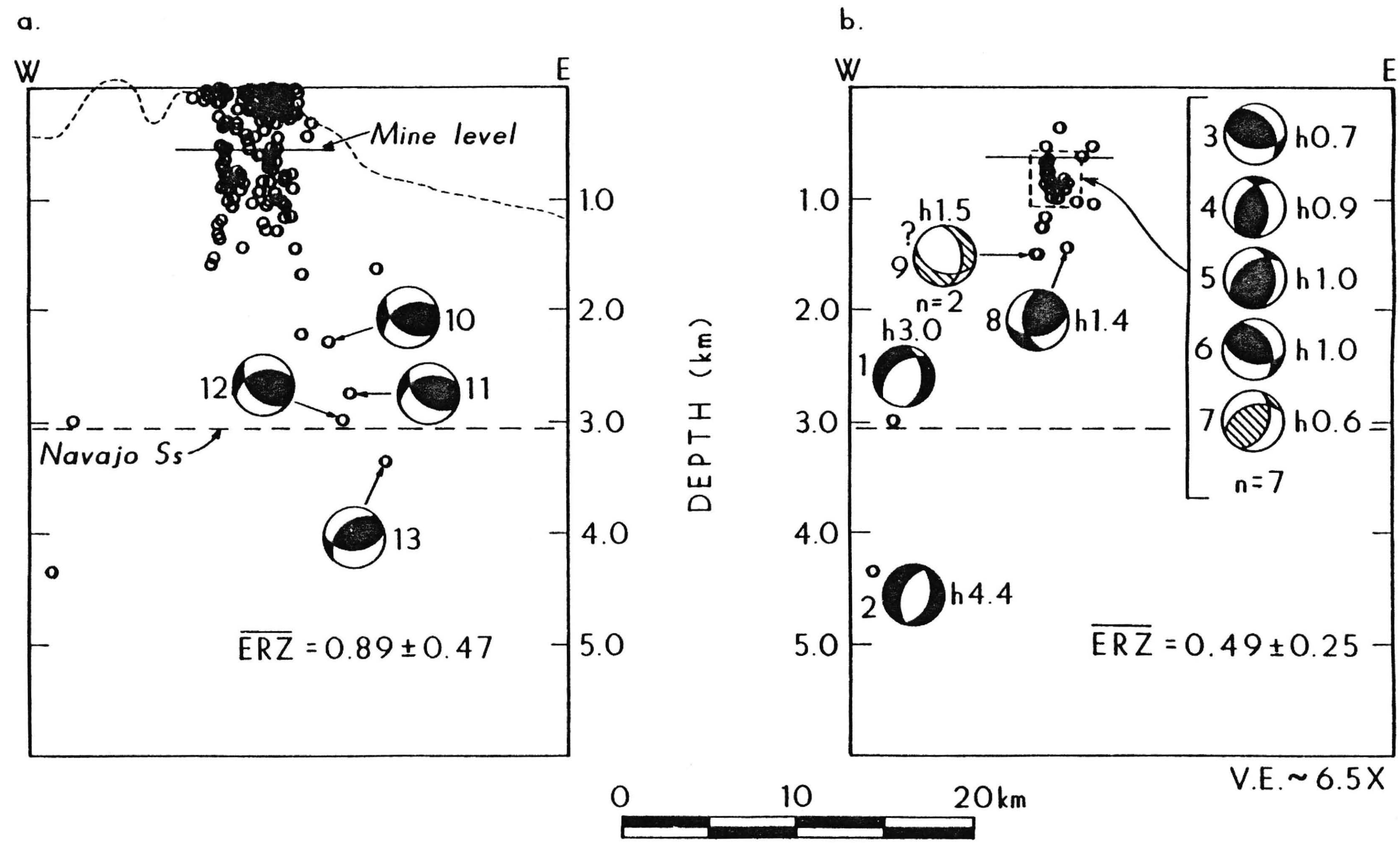
a.
b.
W
E
Mine level
Navajo Ss
DEPTH (km)
1.0
2.0
3.0
4.0
5.0
10
11
12
13
$\overline{ERZ}$ = 0.89 ± 0.47
h1.5
?
9
n=2
8
h1.4
h3.0
1
2
h4.4
3 h0.7
4 h0.9
5 h1.0
6 h1.0
7 h0.6
n=7
$\overline{ERZ}$ = 0.49 ± 0.25
V.E. ~ 6.5X
0
10
20km

Figure 15

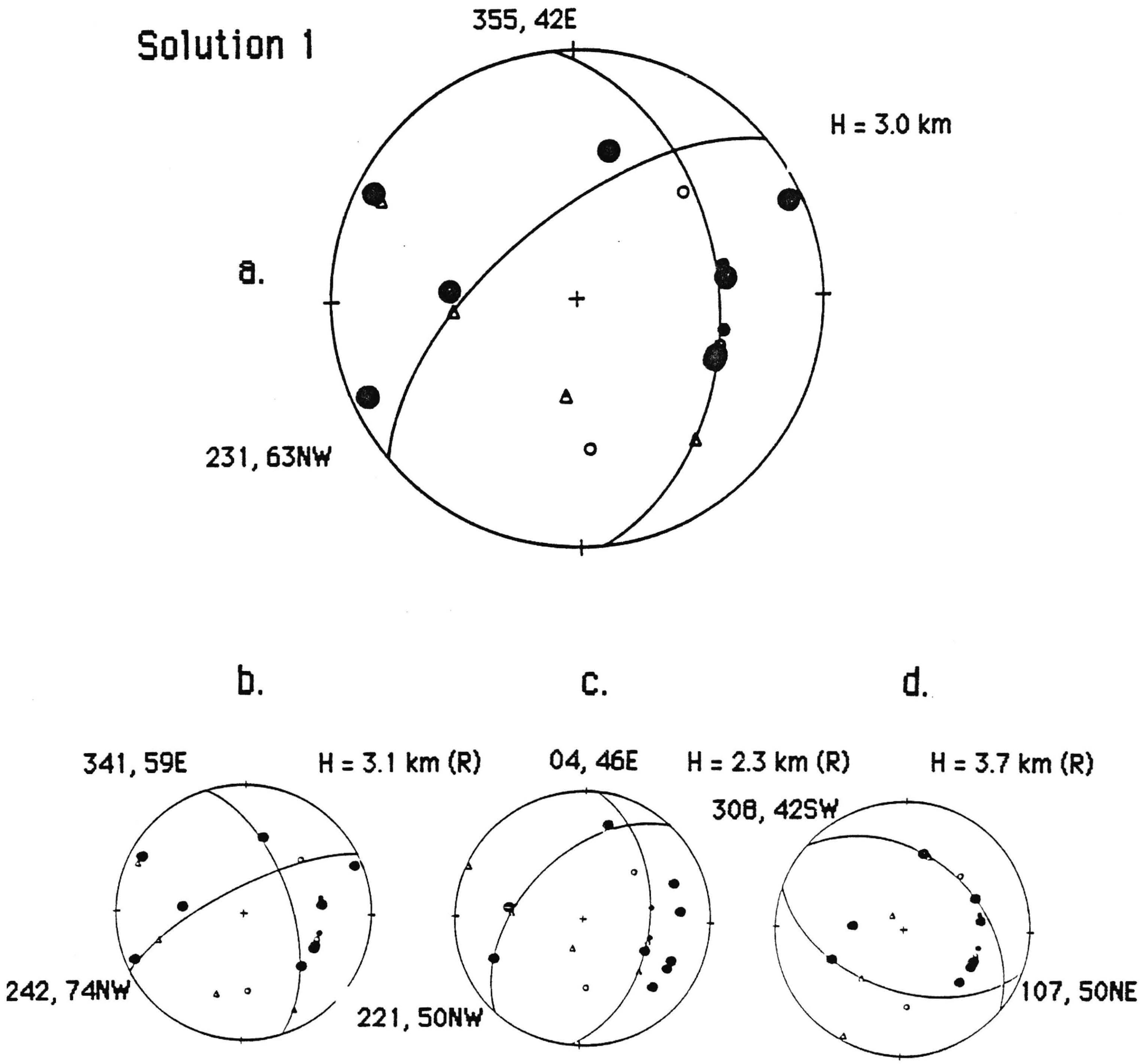
Solution 1
355, 42E
H = 3.0 km
a.
231, 63NW
b.
c.
d.
341, 59E
H = 3.1 km (R)
04, 46E
H = 2.3 km (R)
H = 3.7 km (R)
308, 42SW
242, 74NW
221, 50NW
107, 50NE

Figure 16

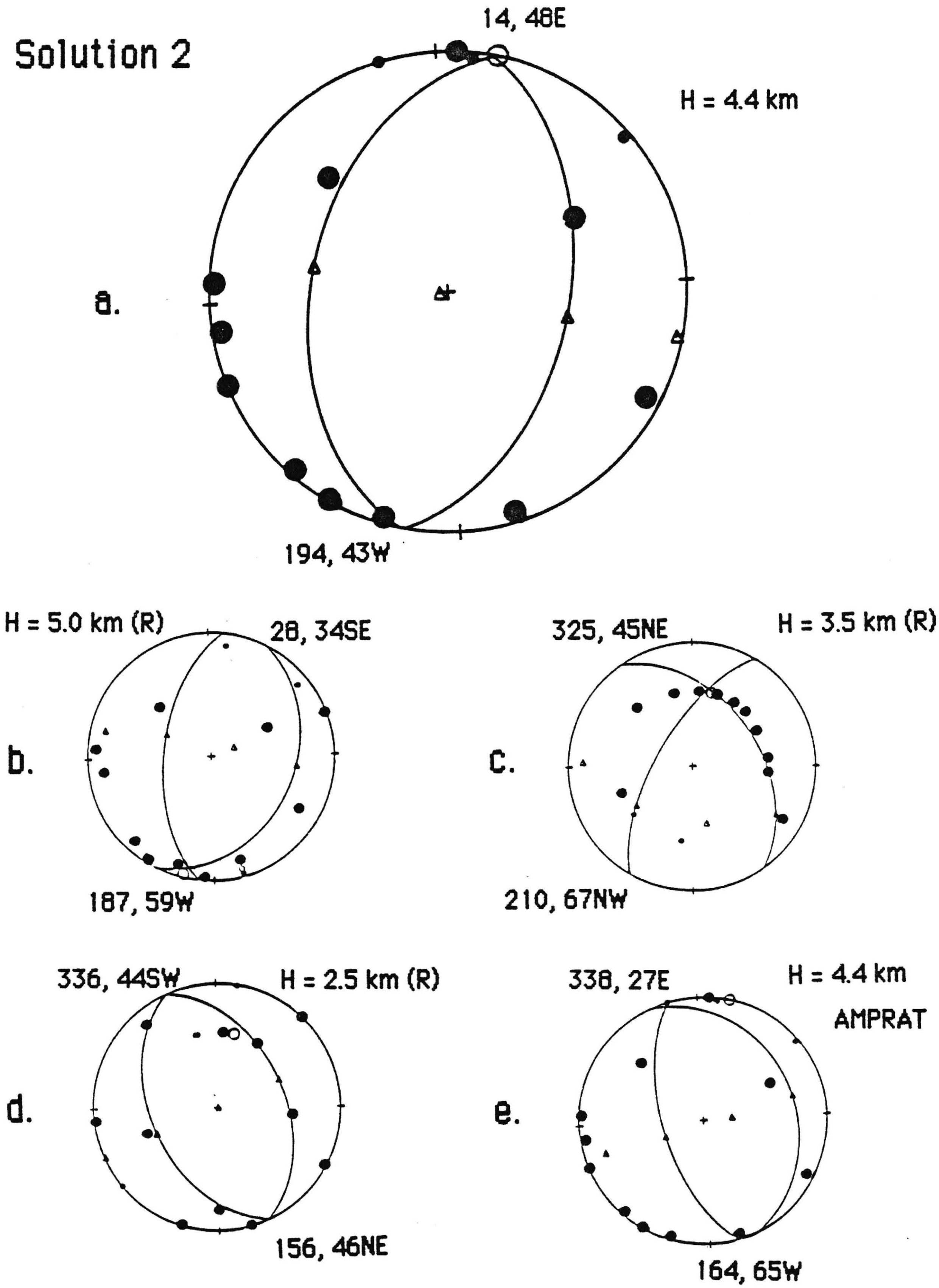

Solution 2
14, 48E
H = 4.4 km
a.
194, 43W
H = 5.0 km (R)
28, 34SE
b.
187, 59W
325, 45NE
H = 3.5 km (R)
c.
210, 67NW
336, 44SW
H = 2.5 km (R)
d.
156, 46NE
338, 27E
H = 4.4 km
AMPRAT
e.
164, 65W

Figure 17

a.

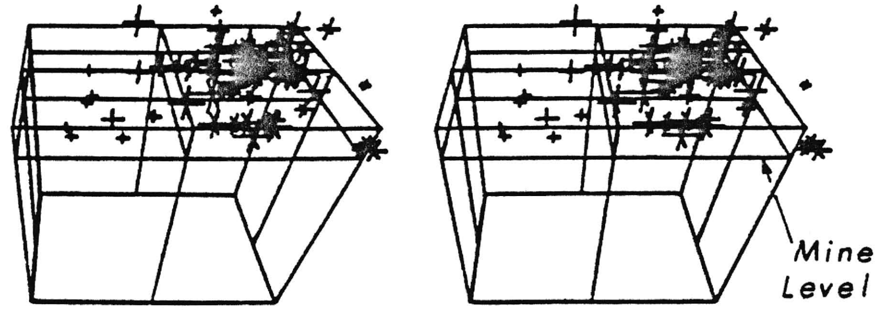

b.

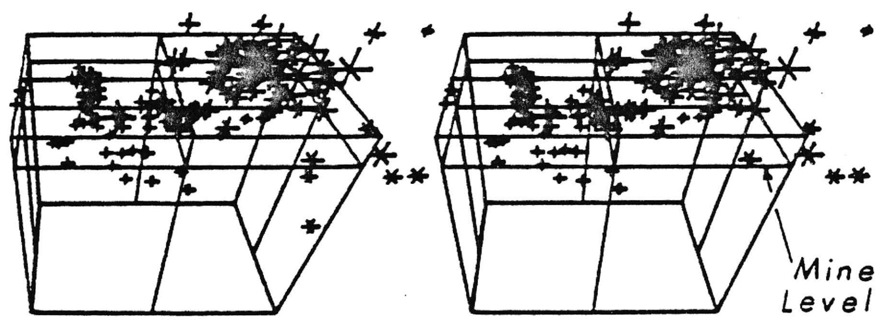

Figure 18

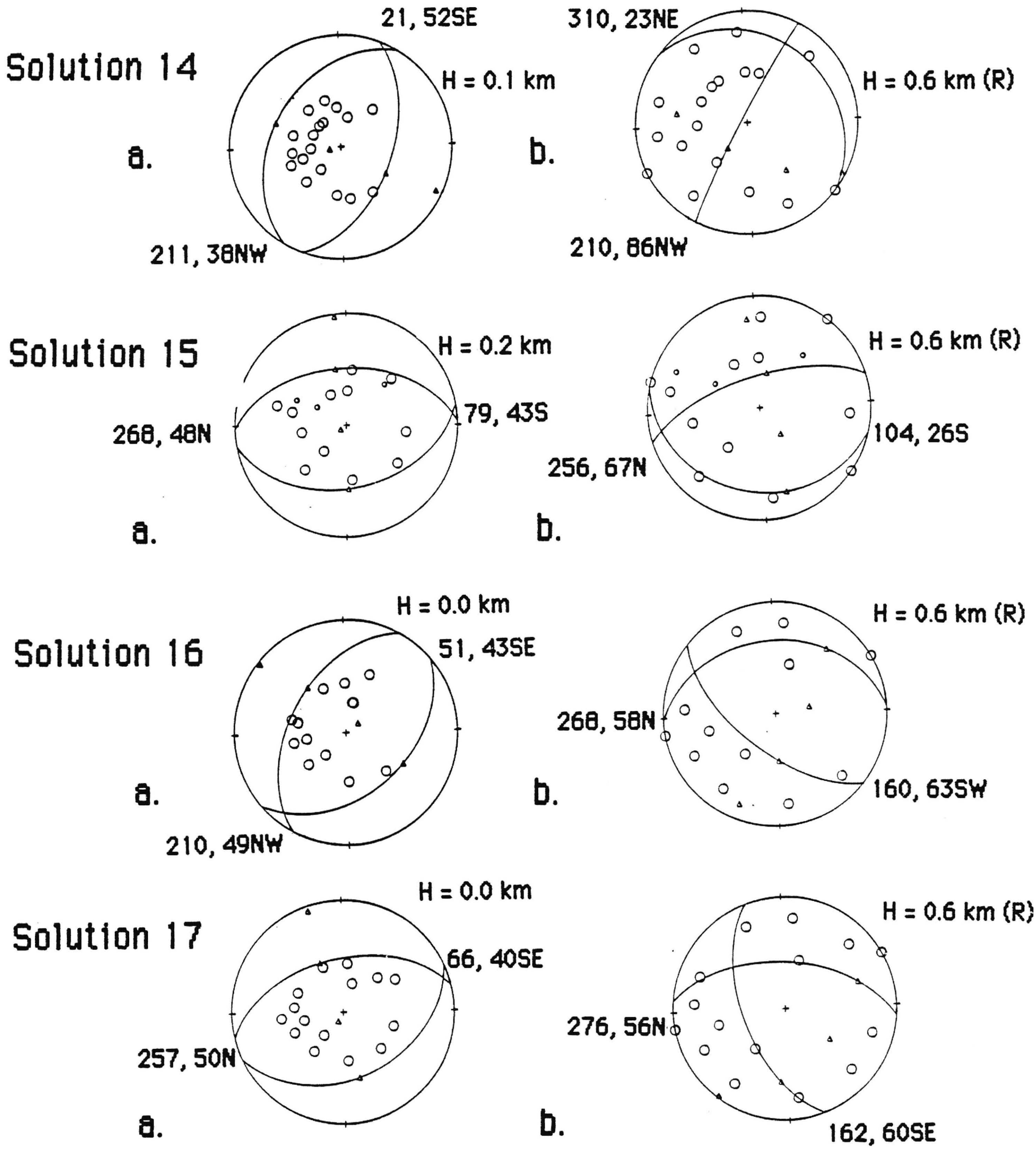
Solution 14
a.
21, 52SE
H = 0.1 km
211, 38NW
b.
310, 23NE
H = 0.6 km (R)
210, 86NW
Solution 15
a.
H = 0.2 km
268, 48N
79, 43S
b.
H = 0.6 km (R)
104, 26S
256, 67N
Solution 16
a.
H = 0.0 km
51, 43SE
210, 49NW
b.
H = 0.6 km (R)
268, 58N
160, 63SW
Solution 17
a.
H = 0.0 km
66, 40SE
257, 50N
b.
H = 0.6 km (R)
276, 56N
162, 60SE

Figure 19

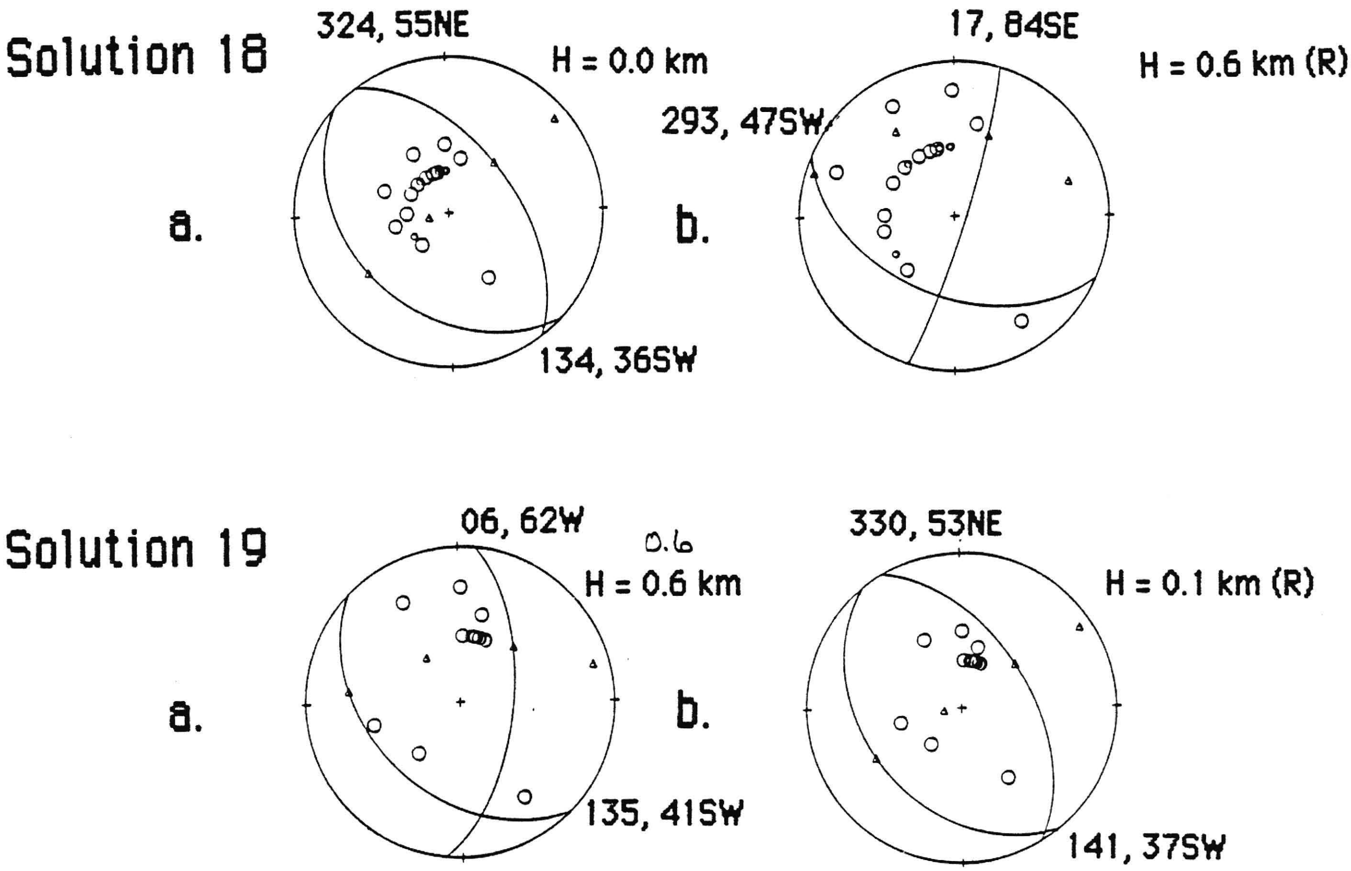
Solution 18
324, 55NE
H = 0.0 km
a.
134, 36SW
17, 84SE
H = 0.6 km (R)
293, 47SW
b.
Solution 19
06, 62W
0.6
H = 0.6 km
a.
135, 41SW
330, 53NE
H = 0.1 km (R)
b.
141, 37SW

Figure 20

REFERENCES

Angelier, J. (1979). Determination of the mean principle directions of stresses for a given fault population, Tectonophysics., 56 T17-T26.

Arabasz, W.J. (1983). Seismological studies across the Basin and Range-Colorado Plateau transition in Utah, Final Report to the National Science Foundation, Grant no. EAR-8008799.

Arabasz, W.J. (1983). Geometry of active faults and seismic deformation within the Basin and Range-Colorado Plateau transition, central and southwest Utah (abs.) Earthquake Notes 54, no.1, 48.

Arabasz, W.J., and D.R. Julander (1986). Geometry of active faults and crustal deformation within the Basin and Range-Colorado Plateau transition in Utah, BSSA?

Arabasz, W.J., R.B. Smith, and W.D. Richins (1979). Earthquake studies in Utah, 1850-1978, University of Utah Seismograph Stations, 57-251.

Baer, J.L. (1976). Structural evolution of central Utah- late Permian to recent, in Geology of the Cordilleran Hingeline J.G. Hill, editor, 1976 Symposium, Rocky Mtn. Assoc. of Geologists, Denver, Colorado, 37-45.

Baer, J.L. and E. Callaghan, Editors (1972). Plateau-Basin and Range Transition Zone, Central Utah, 1972, Utah Geol. Assoc. Publ. 2, 125 pp.

Bakun, W.J. and A.G. Lindh (1977). Local magnitudes, seismic moments, and coda durations for earthquakes near Oroville, California Bull. Seis. Soc. Am. 67, 615-629.

Best, M.G. and W.K. Hamblin (1978). Origion of the Northern Basin and Range province: implications from the geology of its eastern boundry, Geol. Soc. Am. Memoir 152, 313-340. Blake, W., F. Leighton, and W.I. Dinwall (1974). Microseismic techniques for monitoring the behavior of rock structures, U.S. Bur. Mines Bull. 655, 65 pp.

Das, S., and C.H. Scholtz (1983). Why large earthquakes do not nucleate at shallow depths, Nature, 305, 1669-1675.

Doelling, H.H. (1972). Central Utah Coal Fields: Sevier-Sanpete, Wasatch Plateau, Book Cliffs, and Emery, Utah, Geol. Mineralog. Surv. Mon. Ser. No. 3, 571 pp.

Dunrud, C.R. and F.W. Osterwald (1965). Seismic study of coal mine bumps, Carbon and Emery, Utah, Trans. Am. Inst. Mining Met. Petrol. Engr. 232, 174-182.

Dunrud, C.R., F.W. Osterwald, and J. Hernandez (1973). Summary of activity and its relation to geology and mining in the Sunnyside mining district, Carbon and Emery Counties, Utah during 1967-1970, Geological Survey Open File Report, 73-63.

Griscom, M. and W.J. Arabaz (1979). Space-time seismicity pattersn in the Utah Region: A 300-km-long seismicity gap in the Intermountain seismic belt (abstract), Earthquake Notes 50 (4), 69.

Gibowicz, S.J., Z. Droste, B. Guterch, and J. Hordejuk (1981). The Belchatow, Poland earthquakes of 1979 and 1980 induced by surface mining, Engr. Geol., 71, 257-271.

Hanks, T.C. (1982). fmax, Bull. Seism. Soc. Am. 72, 1867-1879.

Hardy, H.R., Jr. (1975). Evaluating the stability of geologic structures using acoustic emission, Am. Soc. for Testing and Materials, Spec. Tec. Publ. 571, 80-106.

Hintze, L.F. (1973). Geologic history of Utah, Brigham Young Univ. Geol. Studies 20, Pt. 3, 181 pp.

Johnston, A.C., D.J. Reinbold, and S.I. Brewer (1984). Seismotectonics of the southern Applachians, Bull. Seism. Soc. Am. 75, 291-312.

Julalnder, D.R. (1983). Seismicity and correlation with fine structure in the Sevier Valley area of the Basin and Range-Colorado Plateau transition, south-central Utah, M.S. Thesis University of Utah, Salt Lake City, Utah, 143 pp.

Keller, G.R., R.B. Smith, and L.W. Braile (1975). Crustal structure along the Great Basin-Colorado Plateau transition from seismic refraction profiling, J. Geophy. Res. 80, 1093-1098.

Kisslinger, C. (1976). A review of theories of mechanics of induced seismicity, Engr. Geol., 10, 85-98.

Kisslinger, K., J.R. Bowman, and K. Koch (1981). Procedures for computing focal mechanisms from local $(SV/P)_z$ data, Bull. Seism. Soc. Am. 71, 1719-1729.

Klein, F.W., (1978). Hypocenter location Program: HYPOINVERSE, U.S. Geol. Surv. Open File Rep. 78-694.

Kusznir, N.J., D.P. Ashwin, and A.G. Bradely (1980). Mining induced seismicity in the North Staffordshire Coalfield, England. Int. J. Rock Mech. Min. Sci. & Geomech. Abstr. 17, 45-55.

Lindseth, R.O. (1982). Digital Processing of Geophysical Data A Review, Teknica Resource Development, LTD, Calgary, Alberta

McGarr, A., (1982). Analysis of states of stress between provinces of constant stress, J. Geophys. Res. 87, 9279-9288.

McGarr, A., S.M. Spottiswood, and N.C. Gay (1975). Relation of mine tremors to induced stresses and to rock properties in the focal region, Bull. Seism. Soc. Am. 65, 981-993.

McGarr, A., (1982). Analysis of states of stress between provinces of constant stress, J. Geophys. Res. 87, 9279-9288.

McKee, M.E., 1982, Microearthquake studies across the Basin and Range-Colorado Plateau transition zone in central Utah M.S. Thesis, Salt Lake City, University of Utah, 118 p.

McKee, M.E., and Arabasz, W.J., 1982, Microearthquake studies across the Basin and Range-Colorado Plateau transition in central Utah, in Overthrust Belt of Utah, Nielson, D.L., ed, Utah Geological Association Publication 10, p. 137-149.

Osterwald, F.W. and C.R. Dunrud (1965). Geology applied to the study of coal mine bumps at Sunnyside, Utah, Trans. Am. Inst. Mining Met. Petr. Engrs. 232, 168-174.

Royse, F. (1983). Extensional faults and folds in the foreland thrust belt, Utah, Wyoming, Idaho: Geol. Soc. Am. abstr. 15, 295.

Sbar, M.L., M. Barazangi, J. Dorman, C.H. Scholz, and R.B. Smith (1972). Tectonics of the Intermountain seismic belt, western United States: microearthquake seismicity and composite fault plane solutions, Geol. Soc. Am. Bull. 83, 13-28.

Scholz, C.H. (1968). The frequency-magnitude relation of microfracturing in rock and its relation to earthquakes, Bull. Seism. Soc. Am. 58, 399-415.

Scholz, C.H. (1968). Experimental study of the fracturing process in brittle rock, J. Geophys. Res. 73, 1447-1454.

Smith, R.B. (1978). Seismicity, crustal structure, and intraplate tectonics of the interior of the western cordillera, G.S.A. Mem. 152, R.B. Smith and G. Eaton, ed., 111-144.

Smith, R.B., and M.L. Sbar (1974). Contempory tectonics and seismicity of the western United States with emphasis on the Intermountain seismic belt, Geol. Soc. Am. Bull., 85, 1205-1218.

Smith, R. B., P.L. Winkler, J.G. Anderson, and C.H. (1974). Source mechanisms of microearthquakes associated with underground mines in eastern Utah, Bull. Seism. Soc. Am. 64, 1295-1317.

Spieker, E.M. (1949). The transition between the Colorado Plateaus and the Great Basin in central Utah: Salt Lake City, Utah geological society, Guidebook to the geology of Utah,4, 106 p.

Standlee, L.A. (1982). Structure and stratigraphy of Jurassic rocks in central Utah: Their influence on tectonic development of the Cordilleran foreland and thrust belt in: Powers, R.B., ed., Geologic studies of the Cordilleran thrust belt, 1, Denver, Rocky Mountain Association of Geologists, 357-382.

Spottiswoode, S.M. and A. McGarr (1975). Source parameters of tremors in a deep level coal mine, Bull. Seism. Soc. Am. 65, 93-112.

Stokes, W.L. (1977). Subdivisions of the major physiographic provinces in Utah, Utah Goelogy, 4, (1), 1-17.

Suteau, A.M., and Whitcomb, J.H., 1979, A local earthquake coda magnitude and its relation to deviation, moment M_o, and local Richter magnitude M_L: Seismological Society of America Bulletin, v. 69, p. 353-368.

Tibbets, B.L., C.R. Dunrud, and F.W. Osterwald (1966). Seismic-refraction measurements at Sunnyside, Utah, U.S. Geol. Surv., Prof. Paper 550-D, D132-D137.

Whitcomb, J.H. (1973). The 1971 San Fernando Earthquake Series Focal Mechanisms and Tectonics, Ph.D. Thesis (Part II), Calif. Inst. of Technol., Pasadena, Calif.

Witkind, I.J., J.D. Lidke, and L.A. McBroome (1978). Preliminary geologic map of the Price 1 X 2 quadrangle, Utah, U.S. Geol. Surv., Open-File Rept. 78-465.

Wong, I.G. and R.B. Simon (1981). Low-level histroical and contempory seismicity in the Paradox Basin, Utah and its tectonic implications, Geology of the Paradox Basin, edited by D. Wiegand, Rocky Mountain Association of Geologists, 169-185.

Wong, I.G. (1982). Mining-induced seismicity in the Colorado Plateau, western United States, and its implications for the siting of an underground high level nuclear waste repository, in Seismicity in Mines, South African Inst. of Mining and Metallurgy (in press).

Wong, I.G. (1983). Mechanisms for mining induced seismicity in the Book Cliffs and Eastern Wasatch Plateau, Utah, U.S.A., Int. Jour. of Rock Mech. Min. Sci. and Geomech. Abstr. 22, 263-270.

Zoback, R.B. and M. Zoback (1980). State of Stress in the conterminous United States, J. Geophys. Res. 85, 6113-6156.

APPENDIX A

STATION DATA SUMMARY

WASATCH PLATEAU STATION DATA

Station	Lat. (N)	Long. (W)	Elevation (m)	Operating Dates (1984)	Polarity
JV1B	39-13.94	111-14.19	2914	Jul 6 - Aug 11	N
JV2B	39-14.07	111-19.35	3036	Jul 6 - Aug 11	N
JV3B	39-20.57	111-20.31	3048	Jul 6 - Aug 11	N
JV4B	39-25.61	111-19.06	3377	Jul 6 - Aug 11	N
JV5B	39-29.66	111-17.18	3231	Jul 6 - Aug 11	N
JV6B	39-28.52	111-12.97	3274	Jul 7 - Aug 11	N
BLCB	39-23.02	111-16.99	2566	Jul 29 - Aug 10	N
POTB	39-27.71	111-16.42	2853	Jul 28 - Aug 10	N
TRMB	39-21.49	111-14.46	3002	Jul 2 - Jul 10	N
RPTB	39-18.92	111-15.13	2670	Jul 10 - Jul 12	R
JVRB	39-18.94	111-16.04	2249	Jul 13 - Aug 12	N
BLMB*	39-24.76	111-12.56	3133	Jul 31 - Aug 10	?
TMNB*	39-22.42	111-14.50	3030	Jul 24 - Aug 10	?
BTDU*	39-20.31	111- 8.43	2920	Jul 4 - Jul 12	N
BTSU	39-20.31	111- 8.43	2920	Jun 26 - Jul 27	N
CRCU	39-27.61	111-10.34	2463	Jul 27 - Aug 11	R
DRYU	39-22.41	111-13.43	2676	Jun 26 - Aug 10	N
(EMTB)*	39-19.61	111- 9.71	2292	Jul 6 - Jul 9 Jul 20 - Jul 27	N
EMTU*	39-19.61	111- 9.71	2932	Jun 26 - Jul 4 Jul 12 - Aug 10	N
ECRU	39-20.86	111- 6.35	2725	Jul 2 - Jul 27	R
FDUU	39-45.41	110-59.40	2975	continuous	?

WASATCH PLATEAU STATION DATA

Station	Lat. (N)	Long. (W)	Elevation (m)	Operating Dates (1984)	Polarity
FLCU	39-20.60	111-10.32	2926	Jun 23 - Jul 27	N
GASU	39-35.42	111-11.09	2627	Jul 24 - Aug 11	R
HOGU	39-34.48	111-13.69	2707	Jul 27 - Aug 11	N
HUCU	39-35.51	111-11.21	2606	Jul 12 - Jul 23	R
LFHU	39-30.21	111-10.09	2365	Jul 26 - Aug 11	R
NMTU	39-14.89	111- 6.76	1897	Jun 21 - Jul 25	R
NMHU	39-23.19	111- 6.93	2173	Jun 27 - Aug 11	N
NKWU	39-32.40	111- 7.67	2588	Jul 28 - Aug 11	R
OTTU	39-24.48	111- 1.79	2219	Jun 22 - Jul 28	R
RILU	39-24.28	111- 9.58	2414	Jun 21 - Aug 11	N
SNLU	39-18.51	111- 9.21	2926	Jun 26 - Jul 27	R
SNOU	39-18.86	111-32.28	2446	continuous	?
SQNU*	39-19.64	111- 6.95	2688	Jul 6 - Jul 12 Jul 13 - Jul 15	R
SPFU	39-19.83	111- 5.00	2341	Jun 22 - Jul 24	R
SPUT	39-31.35	111- 2.60	2365	?Jun 18 -Aug 31	?
TI2U	39-28.34	111- 6.85	2475	Jun 20 - Aug 1	R
TOWU	39-34.83	111-18.95	3109	Jul 27 - Aug 11	N
TTUT	39-19.02	111- 5.63	2816	Jun 15 - Aug 31	?
BRW	39-27.95	111- 2.88	2847	Jul 13 - Aug 24	?
CAW	39-29.66	111- 4.60	2983	Jul 13 - Jul 15	?
FGW	39-28.73	111- 4.50	2957	Jul 13 - Aug 24	?
GEW	39-29.86	111- 6.18	2998	Jul 29 - Aug 24	?
GRW	39-29.22	111- 6.22	2952	Jul 13 - Jul 25	?

WASATCH PLATEAU STATION DATA

Station	Lat. (N)	Long. (W)	Elevation (m)	Operating Dates (1984)	Polarity
GSW	39-31.03	111- 6.28	3027	Jul 28 - Aug 25	?
HRW	39-31.37	111- 4.93	3060	Aug 15 - Aug 24	?
HTW	39-30.22	111- 3.69	2524	Jul 14 - Aug 25	?
(K41W)	39-29.74	111- 4.45	2476	Jul 15 - Aug 25	?
(K42W)	39-30.56	111- 4.51	2521	Jul 15 - Aug 25	?
(K43W)	39-30.86	111- 4.53	2533	Aug 20 - Aug 25	?
(K61W)	39-28.92	111- 3.49	2439	Jul 17 - Aug 25	?
LFW	39-27.48	111- 4.52	2929	Jul 13 - Aug 15	?
LPW	39-32.30	111- 5.99	2896	Jul 14 - Aug 25	?
MHW	39-27.72	111- 5.85	2890	Aug 16 - Aug 24	?
PSW	39-29.74	111- 4.45	2979	Jul 15 - Aug 14	?
RFW	39-30.00	111- 1.96	2310	Jul 14 - Jul 26	?
SPW	39-31.60	111- 3.01	2952	Jul 14 - Aug 10	?
STW	39-31.77	111- 4.02	2969	Aug 10 - Aug 25	?

[1]Ending of station code indicates operator; U (UT), University of Utah; B, U.S. Bureau of Reclamation; W, Woodward-Clyde Consultants. Parentheses indicate stations operated in subsurface mines. Asterisk identifies station with digital portable seismograph. At other stations, smoked-paper-type portable seismographs were operated--except for stations FDUU, SNOU, SPUT, and TTUT, which operated as telemetry stations of the University of Utah seismic network.

[2]N = Normal, R = Reverse

APPENDIX B

FOCAL MECHANISM DATA

Hypocentral Information for Fault Plane Solutions Described in Text

solution	yr	date	orig	time	lat-n	long-w	depth	mag	no	gap	dmn	rms
1	84	708	1825	22.58	39-22.50	111-14.87	3.0	0.8	20	127	2	0.17
2	84	806	34	46.87	39-23.79	111-15.12	4.3	1.5	26	51	3	0.17
3	84	724	1905	45.91	39-20.37	111- 7.55	0.7	0.9	12	74	1	0.12
4	84	718	819	43.03	39-19.44	111- 9.06	0.9	0.4	11	90	0	0.19
5	84	723	2036	22.40	39-19.96	111- 9.48	1.0	0.	10	105	0	0.06
6	84	724	2027	20.69	39-19.81	111- 7.79	1.0	0.	13	56	1	0.09
7	84	722	121	49.70	39-19.91	111- 8.21	0.6	0.7	17	54	0	0.08
	84	723	1037	15.97	39-20.06	111- 9.55	0.6	0.	10	103	0	0.06
	84	723	2031	4.38	39-20.01	111- 9.58	0.6	0.	9	112	0	0.04
	84	724	109	43.91	39-20.02	111- 9.65	0.7	0.4	14	73	0	0.06
	84	724	950	44.35	39-20.06	111- 9.65	0.7	0.	11	74	0	0.06
	84	724	1147	26.56	39-20.06	111- 9.70	0.7	0.	12	79	0	0.06
	84	725	333	49.89	39-20.02	111- 9.69	0.5	0.4	11	76	0	0.08
8	84	724	337	31.13	39-19.38	111- 9.12	1.4	0.	9	80	0	0.22
9	84	724	2020	4.03	39-20.03	111-10.03	1.5	0.	6	184	0	0.05
	84	725	320	57.13	39-20.09	111-10.12	1.6	0.4	7	190	1	0.06
10	84	731	1311	27.94	39-20.89	111- 4.71	2.3	0.8	12	194	3	0.31
11	84	805	828	54.86	39-20.23	111- 4.15	2.8	0.8	16	219	3	0.21
12	84	731	1954	17.33	39-20.34	111- 4.42	2.9	0.4	13	230	3	0.33
13	84	803	1140	31.82	39-19.71	111- 2.92	3.4	0.9	14	236	4	0.27
14	84	712	1657	52.10	39-20.98	111- 6.00	0.1	0.6	21	104	2	0.31
15	84	717	714	31.32	39-20.09	111- 7.38	0.2	0.8	19	52	1	0.18
16	84	721	1446	29.77	39-20.01	111- 6.88	0.	0.9	15	111	1	0.51
17	84	723	50	48.06	39-20.42	111- 7.37	0.0	1.0	20	48	1	0.17
18	84	803	2004	3.68	39-20.60	111- 6.80	0.0	1.8	20	136	3	0.16
19	84	804	837	39.47	39-20.70	111- 7.00	0.6	1.0	17	124	3	0.21

Solution 3

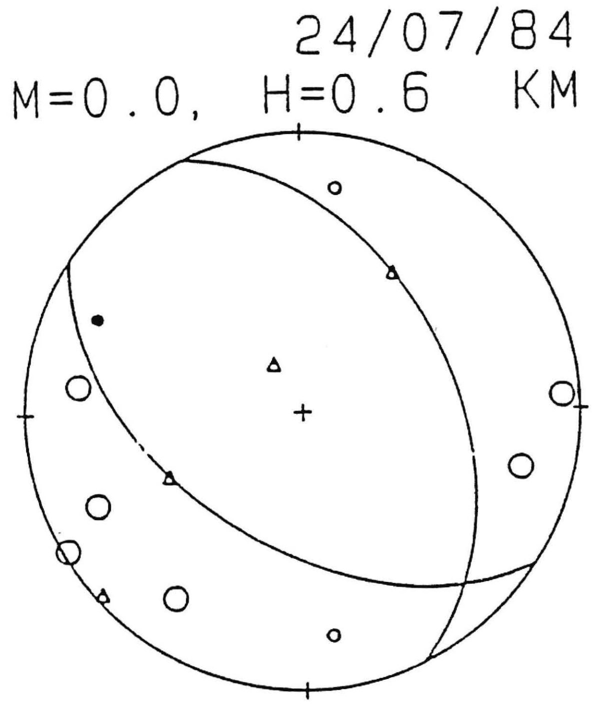

24/07/84
M=0.0, H=0.6 KM

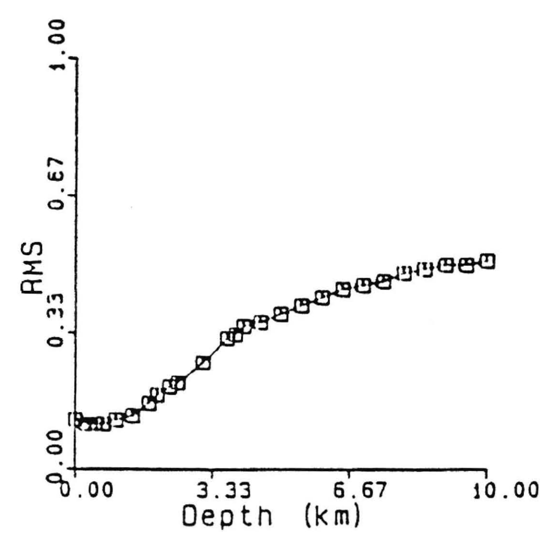

RMS
0.00
0.33
0.67
1.00
0.00
3.33
6.67
10.00
Depth (km)

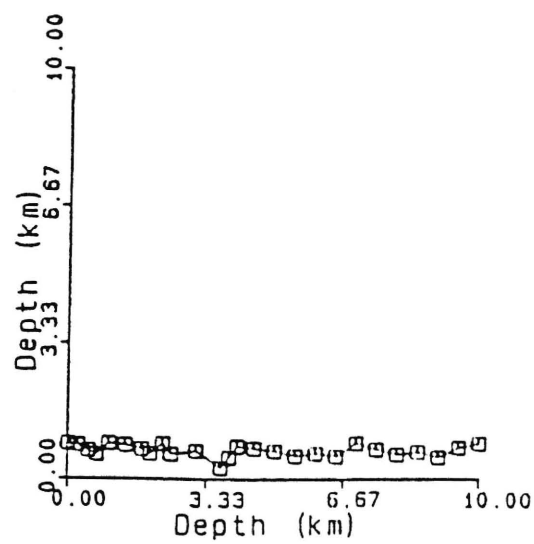

Depth (km)
0.00
3.33
6.67
10.00
0.00
3.33
6.67
10.00
Depth (km)

Solution 4

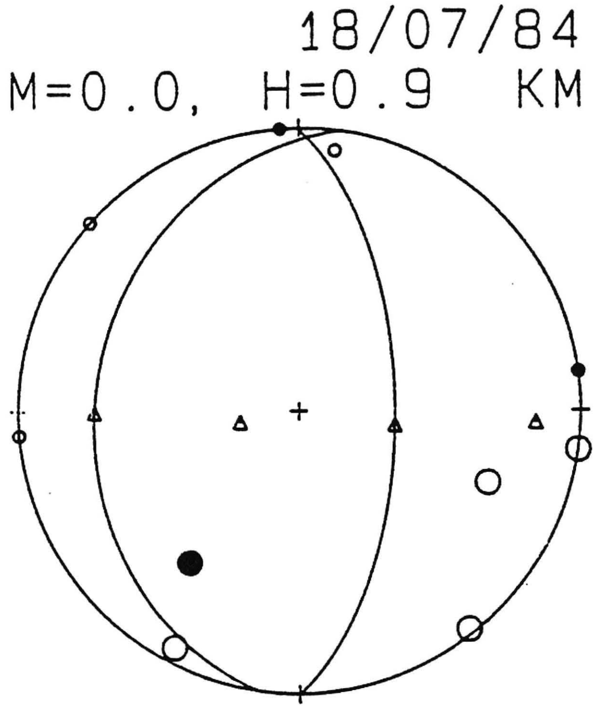

18/07/84
M=0.0, H=0.9 KM

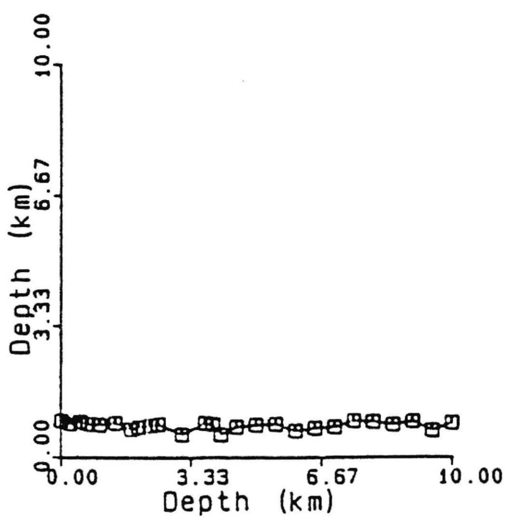

10.00
6.67
3.33
0.00
Depth (km)
0.00
3.33
6.67
10.00
Depth (km)

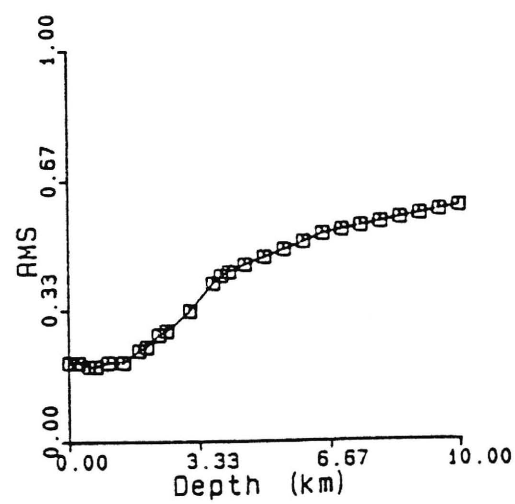

1.00
0.67
0.33
0.00
RMS
0.00
3.33
6.67
10.00
Depth (km)

Solution 5

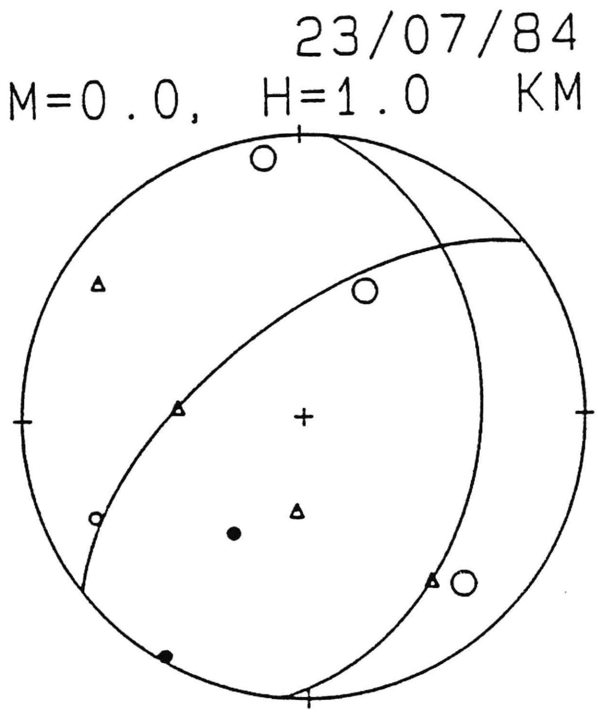
23/07/84
M=0.0, H=1.0 KM

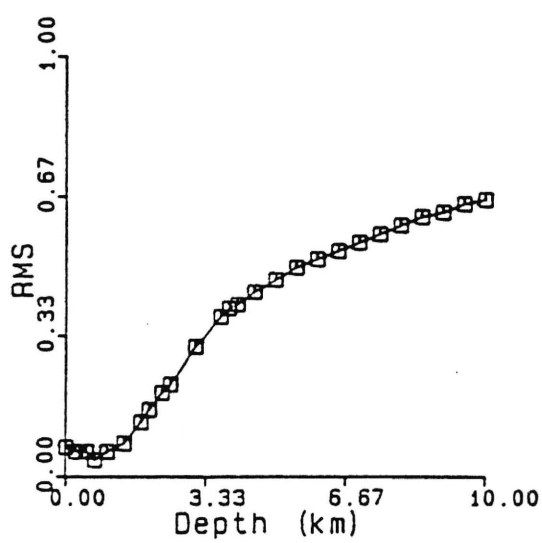
RMS
0.00
0.33
0.67
1.00
0.00
3.33
6.67
10.00
Depth (km)

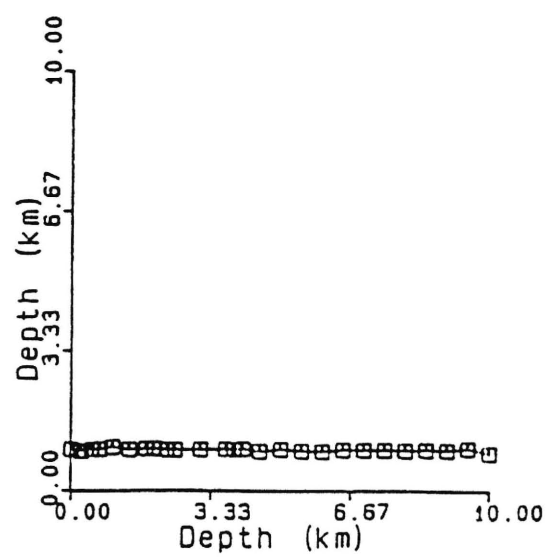
Depth (km)
0.00
3.33
6.67
10.00
0.00
3.33
6.67
10.00
Depth (km)

Solution 6

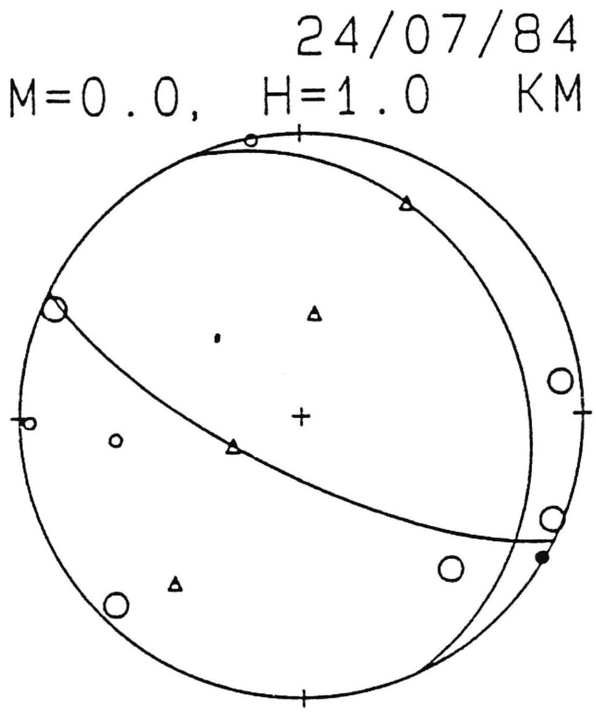

24/07/84
M=0.0, H=1.0 KM

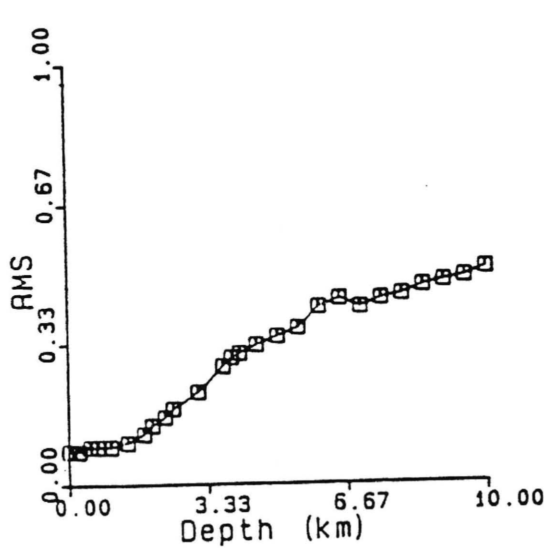

RMS
0.00
0.33
0.67
1.00
0.00
3.33
6.67
10.00
Depth (km)

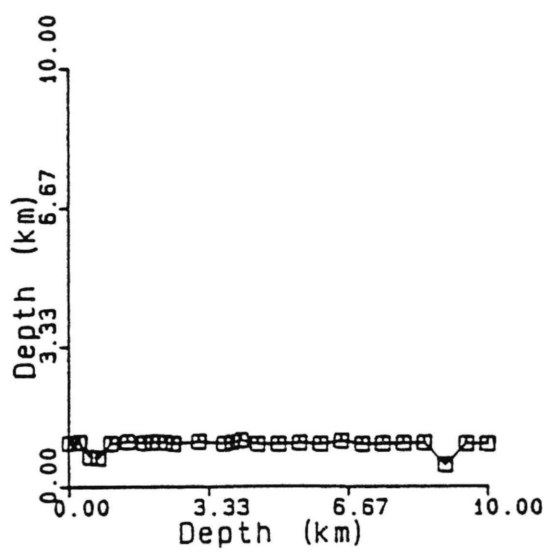

Depth (km)
0.00
3.33
6.67
10.00
0.00
3.33
6.67
10.00
Depth (km)

Solution 7

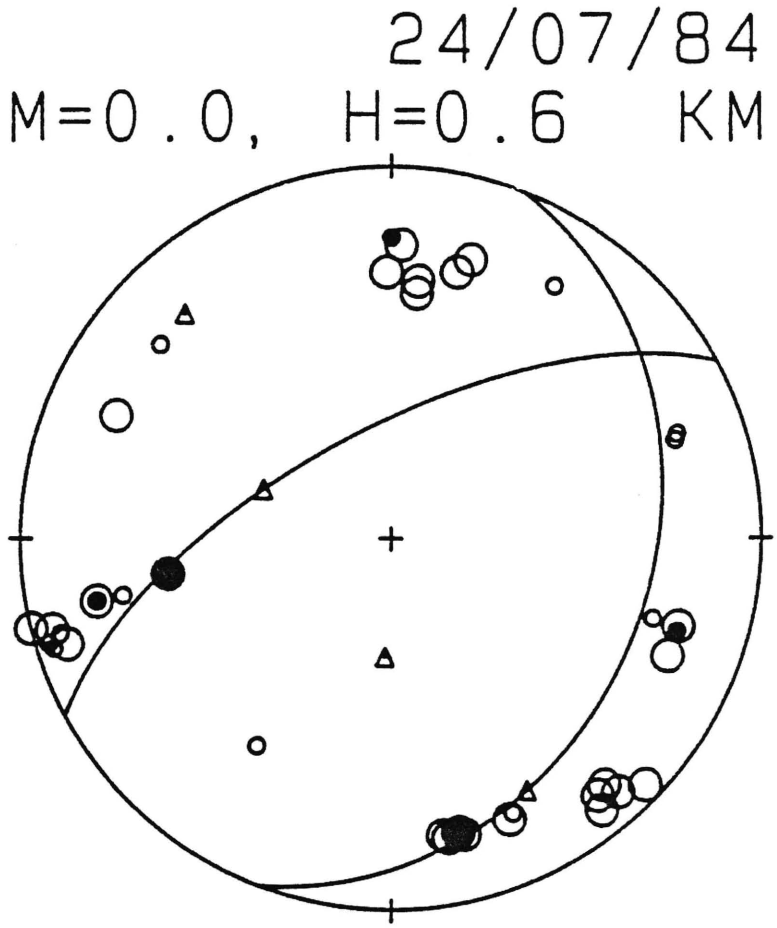

Solution 8

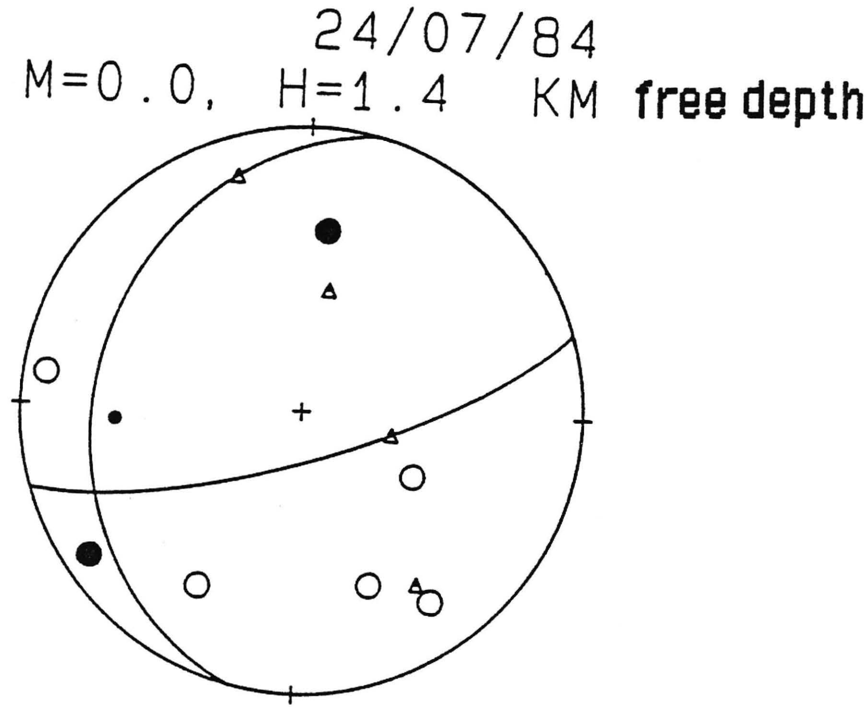
24/07/84
M=0.0, H=1.4 KM free depth

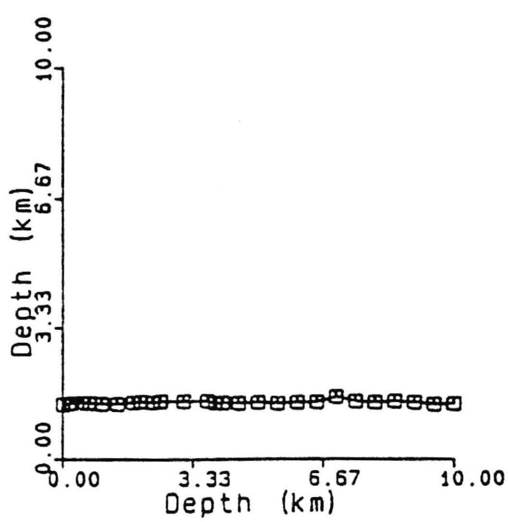
10.00
6.67
3.33
0.00
Depth (km)
0.00
3.33
6.67
10.00
Depth (km)

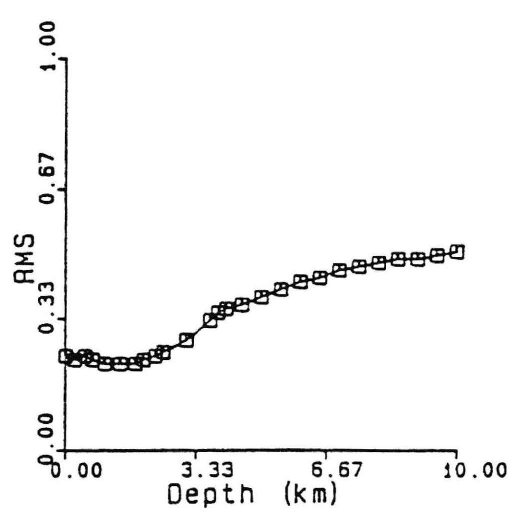
1.00
0.67
0.33
0.00
RMS
0.00
3.33
6.67
10.00
Depth (km)

Solution 8

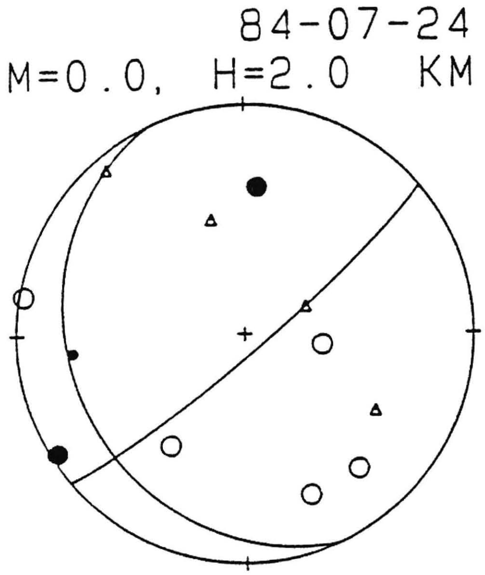
84-07-24
M=0.0, H=2.0 KM

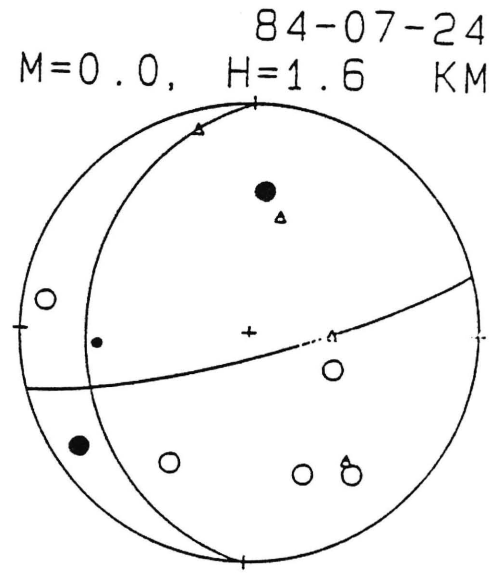
84-07-24
M=0.0, H=1.6 KM

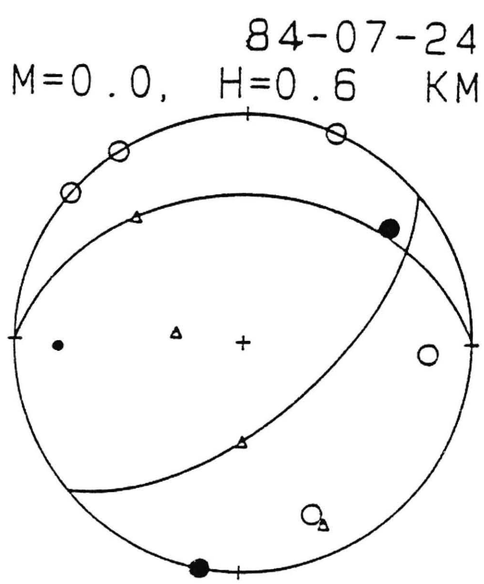
84-07-24
M=0.0, H=0.6 KM

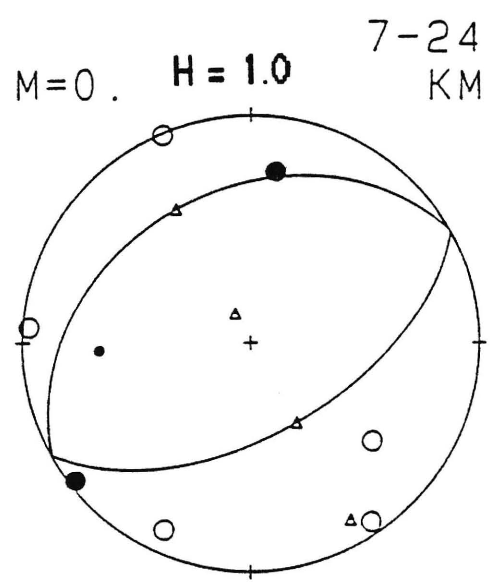
7-24
M=0.
H = 1.0
KM

Solution 9

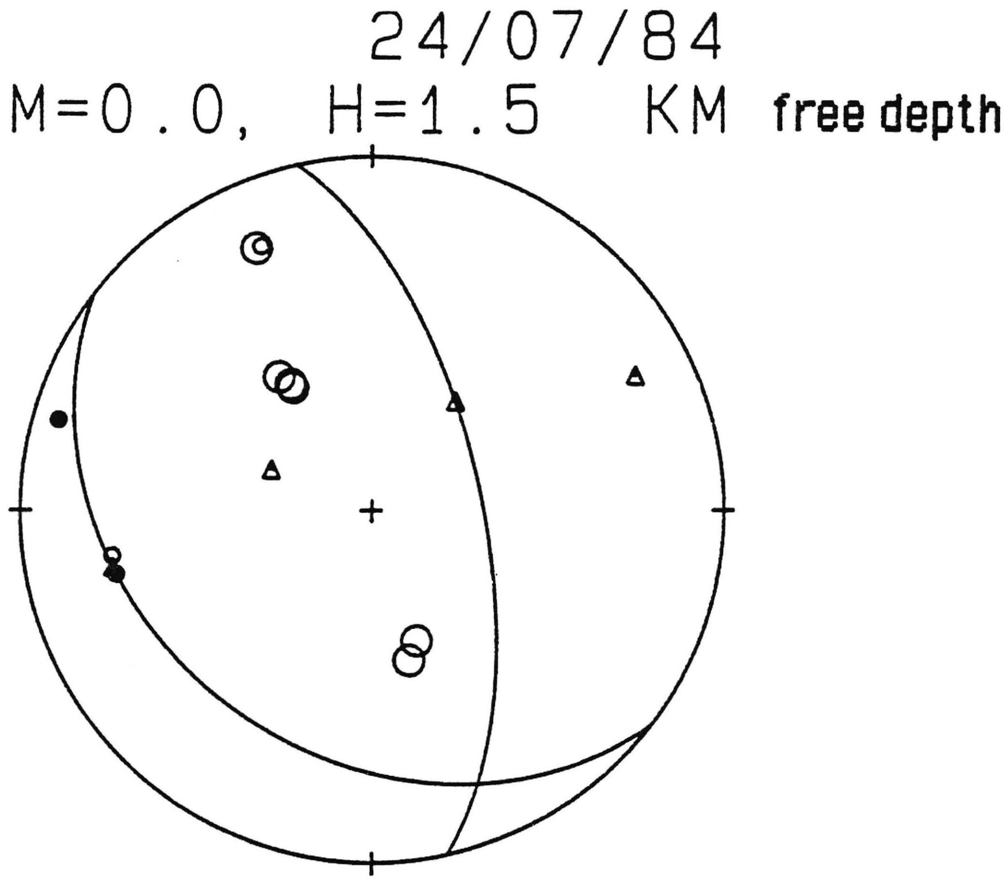

Solution 9

840725 2020

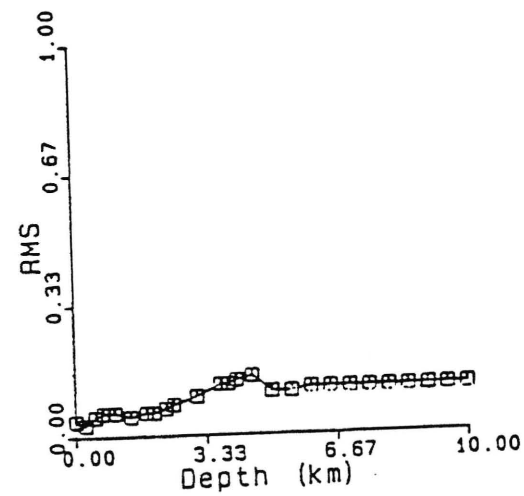

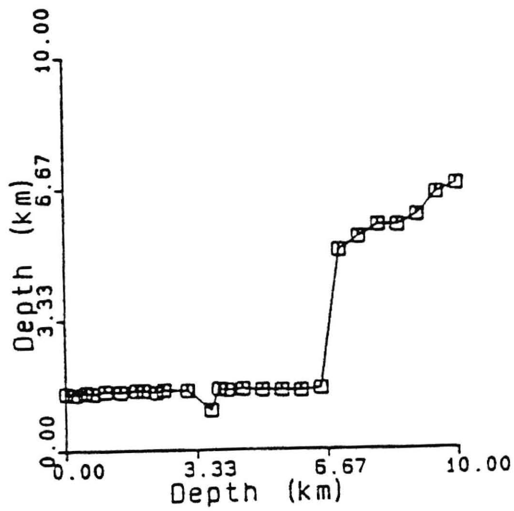

840725 0320

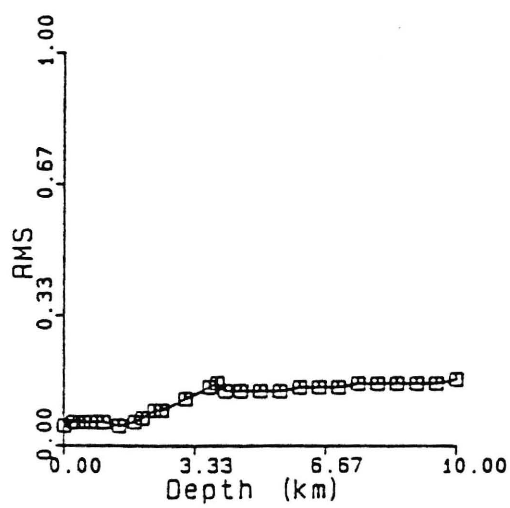

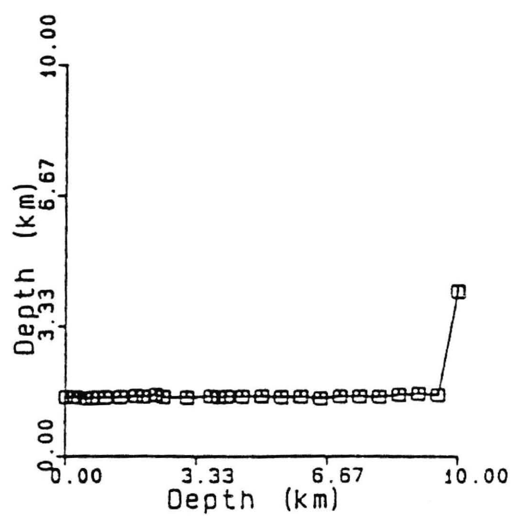

Solution 9

84-07-24
M=0.0, H=2.0 KM

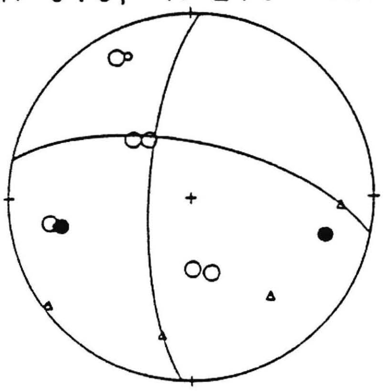

84-07-24
M=0.0, H=1.6 KM

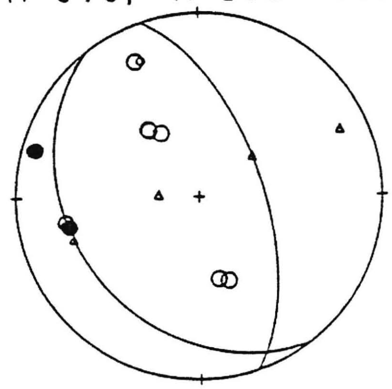

84-07-24
M=0.0, H=1.4 KM

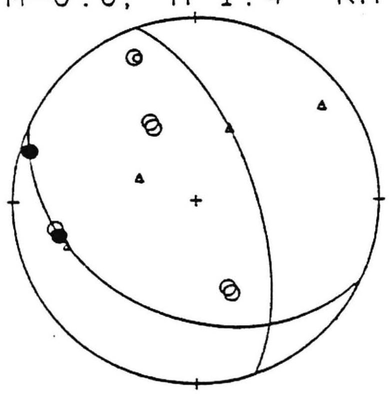

84-07-24
M=0.0, H=0.6 KM

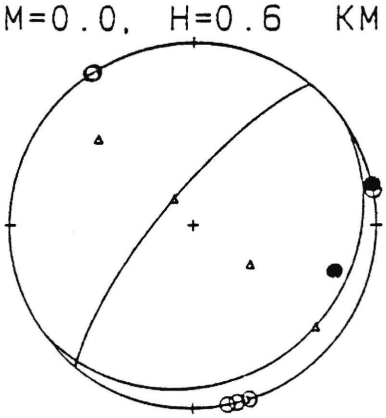

84-07-24
M=0.0, H=1.0 KM

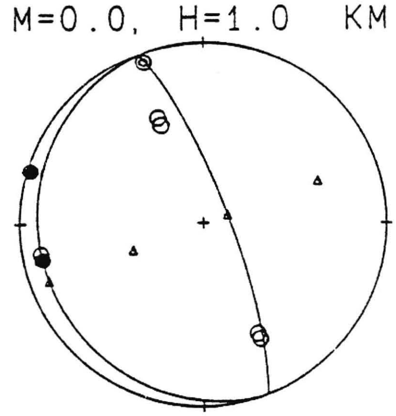

Solution 10

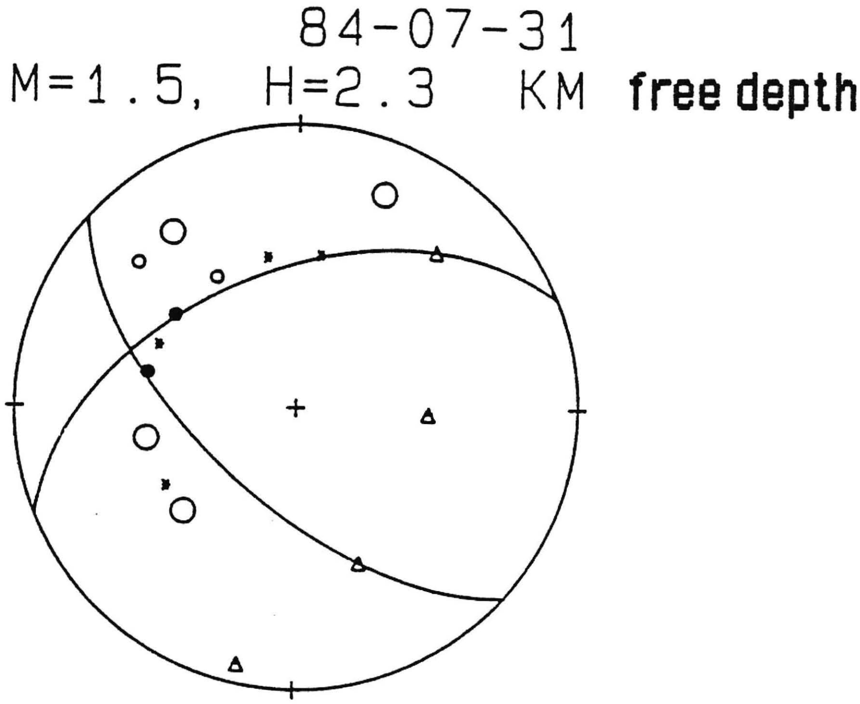

84-07-31
M=1.5, H=2.3 KM free depth

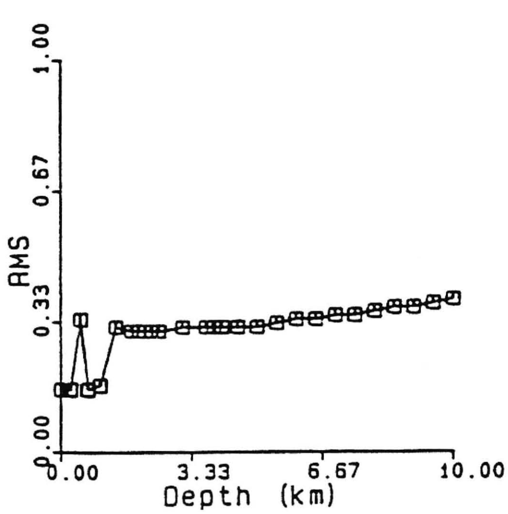

RMS
0.00
0.33
0.67
1.00
0.00
3.33
6.67
10.00
Depth (km)

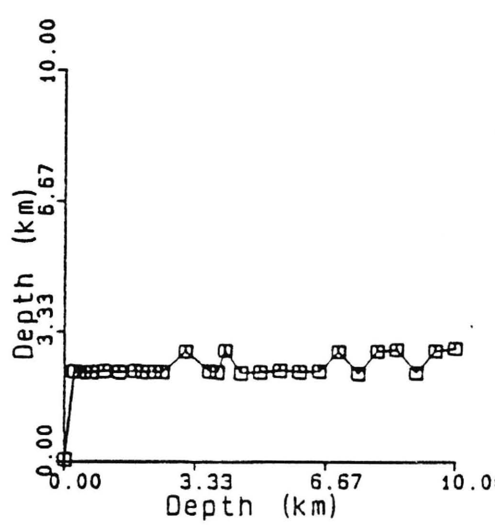

Depth (km)
0.00
3.33
6.67
10.00
0.00
3.33
6.67
10.00
Depth (km)

Solution 10

84-07-31
M=1.5, H=2.9 KM

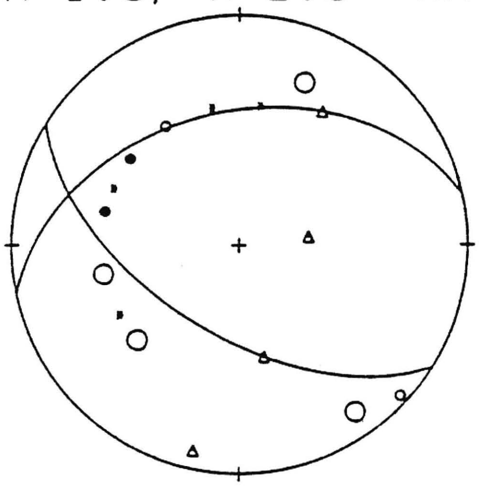

84-07-31
M=1.5, H=1.5 KM

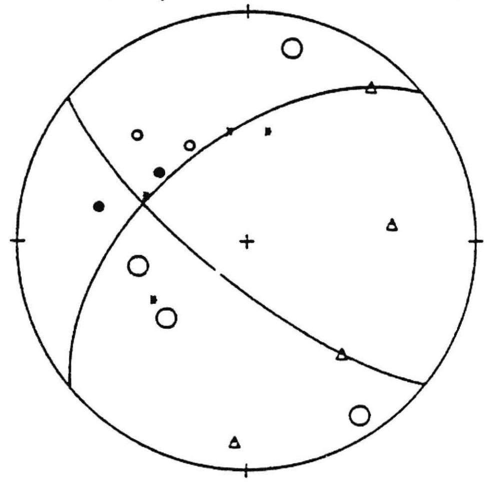

84-07-31
M=1.5, H=0.6 KM

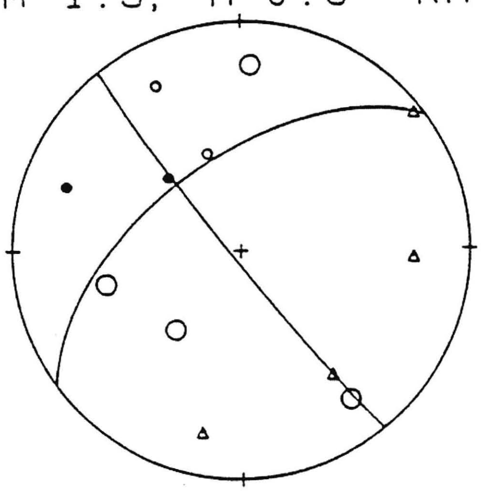

84-07-31
M=1.5, H=1.0 KM

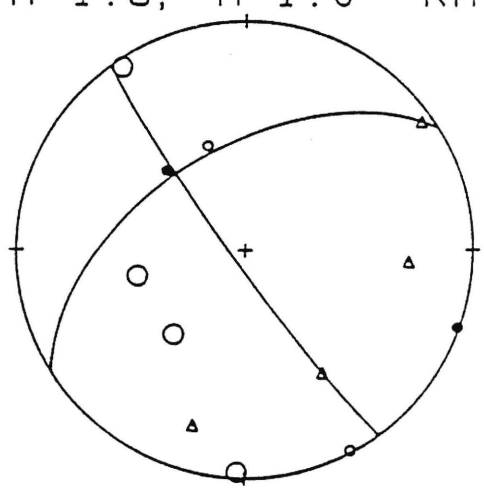

Solution 11

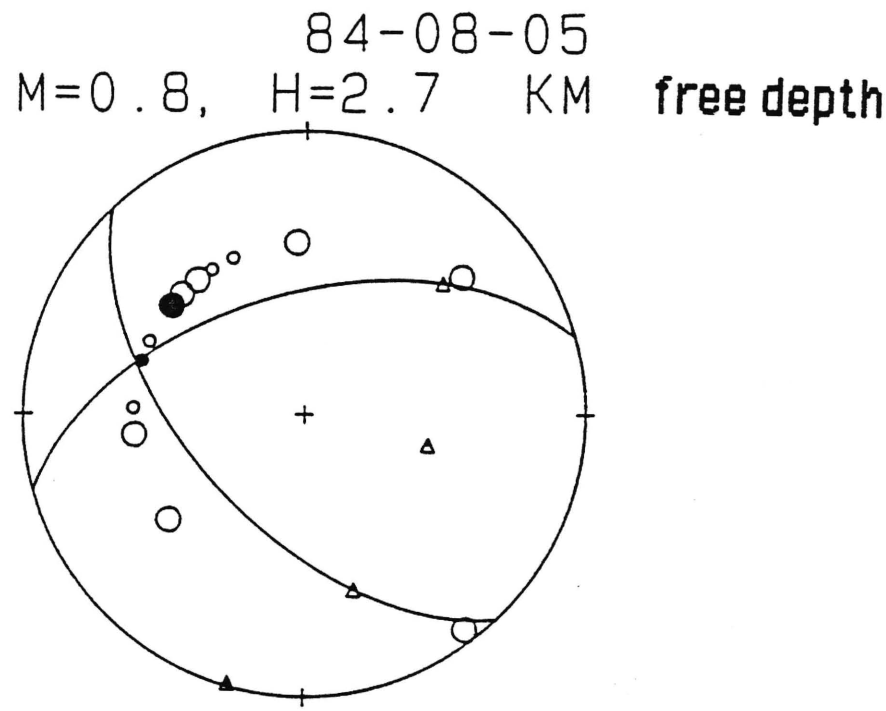

84-08-05
M=0.8, H=2.7 KM
free depth

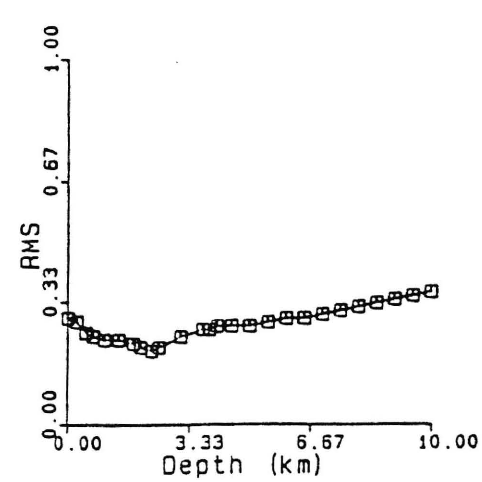

RMS
0.00
0.33
0.67
1.00
0.00
3.33
6.67
10.00
Depth (km)

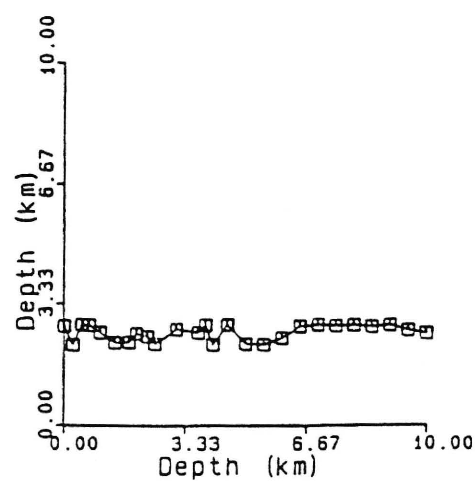

Depth (km)
0.00
3.33
6.67
10.00
0.00
3.33
6.67
10.00
Depth (km)

Solution 11

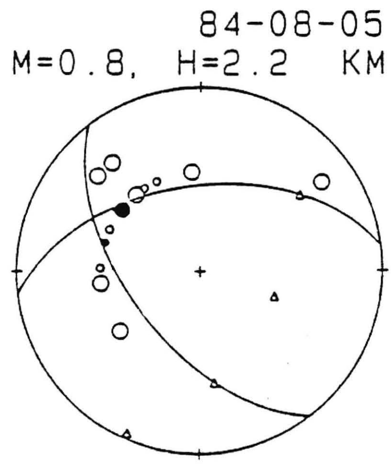
84-08-05
M=0.8, H=2.2 KM

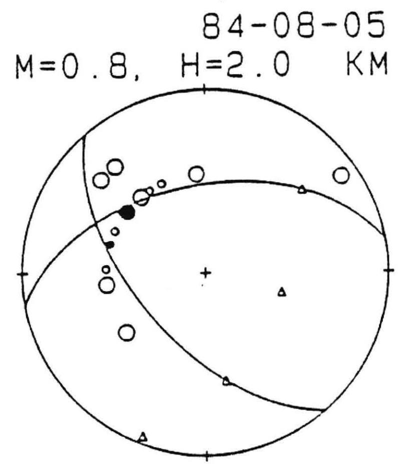
84-08-05
M=0.8, H=2.0 KM

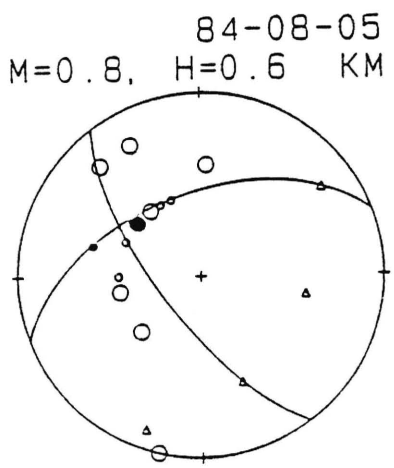
84-08-05
M=0.8, H=0.6 KM

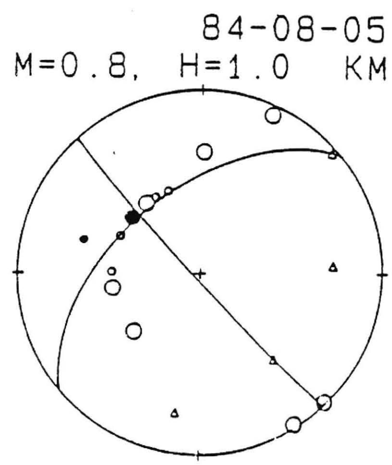
84-08-05
M=0.8, H=1.0 KM

Solution 12

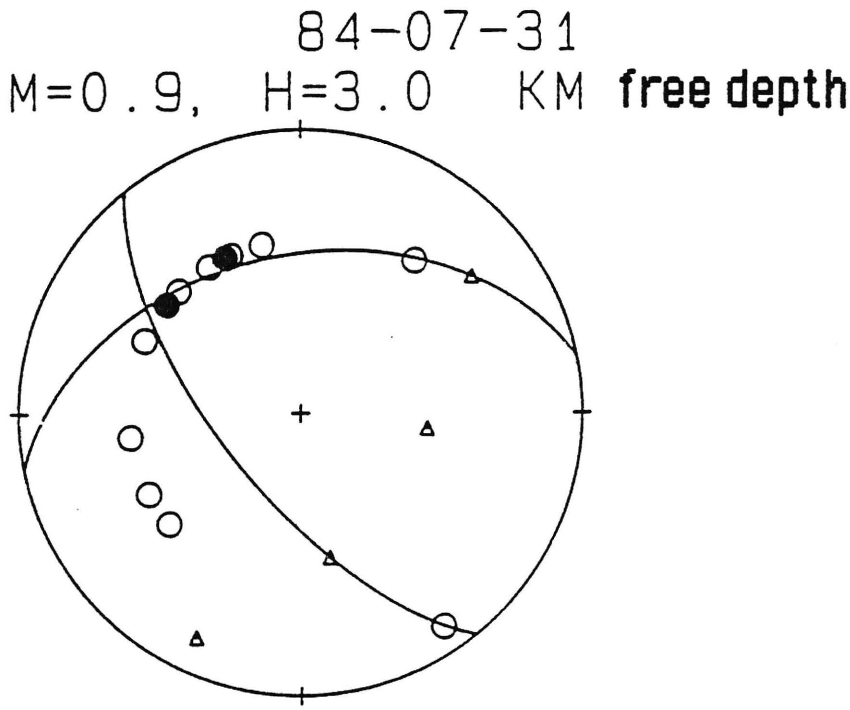
84-07-31
M=0.9, H=3.0 KM free depth

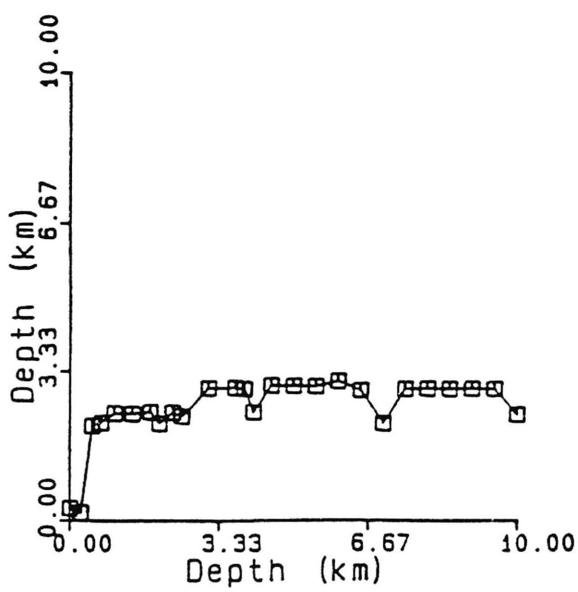
10.00
6.67
3.33
0.00
Depth (km)
0.00
3.33
6.67
10.00
Depth (km)

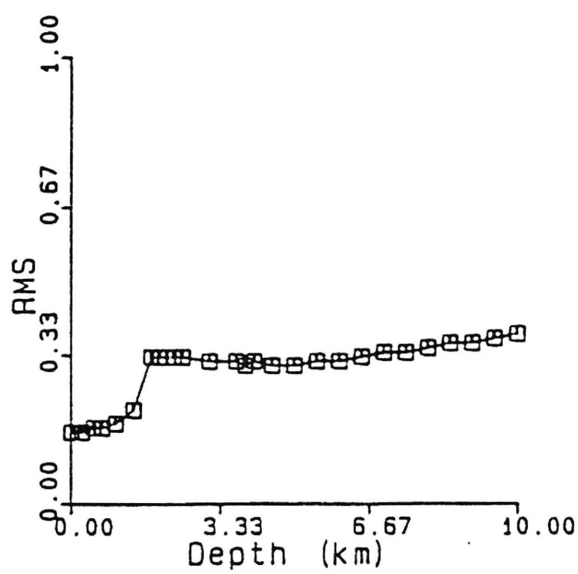
1.00
0.67
0.33
0.00
RMS
0.00
3.33
6.67
10.00
Depth (km)

Solution 12

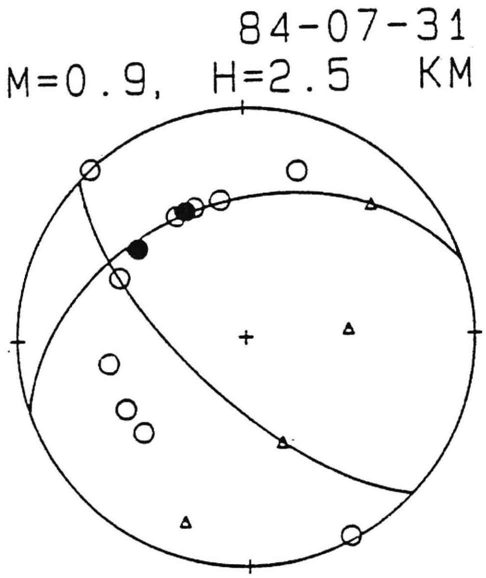
84-07-31
M=0.9, H=2.5 KM

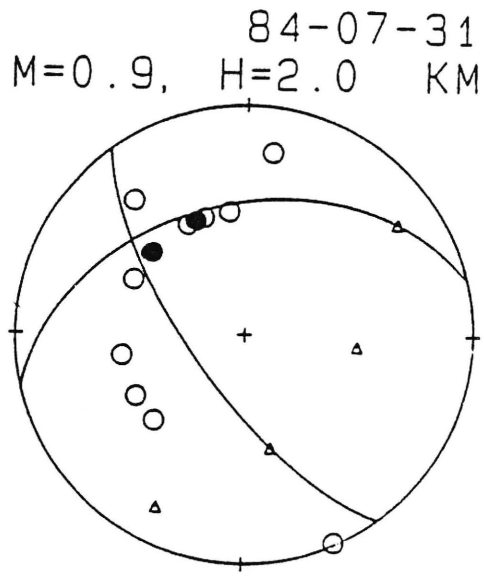
84-07-31
M=0.9, H=2.0 KM

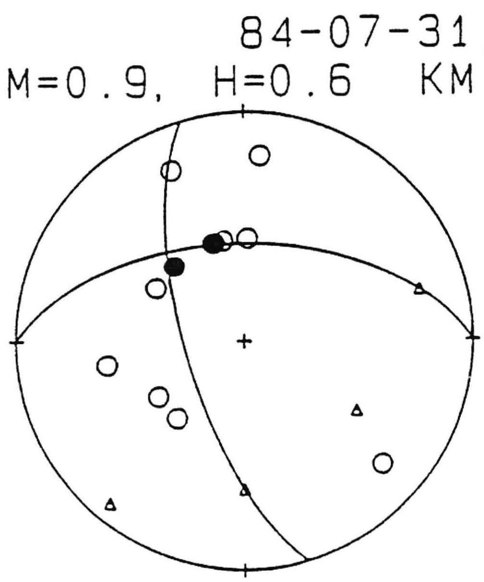
84-07-31
M=0.9, H=0.6 KM

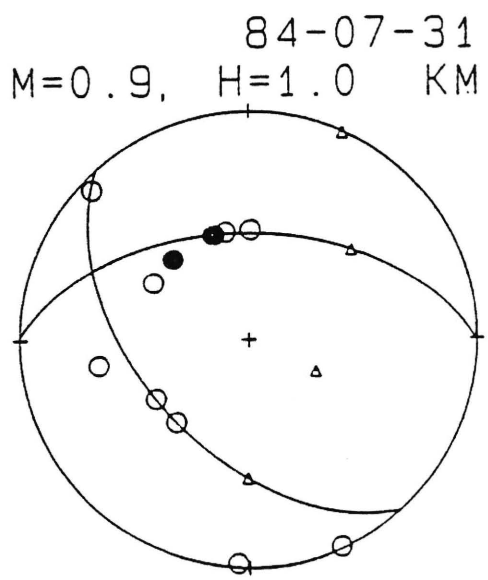
84-07-31
M=0.9, H=1.0 KM

Solution 13

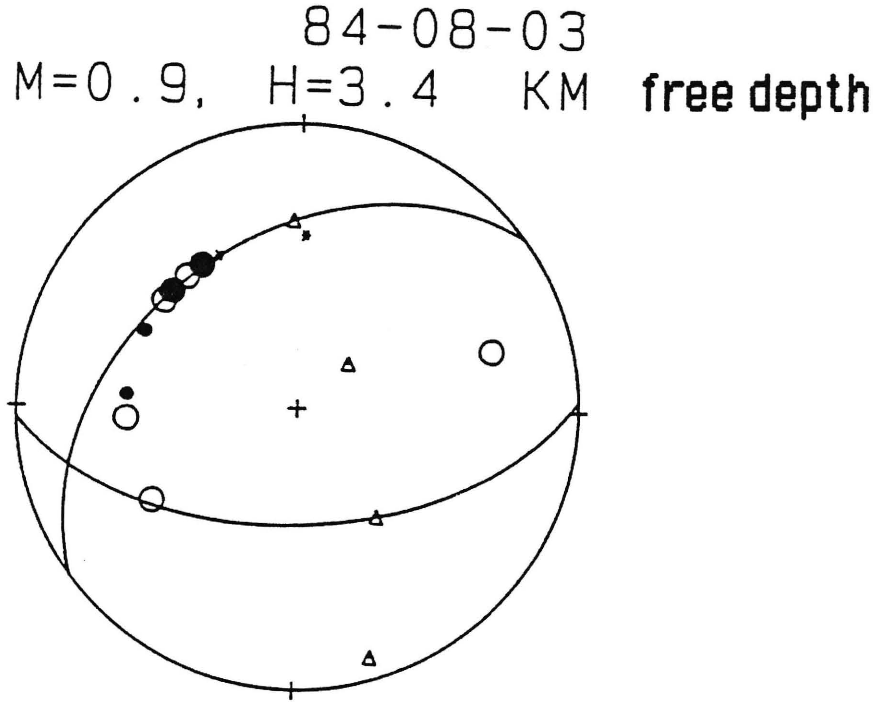
84-08-03
M=0.9, H=3.4 KM free depth

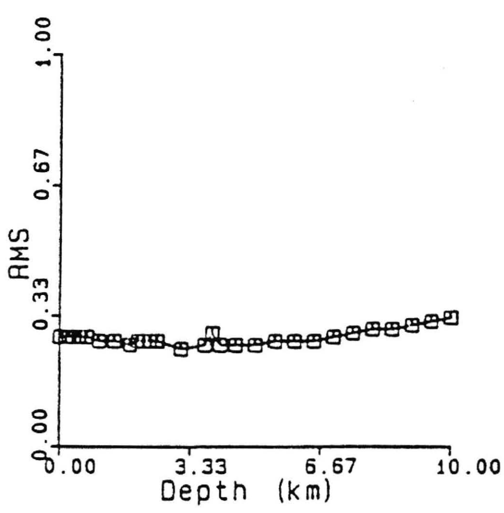
RMS
0.00
0.33
0.67
1.00
0.00
3.33
6.67
10.00
Depth (km)

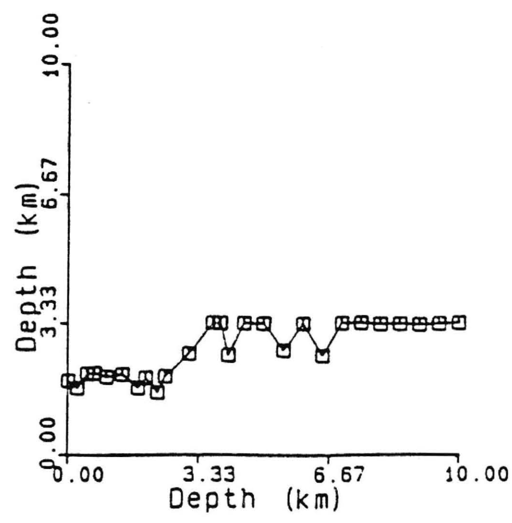
Depth (km)
0.00
3.33
6.67
10.00
0.00
3.33
6.67
10.00
Depth (km)

Solution 13

84-08-03
M=0.9, H=2.5 KM

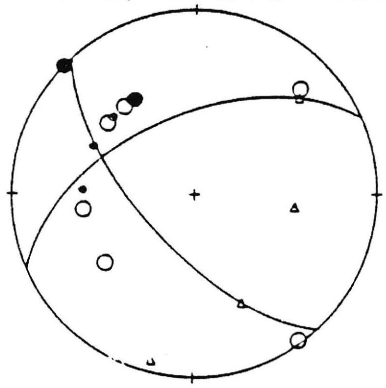

84-08-03
M=0.9, H=2.0 KM

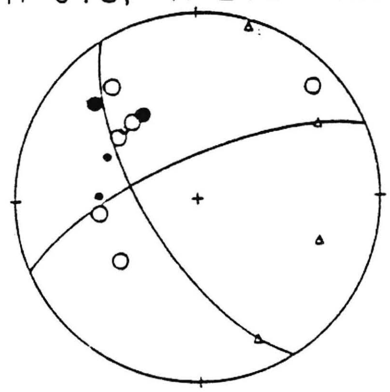

84-08-03
M=0.9, H=1.7 KM

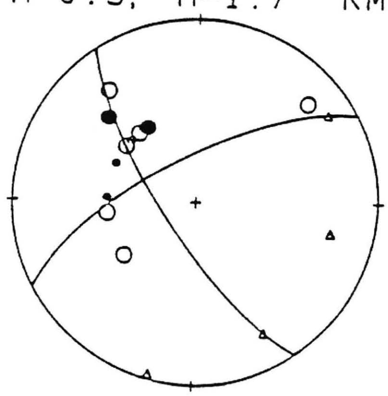

84-08-03
M=0.9, H=0.6 KM

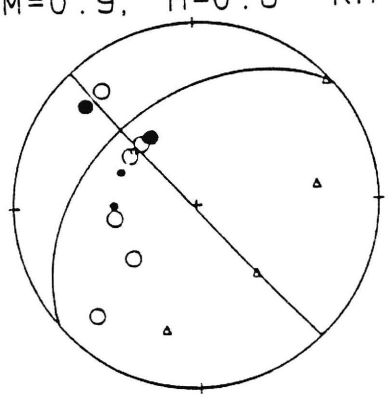

84-08-03
M=0.9, H=1.0 KM

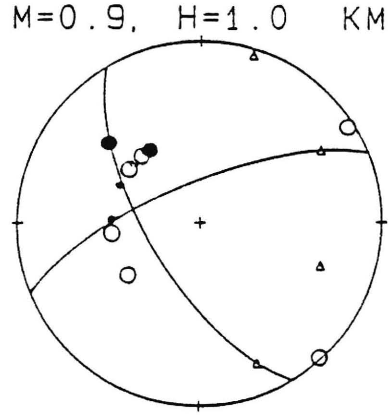

Part II. f_{max} Experiment

by J. C. Pechmann

The objective of this experiment was to investigate apparent attenuation in the upper several hundred meters of the crust using three-component digital recordings of sub-mine earthquakes obtained from instruments located both at underground mine level and at the surface. For this purpose, it was necessary to record earthquakes with ray paths that did not transect the mine workings on their way to the recording stations. We were able to design our experiment so that this condition would be met for earthquakes with hypocenters located to the west of the recording stations (Figure 1).

Simultaneous recordings on a digital seismograph located within the Wilberg Mine (EMB) and a matched instrument located 654 m directly above it on the surface (EMT) was successfully carried out for the five-day period July 21-25, 1984. Of the 172 local seismic events recorded at EMB during this period, 76 were also recorded at EMT. First motion directions for all three components at both stations were carefully tabulated for these events. Unfortunately, the first motion patterns indicate that all of these events were located to the east of EMB/EMT. Although the epicenters determined for some of these events plot slightly to the west of EMB/EMT, the error bars for these locations are large enough to permit the epicenters to actually lie to the east of EMB/EMT (Figure 2). Since we consider the first motion data to be definitive, it appears that none of the local seismic events that we recorded are suitable for the f_{max} study.

Although none of the local seismic events that we recorded were located to the west of EMB/EMT, we did manage to record on both instruments a nuclear blast from the Nevada Test Site, located approximately 500 km WSW of the recording sites (Figure 3). The horizontal-component seismograms recorded at the surface appear to have less high frequency energy than those recorded in the mine. This is particularly noticeable on the EW component. However, because of the complexity of these waveforms and the drastic differences between the waveforms recorded at EMB and EMT, it is premature to interpret this as a simple attenuation effect. Before drawing any firm conclusions about attenuation from these data, we will perform a more detailed analysis of the seismograms than the simple spectral analysis that we originally proposed. Such a study is under way.

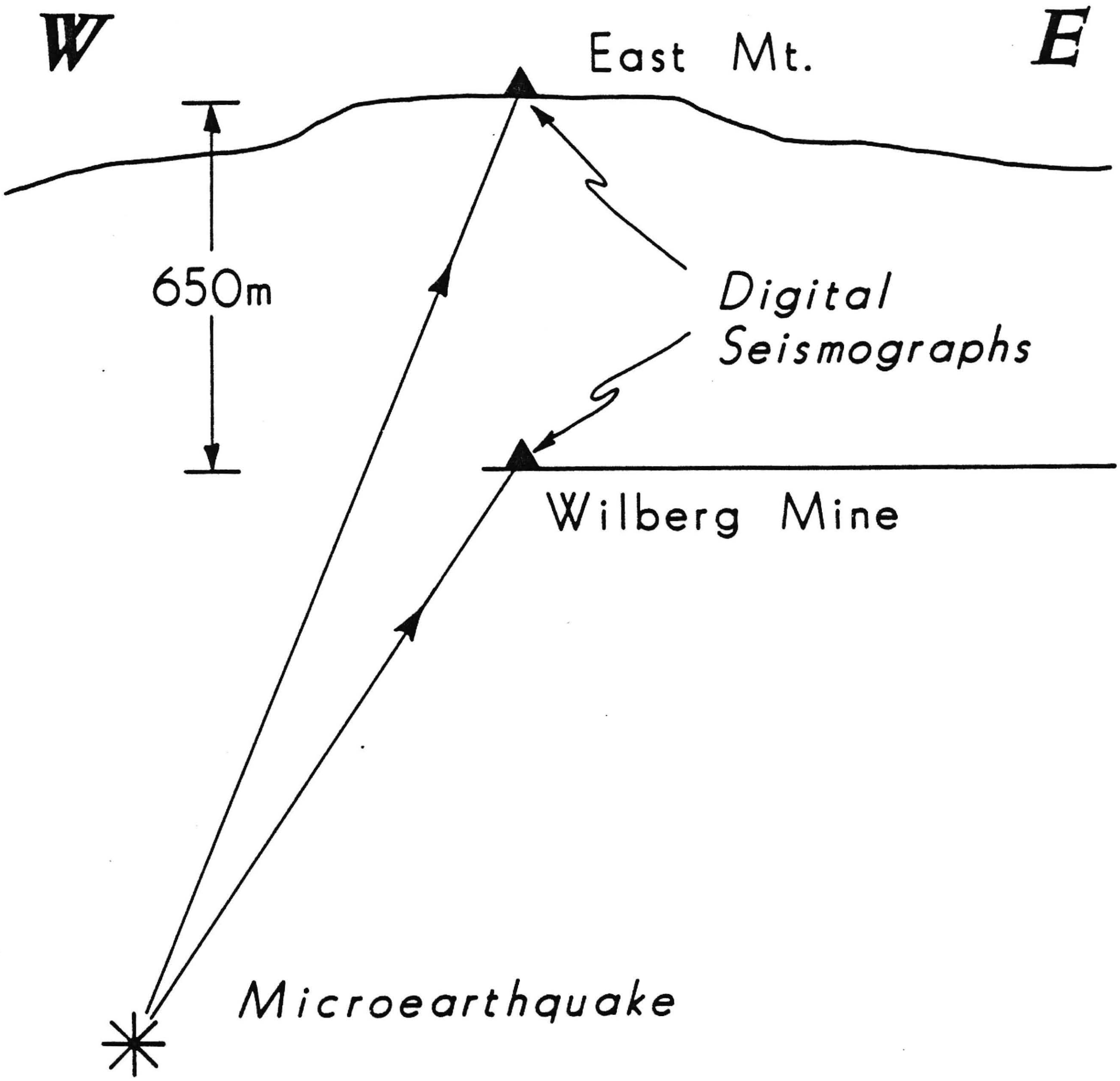

Figure 1. Cross section illustrating the recording setup for the f_{max} experiment. A hypothetical earthquake having the desired ray-path geometry for the experiment is also shown. Topography is drawn to scale with no vertical exaggeration.

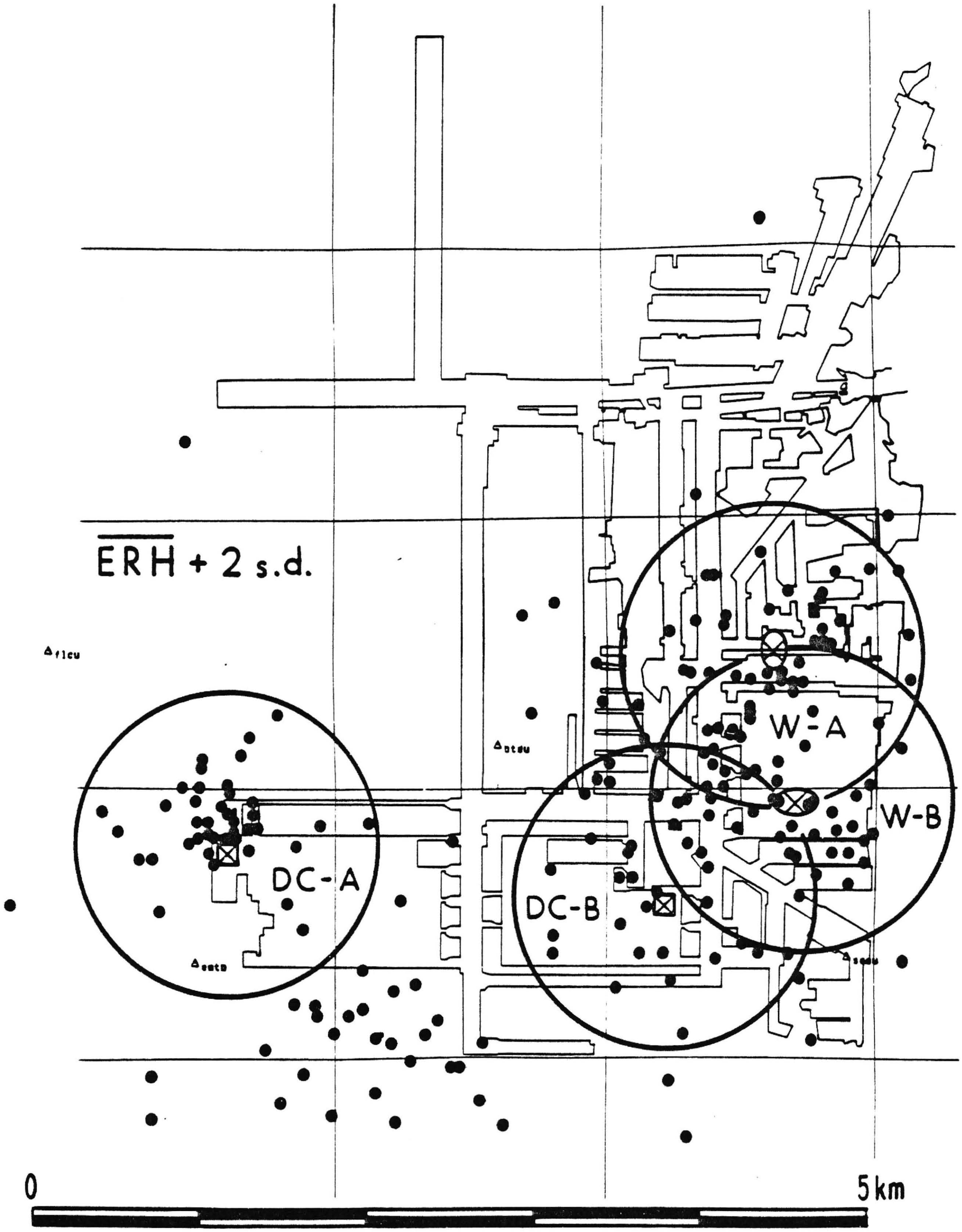

Figure 2. Epicentral plot of events from subset A superimposed on outline of the Deer Creek Mine workings. Squares represent active mine sites within the Deer Creek Mine; ovals show active mine sites within the Wilberg Mine. Circles drawn about each site correspond to the mean epicentral precision plus 2 standard deviations.

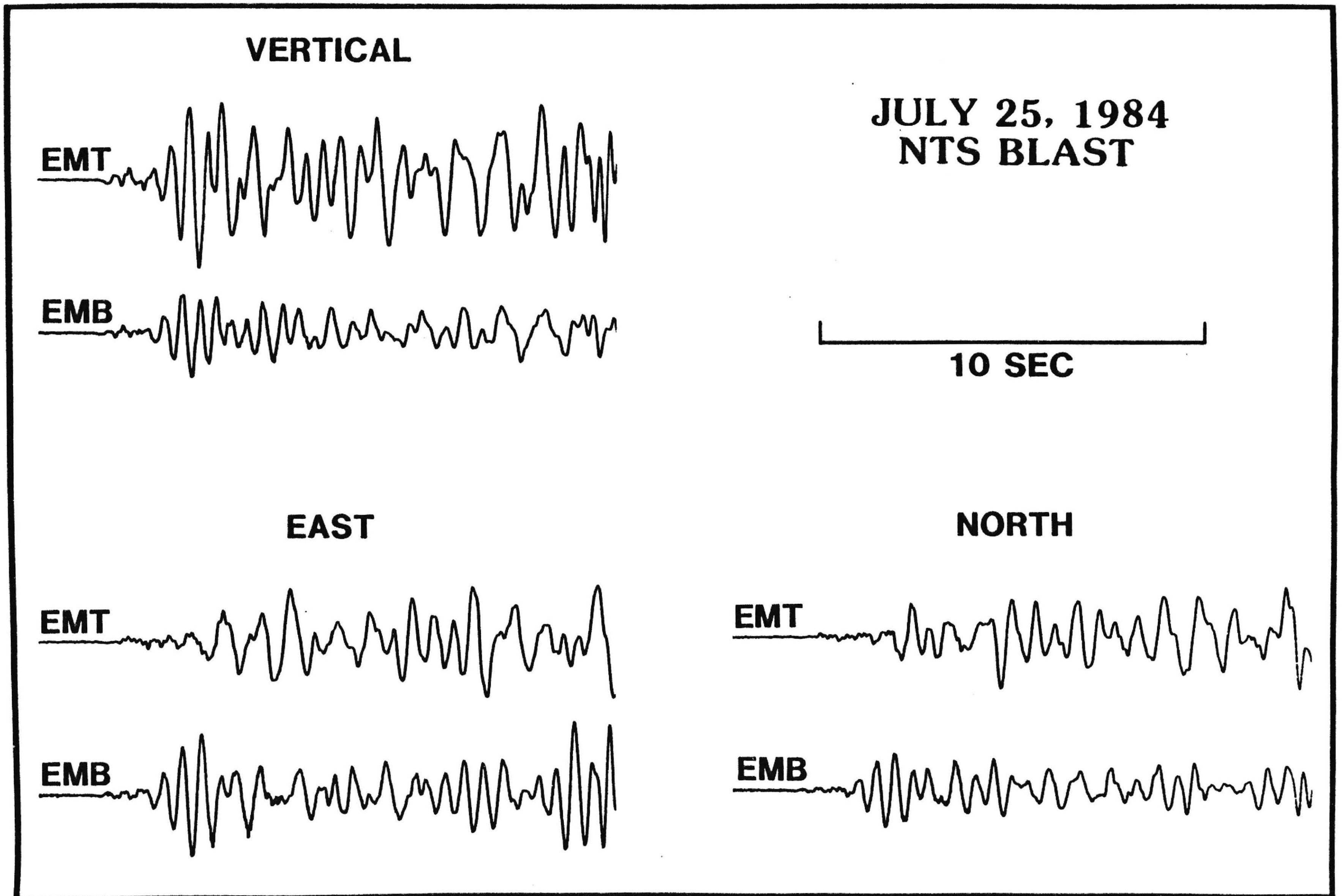

Figure 3. Three-component digital seismograms of a nuclear blast at the Nevada test site on July 25, 1984, recorded at station EMT on East Mountain and station EMB located 654 m directly below EMT in the Wilberg Mine. Note the large differences in waveform between the two sites, and the overall lower frequency character of the east and north components from EMT compared to the same components from EMB.

PART III: SELECTED ABSTRACTS WITH ADDITIONAL INFORMATION

Arabasz, W.J., J.C. Pechmann, D.Williams, R.A. Martin, Jr., C.K. Wood, I.G. I.G. Wong, J.R. Humphrey, and J.A. Adams, 1985. Collaborative study of coal-mining induced and tectonic seismicity, eastern Wasatch Plateau, central Utah—A preliminary report (abstract): Earthquake Notes 55 (1), 24.

During June to August, 1984, a joint field experiment was carried out in the East Mt.-Gentry Mt.-Joes Valley area of the Wasatch Plateau by the University of Utah, the U.S. Bureau of Reclamation, and Woodward-Clyde Consultants. Up to 40 analog and digital seismographs were operated simultaneously within a 40x25 km area located in the eastern part of the Basin & Range (BR)-Colorado Plateau (CP) transition. Multiple objectives included: (1) precise resolution of intense mining-induced seismicity—both at and below levels of active underground coal mining in two target areas; (2) source characterization of mining-induced and tectonic earthquakes (neighboring both vertically and laterally), especially in relationship to an inferred subjacent detachment and Holocene faulting in the Joes Valley area; (3) digital recording of steeply incident waves, both at underground mine level and at surface, to investigate path/site effects on high-frequency spectral content; (4) investigation of near-field ground motion at mine level (by WCC); and (5) spatial mapping of stress orientation within the BR-CP transition. Thousands of seismic events (M<2), predominantly mining-related, were recorded—including abundant mine-level events with ubiquitous dilatational first motions. Shear events reflecting tectonic stress release occur below mine level down to about 4 km, and also beneath the adjacent Joes Valley area at similar depth. Simultaneous subsurface/surface digital recordings were achieved in two separate target areas. The primary purpose of this presentation is to communicate experiment design, accomplishments, and preliminary results.

Williams, D.J., and W.J. Arabasz, 1985. Mining-related seismicity in the East Mountain area, Wasatch Plateau, central Utah (abstract): EOS, Trans. Am. Geophys. Union 66, 954-955.

As part of a multi-institutional field experiment during the summer of 1984 investigating the seismicity of the eastern Wasatch Plateau (see Arabasz et al., 1985, Earthquake Notes 1, 24), a 20-station array of portable seismographs was operated for 1 mo in the East Mt. area, an area of active underground coal mining. Eight stations of the array were concentrated on top of East Mt. at an average spacing of 3 km, and 2 key digital stations—with one 600 m below surface at mine level. Principal issues are (1) precise resolution and spatial correlation of intense microseismicity (>200 events/d<M2) with areas of active mining, (2) mechanisms of mining-related and neighboring tectonic seismicity, and (3) temporal correlation of local seismicity with underground coal extraction.

High-resolution seismic profiles and drill-hole sonic logs were used for a refined velocity model. Accurately-located epicenters (n>400; $\pm$400 m) cluster within an area <2.5 km in diameter that encompasses three zones of significant coal extraction during the study period—but the observed seismicity does not correlate simply, either spatially or temporally, with active mine faces. Abundant focal depths extend to 2 km below mine level, and continuous monitoring for a 60-d period (June 15-Aug. 15) bracketed a 16-d mining shutdown (July 7-22) during which significant seismicity, comparable to that observed before the shutdown, was observed. P-wave first motions indicate two populations of events: (1) enigmatic events located at or close to mine level with ubiquitous dilatational first motions, and (2) double-couple mechanisms, predominantly of compressional type (thrust and ss), with NW- to NE-trending P-axes. Incomplete evidence suggests a change to normal-faulting mechanisms (depth <4 km) immediately west of the mining area.

Arabasz, W.J., 1986. Seismotectonics of the Basin and Range-Colorado Plateau transition in Utah (abstract): Geol. Soc. America Abstracts With Programs 18 (in press; 1986 Rocky Mt. Section Meeting).

Results of seismic monitoring by the University of Utah since 1962, and of short-term seismographic field experiments carried out between 1979 and 1984, allow an overview of the seismotectonics of the NW boundary of the Colorado Plateau. Key observations relate to the correlation of diffuse background seismicity with geologic structure, geometry of faulting, change in regional stress across the transition between the Basin and Range and Colorado Plateau provinces, and implications of recurrent Holocene surface faulting vis-a-vis hypotheses of "thin-skinned" extension.

There has been no documented instance of historical surface faulting in the transition region, and the largest historical shock was one of about M6.5 near Richfield, Utah, in 1901. Low-angle structural discontinuities in the study area appear to play a fundamental role in separating locally intense upper-crustal seismicity above 6-8 km depth from less frequent background earthquakes at greater depth, down to about 15 km. Seismic slip predominates on fault segments of moderate (>30°) to high-angle dip—at least for small to moderate-size earthquakes (M<5)—based both on fault-plane solutions and hypocentral distributions. No convincing evidence has yet been found for seismic slip on either a downward-flattening or a low-angle normal fault in the region although such faults are known to exist.

More than sixty fault-plane solutions provide significant detail for mapping changes in upper-crustal stress orientation across the transition region. Important observations include eastward changes through the transition region from normal faulting to strike-slip faulting to mixed faulting, including compressional reverse faulting.